DEVELOPMENT OF A REAL-TIME PCR INCORPORATING HIGH RESOLUTION MELTING ANALYSIS TO SCREEN HIV-1 SAMPLES FOR RESISTANCE-RELATED CODONS

David Sacks

Dissertation submitted to the Faculty of Health Sciences, University of the Witwatersrand, Johannesburg, in fulfillment of the requirements for the degree of Master of Science in Medicine

Johannesburg, 2010

Declaration

I, David Sacks, declare that this dissertation is my own work. It is being submitted for the degree of Master of Science in Medicine in the University of the Witwatersrand, Johannesburg, South Africa. It has not been submitted before for any degree or examination at this or any other University.

…….
David Sacks

…….
Date

Presentations

Sacks, D., Ledwaba, J., Morris, L. and Hunt, G. Development of a Real-Time PCR Incorporating High Resolution Melting Analysis to Detect Resistance-Related Single Nucleotide Polymorphisms in the HIV-1 Reverse Transcriptase Gene. 2nd Postgraduate Cross Faculty Symposium (Johannesburg, 2009). Poster.

Sacks, D., Ledwaba, J., Morris, L. and Hunt, G. Development of a Real-Time PCR Incorporating High Resolution Melting Analysis to Detect Resistance-Related Single Nucleotide Polymorphisms in the HIV-1 Reverse Transcriptase Gene. 10th Annual Symposium on Antiviral Drug Resistance: Targets and Mechanisms (Richmond, Virginia USA, 2009). Poster.

Sacks, D. Development of a Real-Time PCR Incorporating High Resolution Melting Analysis to Screen HIV-1 Samples for Resistance-Related Codons. NICD Research Forum (Johannesburg, 2010). Presentation.

Abstract

Introduction

High resolution melting analysis (HRMA) accurately, rapidly and cost effectively detects single nucleotide polymorphisms by monitoring DNA dissociation kinetics. This technology was applied to HIV samples to assess whether it could be used to detect clinically relevant drug resistance mutations.

Methods

HRMA-PCR assays incorporating unlabeled probes were designed to genotype 12 mutation codons in the HIV-1 *p66/p51* of engineered plasmids and 116 HIV-1 samples.

Results

HRMA correctly genotyped 63%-88% of the K103N, Y181C, M184V, Q151M and G190A mutations. Each assay had a 1.7%-3.4% discordance, most of which was due to the increased analytical sensitivity of HRMA (~5-20%). Only mutant K65R and V106M were correctly identified while the 41, 67, 70, 215 and 225 codons could not be genotyped. Assay modifications had some success in masking the affects of polymorphisms.

Conclusion

These assays can be used for genotyping selected major HIV-1 resistance mutations and should be further developed as a resistance surveillance tool.

Acknowledgments

I would like to sincerely thank the following people:

- Dr. Gillian Hunt for her invaluable supervision, help and insight throughout the course of my Masters.
- Professor Lynn Morris for her guidance and the opportunity to complete my Masters in her laboratory.
- Johanna Ledwaba for all of the help in and out of the laboratory over the years.
- The entire NICD AIDS Virus Research Unit for all the assistance and advice.
- The University of the Witwatersrand, the Poliomyelitis Research Foundation and the National Research Foundation for student grants.
- The National Health Laboratory Service Research Trust for project funding.
- My parents, Brian and Cheryl, for allowing me to study and for all the love and support over the years.
- My brothers, extended family and friends for their support and friendship.

Table of Contents

List of Figures

List of Tables

Abbreviations

°C	Degrees Celsius
µL	Microlitre
µM	Micromolar
3TC	Lamivudine
ABC	Abacavir
AIDS	Acquired immune deficiency syndrome
Amp	Ampicillin
AMV	Avian myeloblastosis virus
ARV	Antiretroviral
AS-PCR	Allele specific-PCR
ATP	Adenosine triphosphate
ATZ/r	Ritonavir boosted Atazanavir
AZT	Zidovudine
bp	Base pair
CCR5	Chemokine (C-C motif) receptor 5
CD4+	Cluster of differentiation 4 positive
cDNA	Complementary DNA
cpz	Chimpanzee
CXCR4	Chemokine (C-X-C motif) receptor 4
d4t	Stavudine
Da	Dalton

ddI	Didanosine
ddNTPs	Dideoxynucleotide triphosphates
-dF/dT	Negative first derivative plot
dH_2O	Distilled water
DMA	DNA melting analysis
DNA	Deoxyribonucleic acid
dNTP	Deoxyribonucleotide/side triphosphate
DRV/r	Ritonavir boosted Darunavir
ds	Double-stranded
DTT	Dithiothreitol
EDTA	Ethylenediaminetetraacetic acid
EFV	Efavirenz
ENF	Enfuvirtide
Env	Envelope
ETR	Etravirine
FN	False negative
FP	False positive
FPV/r	Ritonavir boosted Fosamprenavir
FTC	Emtricitabine
g	Gram
g	Gravitational acceleration
gag	Group antigen
gor	Gorilla

gp	Glycoprotein
HAART	Highly active antiretroviral therapy
HC*l*	Hydrochloric acid
HIV	Human immunodeficiency virus
HIV group M	Major
HIV group N	Non-M/non O
HIV group O	Outlier
HRMA	High resolution melting analysis
HSV	Herpes simplex virus
HU	Hydroxyurea
I	Inosine
IC_{50}	Half maximal inhibitory concentration
IDV/r	Ritonavir boosted Indinavir
kb	Kilobase
kD	Kilodalton
L	Litre
LB	Lysogeny broth
LNA	Locked nucleic acid
LPV/r	Ritonavir boosted Lopinavir
LTR	Long terminal repeats
M	Molar
mg	Milligram
$MgCl_2$	Magnesium chloride

mL	Millilitre
mM	Millimolar
mm^3	Millimetre cubed
Mol	Mole
MVC	Maraviroc
NaCl	Sodium chloride
Nef	Negative replication factor
NFV/r	Ritonavir boosted Nelfinavir
ng	Nanogram
nm	Nanometre
NNRTI	Non-nucleoside RT inhibitor
NRTI	Nucleoside RT inhibitor
NVP	Nevirapine
PCR	Polymerase chain reaction
pH	Potentiometric hydrogen ion concentration
PI	Protease inhibitor
pmol	Picomol
PR	Protease
RAL	Raltegravir
Rev	Regulator of virus protein expression
RNA	Ribonucleic acid
rpm	Revolutions per minute
RRE	Rev responsive element

RT	Reverse transcriptase
RT-PCR	Reverse transcription-PCR
s	Second
sd-NVP	Single-dose NVP
SIV	Simian immunodeficiency virus
sm	Sooty mangabey
SNP	Single nucleotide polymorphism
SOC	Super optimal broth
SQV/r	Ritonavir boosted Saquinavir
ss	Single-stranded
TAE	Tris-acetate-EDTA
TAM	Thymidine analogue mutation
Tat	Transcriptional transactivator of LTR
TDF	Tenofovir
T-lymphocyte	Thymus-lymphocyte
T_m	Melting temperature
TN	True negative
TP	True positive
TPV/r	Ritonavir boosted Tipranavir
Tris	Tris(hydroxymethyl)aminomethane
U	Enzyme unit
Vif	Virion infectivity factor
Vpr	Viral protein R

Vpu	Viral protein U
X-gal	Bromo-chloro-indolyl-galactopyranoside
ZDV	Zidovudine
α	Alpha
β	Beta

DNA bases and incompletely specified bases

A	Adenine
C	Cytosine
T	Thymine
G	Guanine
R	G or A
Y	T or C
M	A or C
S	G or C
W	A or T
H	A or C or T

Amino acids

A	Alanine
C	Cysteine
D	Aspartic acid
E	Glutamic acid

F	Phenylalanine
G	Glycine
H	Histidine
I	Isoleucine
K	Lysine
L	Leucine
M	Methionine
N	Asparagine
P	Proline
Q	Glutamine
R	Arginine
S	Serine
T	Threonine
V	Valine
W	Tryptophan
Y	Tyrosine

Chapter 1: Literature Review

1.1 Human Immunodeficiency Virus

The human immunodeficiency virus (HIV) is the aetiologic agent of acquired immune deficiency syndrome (AIDS) (Barré-Sinoussi et al., 1983; Gallo et al., 1984). Unknown 27 years ago, today it is estimated that 33 million people are infected with HIV, and 25 million people have died from the disease. Annually there are ~2 million AIDS related deaths and a total of 2.8 million new infections worldwide. Sub-Saharan Africa is most severely affected with 67% of all HIV infections and 75% of AIDS deaths (Joint United Nations Programme on HIV/AIDS, 2008). Countrywide more than 16% of South Africans aged 25 and older are infected with HIV, while the prevalence in some regions exceeds 20% (Shisana et al., 2009).

1.1.1 Classification

HIV is part of the Retroviridae family, Othoretrovirinae subfamily and Lentivirus genus. To date, two species of HIV have been identified, namely HIV type 1 (HIV-1) and HIV type 2 (HIV-2). The viruses share ~50% sequence similarity and have a zoonotic origin from simian immunodeficiency virus (SIV) (Knipe et al., 2007). HIV-1 is most closely related to SIV which is found in wild common chimpanzees (*Pan troglodytes*), SIVcpz (Gao et al., 1999; Keele et al., 2006). HIV-2 is most closely related to the SIV that infects sooty mangabeys (*Cercocebus atys*), SIVsm (Chen et al., 1996). HIV-1 is further classified into four groups, which include M, N, O and P. However the majority of viruses fall into the Main (M) group, which is divided into nine genomic clades (A-D, F-H, J, and K), five sub-subtypes (A1-3 and F1-2) and more than 40 circulating recombinant forms (http://www.hiv.lanl.gov). Subtype C viruses account for 50% of all HIV-1 infections worldwide and is ubiquitous in Southern Africa (Hemelaar et al., 2006; Van

Harmelen et al., 1999). The Outlier (O) and Non-M/non-O (N) HIV-1 group viruses are usually found within central Africa and infect a minority of patients (Hemelaar et al., 2006). The newly discovered group P virus is most closely related to SIV in Gorillas (SIVgor) and has been identified in one Cameroonian patient (Plantier et al., 2009).

1.1.2 Structure of HIV

The mature HI virion is icosahedral in shape and ~120 nm in diameter (Gentile et al., 1994; Nermut et al., 1993). The virus is enveloped by a lipid bilayer which is punctuated with glycoprotein (gp) spikes. Protruding from the membrane are gp120 trimers which are non-covalently linked to transmembrane gp41 trimers (Allan et al., 1985; Chan et al., 1997; Kwong et al., 1998; Veronese et al., 1985). The lipid bilayer encloses an elongated conical protein core which holds two strands of positive sense ssRNA and the reverse transcriptase (RT), integrase and protease enzymes (Gelderblom et al., 1987; Knipe et al., 2007) (Figure 1.1). The genome is ~9700 nucleotides in length and codes for nine genes which generate 15 proteins (Figure 1.2). The three largest structural genes include *gag*, *pol* and *env*. The six smaller accessory genes include *vif*, *vpr*, *tat*, *rev*, *vpu* and *nef*. The long terminal repeats (LTR) contain the regulatory elements and flank the rest of the genome (Kuiken et al., 2009).

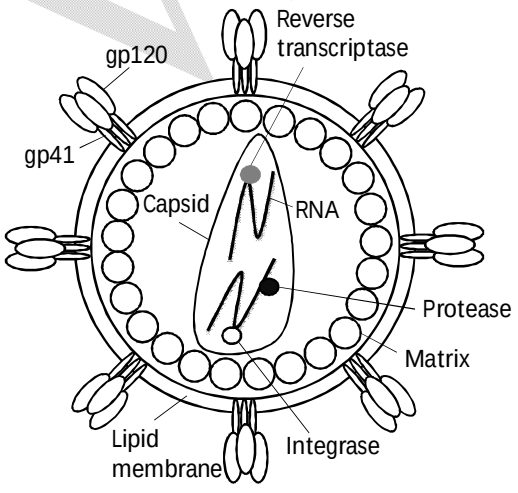

Figure 1.1. Diagrammatic representation of the HIV-1 structure. HIV-1 is 120 nm in diameter and approximately spherical in shape. Glycoprotein spikes protrude from the host-cell derived lipid membrane. The conical protein capsid contains RNA, reverse transcriptase, integrase and protease enzymes. Figure adapted from Knipe et al., 2007.

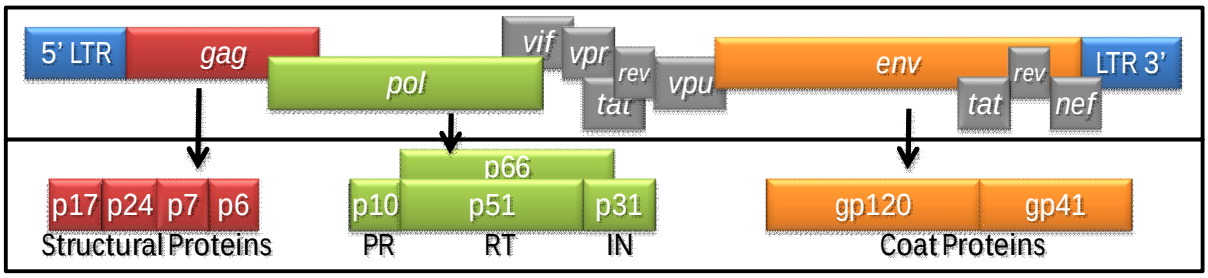

Figure 1.2. Schematic representation of the HIV-1 genome. *Gag* (red) provides structural proteins for the virus. *Pol* (green) provides enzymes involved in reproduction and infection; including the protease, reverse transcriptase and integrase enzymes. *Env* (orange) provides the membrane proteins that allow for viral attachment and fusion to target cells. The regulatory and accessory proteins (grey) play a role in viral transcription and have important virulence factors. The Long Terminal Repeats (LTR, blue) flank the viral genome and are involved in transcription (Knipe et al., 2007). Figure adapted from Kuiken et al., 2009.

The *Gag* gene encodes the matrix (p17 subunit), capsid (p24 subunit), nucleocapsid (p7 subunit) and p6 structural proteins. *Pol* encodes the enzymatic proteins protease (p10 subunit), reverse transcriptase (p51 and p66 subunits) and integrase (p31 subunit). A -1 frame shift allows the Gag-Pol polyprotein to be translated (Kuiken et al., 2009). The Gag and Gag-Pol proteins undergo 12 proteolytic reactions by protease to generate the different structural and enzymatic proteins (Knipe et al., 2007; Oliveira et al., 2003). *Env* encodes the external non-covalently linked trimeric glycoproteins, gp120 and gp41. The accessory proteins are Tat (p16 and p14 subunits), Rev (p19 subunit), Vif (p23 subunit), Vpr (p10-p15 subunits), Vpu (p16 subunit) and Nef (p25-p27 subunits) (Knipe et al., 2007; Kuiken et al., 2009). Each virion consists of ~2000 Gag proteins, ~200 Gag-Pol proteins, two strands of RNA and ~300 Vpr molecules (Muller et al., 2000; Wilk et al., 2001)

Reverse transcriptase is an asymmetric heterodimeric enzyme, consisting of the 66 kD (p66) and 51 kD (p51) subunits (Figure 1.3) (Huang et al., 2008). The p51 subunit consists of the first 440 amino acids of *pol*, while p66 consists of all 560 amino acids of *pol*. The subunits share similar

subdomains but the catalytic sites are located in p66 while p51 plays a structural role (Sarafianos et al., 2009).

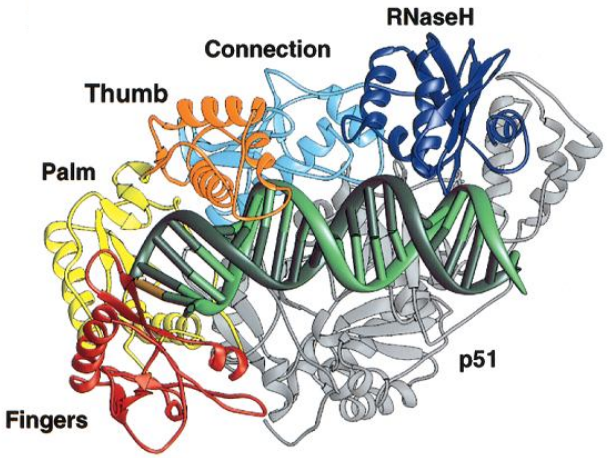

Figure 1.3. Structure of the HIV-1 RNA dependent DNA polymerase. The HIV-1 reverse transcriptase is composed of the p51 and p66 subunits. The p66 subunit consists of the fingers (red), palm (yellow), thumb (orange), connection domains (light blue) and RNase H (dark blue). The p51 subunit is indicated in gray, the DNA template as dark green, and the primer in light green. Diagram adapted from Huang et al., 1998.

1.1.3 HIV Life Cycle

HIV-1 infects cells that express the CD4 receptor including CD4+ T- lymphocytes, macrophages and dendritic cells. The gp120 undergoes structural changes when bound to CD4, which allows the virus to attach to the CCR5 or CXCR4 co-receptors. Once the virus is attached to the target cell the fusion peptide region of gp41 penetrates the cell (Wyatt and Sodroski, 1998). Following lipid membrane fusion, the virus undergoes uncoating, allowing viral particles to enter the cytoplasm of the target cell (Lehmann-Che and Saïb, 2004). Reverse transcriptase (RT) is the virus encoded RNA dependent DNA polymerase and transcribes RNA into DNA. The enzyme also has RNase H function which is required for degradation of the viral RNA allowing for cDNA formation (Sarafianos et al., 2009). A pre-integration complex forms consisting of viral

cDNA, integrase, protease, Vpr and reverse transcriptase. The pre-integration complex moves into the nucleus and integrase mediates the integration of the viral DNA into a transcriptionally active region of the host genome (Lehmann-Che and Saïb, 2004).

Parallel host cell and proviral activation occurs due to gene activation by host transcriptional regulators which bind to the LTR (Kuiken et al., 2009). Short viral transcripts are produced during basal transcription, which form hairpin stem-loops to which Tat binds. Together this structure recruits other factors that allow for the production of full length HIV-1 transcripts (Kuiken et al., 2009; Zheng et al., 2005). The full length transcripts are spliced into 2 kb or 4.4 kb fragments. The former can exit the nucleus easily while the latter require Rev and the Rev response element (RRE) to exit (Zheng et al., 2005). The shorter fragments are translated in the cytoplasm and Tat, Rev and Nef are produced. Rev binds the RRE and shuttles the larger transcripts into the cytoplasm (Pollard and Malim, 1998). During virion assembly the RNA strands and Gag polyproteins assemble at the host cell membrane. p6 causes membrane budding during which, and/or after, protease cleaves gag leading to virion maturation (Bieniasz, 2009; Klein et al., 2007).

1.1.4 Disease Progression

HIV transmission occurs via sexual exposure to an infected partner, exposure to infected blood or blood products or exposure *in utero*, *intrapartum* or via breast feeding (Centers for Disease Control and Prevention, 2005). HIV infection commonly occurs across mucosal surfaces and at these points of entry, dendritic cells interact with the virus and facilitate the infection of CD4+ T-lymphocytes (Geijtenbeek and van Kooyk, 2003). The viral load is high following infection but

decreases as cytotoxic T-lymphocytes control the virus, which establishes a viral set-point (Musey et al., 1997). As the disease progresses the virus continues to targets CD4+ T-lymphocytes and so as the viral load increases the CD4+ T-lymphocytes count decreases. Consequently the CD4+ T-lymphocyte count and viral load are strongly correlated with the development of AIDS (Goedert et al., 1987; Mellors et al., 1995b; Phillips et al., 1991).

The World Health Organization proposes four stages of HIV/AIDS immunodeficiency and the median time from the initial stage, HIV infection, to AIDS is 9.8 years in adults (Osmond, 1989). Patients in the final stage, AIDS, are characterized by a CD4+ T-lymphocyte count of < 200 cells/mm^3 and severe HIV-associated infections (World Health Organization (WHO), 2007).

1.2 Antiretroviral Drug Therapy

Antiretroviral (ARV) therapy suppresses viral replication allowing for the partial reconstitution of the immune system and slowing the progression to AIDS (Connick et al., 2000; Tochikura et al., 1989). However as HIV is integrated into the cellular material of the host immune cells, patients must remain on ARV therapy indefinitely (Weller and Williams, 2001).

By 2007 over two million HIV infected patients in Sub-Saharan Africa were receiving ARV therapy (WHO/UNAIDS, 2008). The ARV drugs in the following Table have been approved by the US Food and Drug Administration (Johnson et al., 2009).

Table 1.1. ARV drugs available in the USA.

Nucleoside reverse transcriptase inhibitors (NRTIs)
Abacavir (ABC)
Didanosine (ddI)
Emtricitabine (FTC)
Lamivudine (3TC)
Stavudine (d4T)
Tenofovir (TDF)
Zidovudine (ZDV/AZT)
Non-nucleoside reverse transcriptase inhibitors (NNRTIs)
Efavirenz (EFV)
Etravirine (ETR)
Nevirapine (NVP)
Protease inhibitors (PIs)
Atazanavir/Ritonavir (ATZ/r)
Darunavir/r (DRV/r)
Fosamprenavir/r (FPV/r)
Indinavir/r (IDV/r)
Lopinavir/r (LPV/r)
Nelfinavir/r (NFV/r)
Saquinavir/r (SQV/r)
Tipranavir/r (TPV/r)
Entry inhibitor
Enfuvirtide (ENF)
CCR5 inhibitor
Maraviroc (MVC)
Integrase inhibitor
Raltegravir (RAL)

Table adapted from Johnson et al., 2009.

Each ARV drug class interferes with a different stage in the viral life-cycle. Highly active ARV therapy (HAART) takes advantage of this, as it consists of at least three drugs in at least two of the drug classes (Clavel and Hance, 2004). The South African Department of Health treatment guidelines for HIV infected adults and adolescents has recommended a first-line combination of the NRTI drugs d4T and 3TC in combination with the NNRTI drugs EFV or NVP. Second-line therapy includes the same NRTI drugs in combination with the Ritonavir boosted protease inhibitor Lopinavir (LPV/r or Kaletra (KAL) or Alluvia) (National Department of Health South Africa, 2004). Recently, the first-line regimen has been changed to include TDF and 3TC or FTC (National Department of Health South Africa 2010, 2010).

1.2.1 Mode of Action

The NRTI drugs are base analogues that are structurally similar to natural nucleosides but lack the 3' hydroxide group. These bases are phosphorylated by host cell kinases and compete with the normal dNTPs for incorporation into the transcribed cDNA. As the base analogue lacks the 3' hydroxide group the next base cannot form the 5'-3' phosphodiester bond and DNA synthesis is terminated (Menendez-Arias, 2008).

The NNRTIs are a structurally diverse set of small (< 600 Da) hydrophobic compounds. Unlike the NRTIs, the NNRTIs do not require host mediated metabolism to function. The NNRTIs prevent RT activity by repositioning the catalytic aspartate residues which are located in RT on a β-sheet in p66. The repositioning prevents the enzyme from undergoing conformational changes, thereby locking the enzyme in an inactive state (De Clercq, 1998).

PIs bind to and prevent protease from cleaving the viral Gag and Gag-Pol polyproteins, thereby preventing viral maturation. The inhibitors have been synthesized to resemble the phenylalanine-proline residues in Gag and Gag-Pol that are cleaved by protease. A hydroxyethylene bond instead of the normal peptidic linkage is located at the site at which the protease attempts to cleave the drug which prevents cleavage (De Clercq, 2001).

The entry inhibitor, Enfuvirtide, binds to gp41 and prevents the protein from undergoing conformational changes required for fusion (Lalezari et al., 2009). The integrase inhibitor, Raltegravir, binds to the catalytic domain of integrase, preventing the insertion of the viral cDNA

into the host genome (Sichtig et al., 2009). The CCR5 inhibitor, Maraviroc, binds to and blocks the CCR5 co-receptors on immune cells from viral attachment (Shafer and Schapiro, 2008).

1.3 Drug Resistance

ARV drug therapy dramatically reduces viral replication and as a consequence of the wide-spread use of HAART (≥ 3 drugs from ≥ 2 classes) the AIDS related mortality and morbidity has decreased (Joint United Nations Programme on HIV/AIDS, 2008). However the development of drug resistance mutations or infection with a resistant virus can lead to treatment failure (Erice et al., 1993; Kozal et al., 1993; Larder et al., 1989). Drug resistance mutations can develop in response to treatment with each available ARV drug (Johnson et al., 2009). In the settings of wild-type, drug susceptible virus, prevention of drug resistance evolution, and by extension, success of ARV drug therapy are dependent upon long-term adherence. Depending on the drug regimen, adherence of > 60–95% is required to achieve virologic suppression and prevent drug resistance development (Gardner et al., 2009).

Inadequate drug exposure can lead to the expansion of drug resistant quasi-species. These sub-populations can quickly out-compete the wild-type virus leading to treatment failure (Gardner et al., 2009). The HIV-1 population within an individual is genetically heterogeneous as a result of three factors. (i) HIV-1 exhibits a high turnover rate as 10^{10} virions/day can be produced (Perelson et al., 1996; Piatak Jr et al., 1993). (ii) RT has a high copy error rate, due to the lack of proofreading (Roberts et al., 1988); substitutions, additions and deletions are introduced with a rate of up to 5 errors/round of replication (Preston et al., 1988). (iii) Recombination can occur if an individual is infected with two different HIV strains (Burke, 1997; Zhuang et al., 2002).

These factors lead to the evolution of highly diverse subpopulations of quasi-species in an infected patient. If any of the random mutations that develop provide a selective advantage in the presence of ARV drugs, then that mutant quasi-species will out-compete the less fit viruses (Simon et al., 2006).

However drug resistance does not always develop *in vivo* in response to sup-optimal ARV drug therapy. While relatively uncommon, transmission of drug resistant HIV does occur and is a growing concern world-wide (Bennett et al., 2008; Erice et al., 1993). In addition natural polymorphisms carried by HIV-2 result in resistance to most NNRTIs (Witvrouw et al., 1999). Similarly, the various HIV-1 subtypes do not respond equally to each ARV drug due to natural polymorphisms (Palmer et al., 1998). In contrast to treatment failure due to drug resistance, drug toxicity often limits the success of therapy and is dependent upon host genetics (Tozzi, 2010).

1.3.1 Mutation Classification

HIV mutations are classified as either primary/major, secondary/minor or compensatory mutations. When present alone the primary mutations are capable of inducing high levels of drug resistance. Secondary mutations are less potent as their presence alone only marginally reduces drug susceptibility. Consequently these mutations are almost exclusively found with other primary/major mutations. Mutations can result in decreased viral fitness, which is compensated for by the development of compensatory mutations, which restore viral fitness (Shafer, 2002).

The genetic barrier of a drug or class of drugs is a measure of the ease with which resistance develops during treatment. One or two single nucleotide polymorphisms (SNPs) lead to high

level resistance to drugs with a low genetic barrier, while a number of SNPs are required for resistance to develop to drugs with a high genetic barrier. Generally the RT inhibitors have a low genetic barrier, while PIs have a high genetic barrier (Luber, 2005).

1.3.2 Major NRTI Mutations

NRTIs resemble natural nucleosides and are incorporated into growing DNA strands. The incorporation of the NRTI prevents continued elongation as the modified bases lacks 3' hydroxide groups (Menendez-Arias, 2008). Two types of NRTI mutations exist; those that result in (i) enhanced discrimination against the base analogue and the (ii) removal of the chain terminating element. Enhanced discrimination retards the incorporation of 3TC, ABC, ddI, FTC and TDF and so viral replication continues (Shafer and Schapiro, 2008). The thymidine analogue drugs (ZDV and d4T) select for the second type of mutation, and are termed thymidine analogue mutations (TAMs) (Clavel and Hance, 2004). The mutant RT has an altered conformation near to the growing DNA chain which allows for ATP binding. ATP bound in this position cleaves the phosphodiester bond between the terminated DNA chain and the base analogue, leading to continued elongation (Boyer et al., 2001). Mutations identified in *p66/p51* of *pol* that induce resistance to the NRTI class of drugs are listed in the following Table.

Table 1.2. Selected HIV-1 NRTI drug resistance mutations.

Codon	Wild-type sequence	Mutant sequence	Amino acid change
M41L	ATG	C/TTG	Methionine (M) → Leucine (L)
K65R	AAA/G	AGG	Lysine (K) → Arginine (R)
D67N	GAC/T	AAC/T	Aspartate (D) → Arginine(R)
K70R	AAA/G	AGG	Lysine (K) → Arginine (R)
Q151M	CAA/G	ATG	Glutamine (E) → Methionine (M)
M184V	ATG	GTG	Methionine (M) → Valine (V)
T215F	ACC	TTC	Threonine (T) → Phenylalanine (F)
T215Y	ACC	TAC	Threonine (T) → Tyrosine (Y)

Table adapted from Clark et al., 2007.

1.3.2.1 M184V

A common NRTI mutation is the change from methionine (M) to valine (V) at codon 184 (M184V) of HIV-1 RT. The mutation occurs as a result of a SNP at this position (ATG → GTG), replacing methionine at the center of the RT catalytic site. The valine blocks the binding of the NRTIs due to steric hindrance. When 3TC is used in mono-therapy, M184V develops within weeks, resulting in high level resistance (Clavel and Hance, 2004). M184V also results in low level resistance to ddI and ABC, but increased susceptibility to ZDV, d4T and TDF (Shafer and Schapiro, 2008). Viruses harbouring M184V have decreased RT processivity and so are significantly less fit than the wild-type virus (Martinez-Picado and Martinez, 2008).

1.3.2.2 Q151M

Codon 151 is situated within a highly conserved region of the finger sub-domain of the polymerase (Iversen et al., 1996). There is a high genetic barrier for the glutamine (G) to methionine (M) mutation to develop as two bases changes are required (CAG → ATG). Additionally, the intermediate viruses are substantially less fit than the wild-type virus (Kosalaraksa et al., 1999). Consequently, the emergence of Q151M is rare, occurring in ~5% of NRTI resistant patients (Clavel and Hance, 2004). The Q151M mutation results in high level resistance to ZDV, d4T, ddI and ABC (Shafer and Schapiro, 2008).

1.3.2.3 K65R

A lysine (K) to arginine (R) change at codon 65 confers resistance to many NRTIs and is selected for by TDF, ABC, ddI, 3TC, FTC and d4T (Xu et al., 2009). The M184V and K65R double mutation is strongly deleterious as K65R also decreases polymerase processivity. A62V

and S68G are compensatory mutations that rescue the unfit viruses harbouring K65R (Martinez-Picado and Martinez, 2008).

1.3.2.4 Thymidine Analogue Mutations (TAMs)

The level of resistance to ZDV, d4T and the other NRTIs is proportional to the number of TAMs present. The resistance mutations fall into two categories, type I and type II TAMS. The type I pattern includes M41L, L210W and T215Y and type II, D67N, K70R, T215F and K219Q/E (Shafer and Schapiro, 2008). K70R and T215Y/F confer moderate resistance to ZDV and d4T (Garcia-Lerma, 2005). The presence of D67N, K70R and T215Y or M41L/T215Y double mutations, are required for high level resistance (Menendez-Arias, 2008). M41L, D67N, L210W and K219Q/E are secondary mutations and only confer resistance when associated with K70R and T215Y/F (Garcia-Lerma, 2005). There is partial re-sensitization of TAM mutants to the NRTIs when K65R, L74V or M184V are present as these mutations prevent the binding of ATP stopping the removal of the blocked base (Goldschmidt and Marquet, 2004).

1.3.3 Minor NRTI Mutations

The majority (95%) of the minor mutations occur in the presence of major mutations. These include, K20R, T39A, K43E/Q/N, E44D/A, T69N/S/I/G/insertion, V75M/A, V118I, G196E, K122E, E203K/D and H208Y (Delaugerre et al., 2001; Gonzales et al., 2003; Mellors et al., 1995a; Saracino et al., 2006; Shafer and Schapiro, 2008; Svicher et al., 2006).

1.3.4 Major NNRTI Mutations

NNRTIs are small compounds that specifically inhibit HIV-1 RT. Currently 30 structurally different classes of NNRTIs have been established. Resistance to these compounds occurs when a NNRTI no longer binds to its target site on RT and so are no longer active against the virus (Martins et al., 2008). Mutations identified in *p66/p51* that confer resistance to the NNRTI class of drugs are listed in the following Table.

Table 1.3. Selected HIV-1 NNRTI drug resistance mutations.

Codon	Wild-type sequence	Mutant sequence	Amino acid change
K103N	AAA/G	AAC/T	Lysine (K)→ Asparagine (N)
V106M	GTA/G	ATG	Valine (V)→ Methionine (M)
Y181C	TAT	TGT	Tyrosine (Y) → Cysteine (C)
G190A	GGG/A/C/T	GCA	Glycine (G) → Alanine (A)
P225H	CCC/T	CAC	Proline (P) → Histidine (H)

Table adapted from Clark et al., 2007.

1.3.4.1 K103N

The lysine (K) to asparagine (N) or serine (S) change at amino acid 103 of HIV-1 RT results in high level resistance to NVP and EFV. A hydrogen bond forms between 103N and 188Y which stabilizes the NNRTI binding pocket drastically reducing NNRTI binding and conferring broad drug resistance (Harrigan et al., 2005; Ren and Stammers, 2008). This mutation carries only a small fitness cost as RNase H activity is marginally slowed, thus K103N can persist at low levels for years in the absence of drugs (Martinez-Picado and Martinez, 2008).

1.3.4.2 Y181C

The tyrosine (Y) to cysteine (C) change at position 181 results in the loss of an aromatic ring interaction between the amino acid residue and ARV drug. As there are more extensive aromatic

interactions between the enzyme and NVP than with EFV, Y181C is associated with strong NVP and moderate EFV resistance (Ren and Stammers, 2008).

1.3.4.3 V106M

Methionine (M) instead of valine (V) at codon 106 decreases the side-chain length thereby weakening the drug contact with RT (Martins et al., 2008). The GTA sequence is usually present at codon 106 in subtype B viruses, with GTG in subtype C viruses. The ATG mutation (V106M) is then more likely to arise in the subtype C GTG background, due to a lower genetic barrier. V106M is selected for by EFV, but results in broad NNRTI resistance (Brenner et al., 2003; Loemba et al., 2002). The virus is only moderately unfit, probably due to slightly slower RNAse H activity (Martinez-Picado and Martinez, 2008).

1.3.4.4 G190A

The glycine (G) to alanine (A) change at codon 190 is selected for by NVP and increases the size of the side-chain at this site. The increased bulk prevents optimal binding of NNRTIs with the hydrophobic binding pocket (Ren and Stammers, 2008). G190A, unlike G190E does not confer severe fitness costs (Boyer et al., 1998). G190C/T/V are rare and confer high level resistance the NNRTIs (Shafer and Schapiro, 2008).

1.3.5 Minor NNRTI Mutations

The minor NNRTI mutations include, A98G, K101P/Q, V108I, I135T/M, V179D/I/E P225H, L283I (De Clercq, 2004; Parkin et al., 2006; Shafer and Schapiro, 2008).

1.3.6 Mutations in Other Drug Classes

In total, more than 80 mutations at more than 40 sites confer resistance to one or more of the PIs. Similar to NNRTI mutations, the PI mutations lead to a decreased affinity of the protease inhibitor to the target site (Ohtaka and Freire, 2005). I47V/A and V82A/F/T/S confer high level PI resistance (Johnson et al., 2009).

The integrase inhibitor, Raltegravir, looses activity when one of the major integrase inhibitor mutations (Q148H/K/R, N155H and Y143R/H/C) is present with one or more minor mutations (L74M, E138A/K and G140S). The most common combination seen in patients failing Raltegravir therapy is Q148H and G140S (Johnson et al., 2009). The mutations alter the integrase inhibitor binding site, decreasing the affinity of the drug for the enzyme (Shafer and Schapiro, 2008).

The CCR5 inhibitor, Maraviroc, binds to CCR5 complexes on host cells, preventing HIV from attaching to these co-receptors. However, resistant viruses are capable of binding to these altered sites on target cells. There is also increased binding to drug-free CCR5 and expansion of pre-existing CXCR4 dependent viruses; which do not require CCR5 co-receptors for binding (Latinovic et al., 2009).

The fusion inhibitor, Enfuvirtide, binds to amino acids 36–45 of gp41. Multiple mutations in this region result in strong Enfuvirtide resistance, but also decrease viral fitness (Greenberg and Cammack, 2004). The N126K, N137K and S138A are compensatory mutations often present in Enfuvirtide resistant viruses (Shafer and Schapiro, 2008).

1.3.7 Prevalence of Mutations

While there are many mutations that confer drug resistance only a minority are found in > 10% patients failing ARV drug therapy. These prevalent mutations in *p66/p51* include M41L, D67N, K70R, L90M, K103N, Y181C, M184V, T215Y and L210W (Cheung et al., 2004; Rhee et al., 2004).

1.4 Resistance Detection

Resistance testing is performed to ascertain to which drugs a particular HI virus is susceptible or resistant. Standardized regimens are highly successful in suppressing viral replication but some patients who have experienced virologic failure respond better to individualized HAART regimens. The personalized regimens are formulated in part from the information generated from resistance testing (Baxter et al., 2000; Durant et al., 1999; Torre and Tambini, 2002; Tural et al., 2002).

1.4.1 Phenotypic Assays

Phenotypic assays test the sensitivity of patient derived virus under ARV drug pressure *ex vivo*. HIV is isolated from patient plasma or peripheral blood mononuclear cells and used to infect HIV free cells. The infected cells are then cultured in increasing concentrations of ARV drugs and the growth is monitored by measuring p24 levels (Alcorn and Faruki, 2000; Baldanti et al., 2004). The IC_{50} from patient derived virus is compared to that of a wild-type control (Alcorn and Faruki, 2000). A 3-10 fold increase in the IC_{50} is associated with intermediate resistance, while > 10 fold increase is considered high level resistance. Alternatively, single-cycle assays can be used, wherein the patient derived RT/PR is cloned into a HIV vector and cultured in cells. Such

assays are more reproducible and have a higher through-put than traditional phenotypic assays (Hanna and D'Aquila, 2001). While phenotypic assays are a direct measure of viral fitness, high cost and long assay time limit the utility of phenotypic testing (Baldanti et al., 2004).

1.4.2 Genotypic Assays

In contrast to phenotypic assays, genotypic assays are used to infer HIV-1 drug resistance from sequence data, rather than directly detecting resistance. While there are numerous genotyping assays available, only a subset are used for HIV-1 drug resistance detection. Genotyping assays involve virus isolation and reverse transcription-PCR (RT-PCR) of the viral RNA. Normally RT and PR are then amplified during a PCR step. Additional regions of the genome, corresponding to other mutational hotspots can be amplified for investigation (Hanna and D'Aquila, 2001).

1.4.2.1 Hybridization Assays

The fragmentation of the HIV genome and its subsequent association with probes is used to determine the viral genotype in hybridization assays. Biotinylated or fluorescently labeled viral nucleic acid is exposed to tens or thousands of labeled/unlabelled probes bound to a surface. The surface is scanned and the levels of reporter signal are used to determine the genotype at mutation codons of interest. Hybrization assays are reusable and show high concordance with sequencing results. However, these assays are subtype specific and cannot reliably genotype insertions and deletions (Stuyver et al., 1997; Vahey et al., 1999; Wallis et al., 2005; Wilson et al., 2000).

1.4.2.2 Dideoxynucleotide Sequencing

The Sanger method is the most widely used sequencing technique and is based on chain-termination. Labeled dideoxyribonucleotide triphosphates (ddNTPs) are added in combination with regular nucleotides to a PCR. During cycling, the ddNTPs cause chain termination as they lack a 3' hydroxyl group. Eventually fragments of all possible lengths are produced, which are separated according to size by polyacrylamide gel electrophoresis. The base pair sequence is then elucidated, as the labeled ddNTPs fluoresce at different wavelengths (Pettersson et al., 2009). While population sequencing is the gold standard for HIV genotyping it is expensive, labour intensive and insensitive (> 20% of mixed species) (Eshleman et al., 2004; Grant et al., 2003; Hanna and D'Aquila, 2001; Vossen et al., 2009a).

Pyrosequencing technology is based on sequencing-by-synthesis. Upon nucleotide incorporation, a pyrophosphate is released which is converted to ATP. The reaction is setup such that this leads to photon emission, which is proportional to the number of dNTPs added to a growing DNA chain (Ahmadian et al., 2006). Pyrosequencing has a high analytical sensitivity as it detects ~1% of mixed species. While this methodology is useful for indentifying important minority populations it is expensive and labour intensive (Ahmadian et al., 2006; Bushmana et al., 2008).

1.4.2.3 Competitive PCR Assays (Real-time PCR)

Real-time PCR allows for hybridization-based allele-discrimination during PCR (Landegren et al., 1998). Real-time PCR differs from traditional PCR due to the inclusion of a fluorescent reporter. The signal produced by the fluorescent reporter, a dye or probe, reflects the amount of PCR product produced in real-time (Kubista et al., 2006).

Allele-specific real-time PCR (AS-PCR), usually an application of real-time PCR, is used for genotyping specific loci (Larder et al., 1991). Primers are designed to match both the wild-type and mutant viral sequences. The PCR is monitored in real-time and the crossing point is used to determine the relative quantities of each measured genotype (Palmer et al., 2006; Toni et al., 2009). While these assays are fast, cheap and sensitive (~ 1%), they are subtype specific and only one mutation at a time can be interrogated (Paredes et al., 2007).

1.4.2.4 Fluorescently Labeled Probes and Real-time PCR

Taqman assays are usually used for HIV quantitation, but can be adapted for mutation identification (Mohey et al., 2005). In Taqman assays, a real-time PCR is setup with a probe that consists of a donor and acceptor dye pair. When the acceptor and donor are in close proximity to one another, the fluorescence produced by the donor is quenched by the acceptor. Cleavage of the probe by Taq polymerase allows the donor dye to fluoresce which is correlated with a particular genotype (Holland et al., 1991; Kubista et al., 2006).

1.4.2.5 DNA Melting Analysis (DMA)

PCR product differentiation by DNA melting analysis (DMA) is dependent upon differences in the melting temperature (T_m) of double stranded (ds) nucleic acids. The T_m of DNA is the temperature at which 50% of dsDNA denatures to single stranded DNA (ssDNA). The T_m is affected by the length of the dsDNA, base composition and the extent of base complementarity. Amplicons with the same base composition and length will have the same T_m; a deviation from this, including a SNP, will alter the T_m. This alteration in T_m is used for genotyping by DMA (Lay and Wittwer, 1997; Reed et al., 2003; Ririe et al., 1997).

An intercalating dye is added to a DMA assay to track product formation during PCR and for melting curve analysis following the PCR. At the end of the temperature cycling, the PCR products are slowly heated. At low temperatures, below the T_m of the nucleic acid, the dye is bound to the dsDNA and fluorescence is at a maximum. As the temperature increases, the fluorescence slowly decreases due to greater internal rotation of the bound dye. When the T_m of the nucleic acid is reached, the DNA melts and the dye dissociates from the ssDNA leading to a dramatic drop in the fluorescence (Figure 1.4). The fluorescence differences, which are T_m dependent, are used to construct melting curves, from which sequence variation can be detected (Kubista et al., 2006).

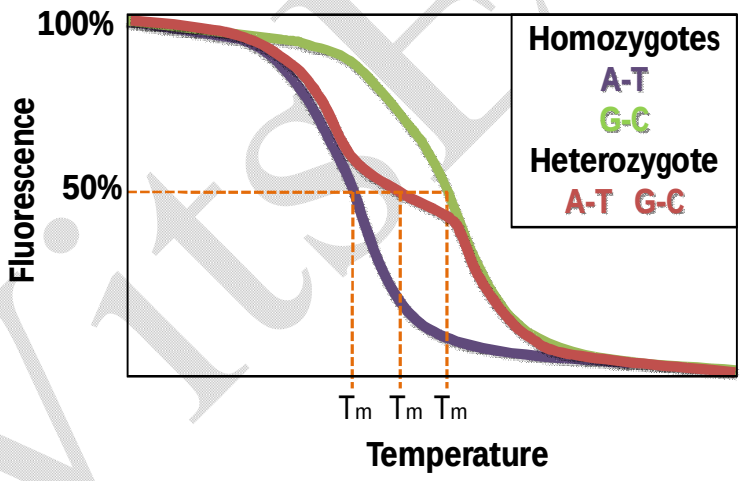

Figure 1.4. Melting curve analysis. Two amplicons that differ by an A (purple) to G (green) transition will have a slightly different T_m, and so the melting curves will be parallel but shifted along the temperature axis. However a heterozygous mixture of these two genotypes produces an altered melting curve shape. Thus homozygous difference are distinguished by T_m differences, while heterozygous genotypes by shape differences (Herrmann et al., 2006a).

DMA is limited to the differentiation of amplicons with major sequence and length differences (Ririe et al., 1997). SNP differentiation is possible if high levels of SYBR Green I or other

fluorescent dyes are added post-PCR. This two-step process is required as high concentrations of certain intercalating dyes, which are required for SNP analysis, inhibit PCR (Lipsky et al., 2001).

DMA allows for mutation scanning along the entire length of the amplicon. The addition of a fluorescein-labeled primer and/or probes allows for the interrogation of a limited region of the amplicon (Gundry et al., 2003; Millward et al., 2002; Wittwer et al., 2001).

1.4.2.6 High Resolution Melting Analysis (HRMA)

HRMA is a variation of DMA that allows for closed-tube, one-step differentiation of PCR products, by SNPs, with specialized dyes and melting instruments with increases melting resolution (Wittwer et al., 2003). Melting resolution depends on a number of factors which vary across melting instruments: (i) tight temperature control, decreasing inter-sample variation both spatially and temporally; (ii) smooth melt gradients (0.1°C/s) and (iii) sensitive temperature and fluorescence detection (Herrmann et al., 2006a; Herrmann et al., 2006b). A new generation of specialized melting instruments can collect up to 100 data points/°C, which allows for small fluorescence changes to be monitored, permitting more accurate genotyping than with DMA (Zhou et al., 2005). HRMA dyes allow for a one-step SNP differentiation procedure as the dyes do not inhibit PCR and do not undergo dye redistribution during melting analysis (Figure 1.5) (Liew et al., 2004; Wittwer et al., 2003). The limit of detection of HRMA assays is ~ 3% of mixed species (Krypuy et al., 2006; Simi et al., 2008; Wojdacz and Dobrovic, 2007).

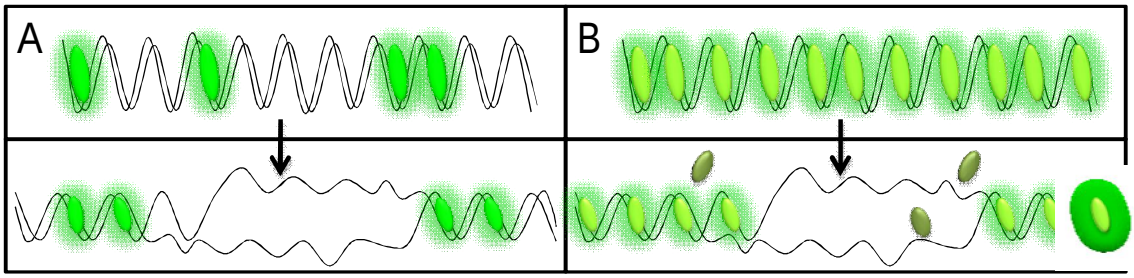

Figure 1.5. Dye redistribution. (**A**) SYBR Green I redistributes to dsDNA during melting. (**B**) The new HRMA dyes can be added in saturating concentrations and therefore not prone to redistribution. This allows for more precise fluorescence monitoring (Gundry et al., 2003; Wittwer et al., 2003). Diagram adapted from Corbett Research, 2006.

1.4.2.6.1 HRMA Incorporating Unlabeled Oligonucleotide Probes

DMA and HRMA indicate base changes within the entire amplicon which is useful for mutation discovery (mutation scanning). However the addition of unlabelled, 3' blocked oligonucleotide probes can signal the presence or absence of a particular genotype (Zhou et al., 2004). In this procedure, two melting peaks are generated, one due to the melting transition of the probe-amplicon duplexes and the other the amplicon-amplicon duplexes. The presence of a SNP prevents the binding of non-corresponding short probes and no melting peak is generated (Figure 1.6) (Zhou et al., 2004). Negative first derivative plots (-dF/dT) are constructed to visualize the genotype differences and are derived from melting curves (example in Figure 1.4).

The amplicon-amplicon duplexes melt with a larger fluorescence transition than the shorter probe duplexes. This signal can overwhelm the smaller probe signal thereby preventing allele detection. To bypass this, asymmetric PCRs are setup to overproduce the strand to which the probe binds; thereby increasing the probe and decreasing the amplicon signal (Montgomery et al., 2007a; Montgomery et al., 2007b; Zhou et al., 2004; Zhou et al., 2005). The probes are blocked at the 3' end to prevent polymerase mediated extension during PCR by 3' phosphorylation, 2',3' di- and deoxynucleotide, 3'-3'linkage or 3'-spacer C3 (Zhou et al., 2004).

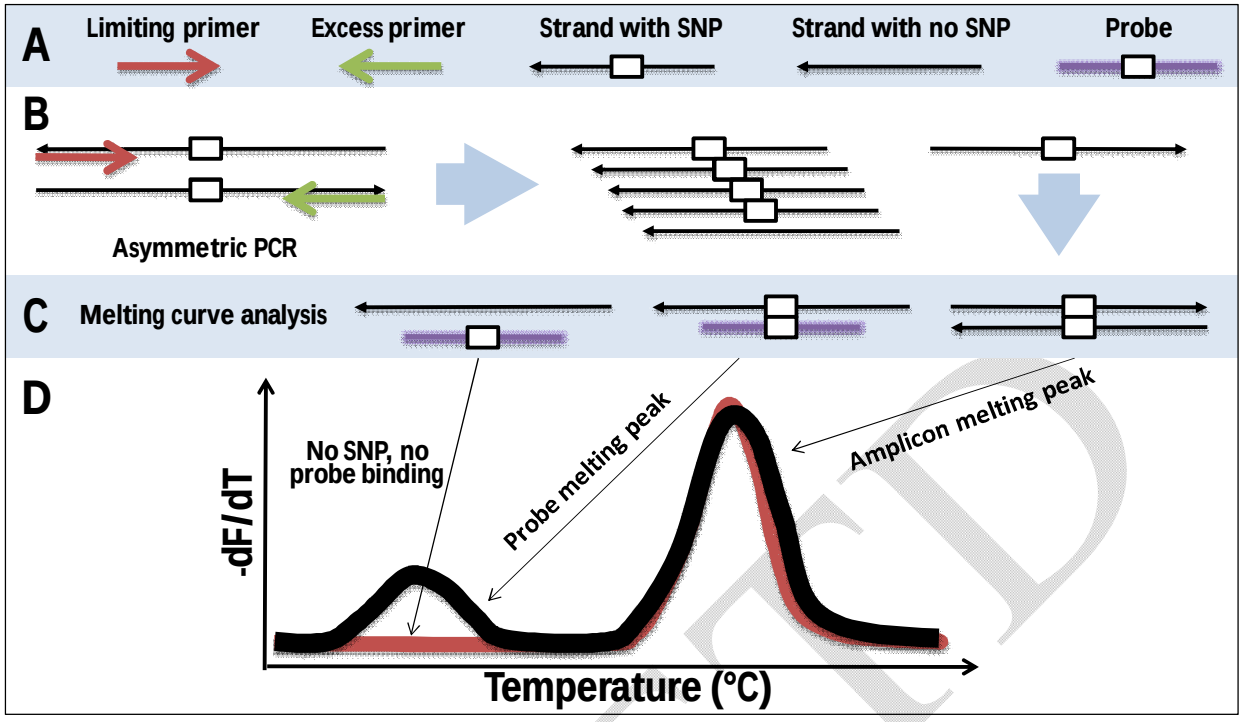

Figure 1.6. HRMA with unlabelled probes. (**A**) Key to diagram. (**B**) For HRMA with probe analysis, an asymmetric PCR is setup, with the excess primer (green) over producing the strand to which the probe (purple) binds. Not each amplicon (black) contains a SNP (box). (**C**) At the end of the PCR, the products are cooled, allowing the formation of duplexes. Short probes do not bind if a mismatch is present between the probe and amplicon. (**D**) Fluorescence is monitored during a temperature increase. Amplicon-amplicon duplexes melt at a higher temperature than the probe-amplicon duplexes. If a probe binds to an amplicon, a probe peak is generated (black curve). If a probe is mismatched to an amplicon no curve is generated (red line) (Erali et al., 2008).

Optimal probe length varies from 10 to 30 bp, with a G+C content of ~30%. The peak corresponding to the melting of the probe increases in height (i.e. intensity) with increasing probe length. Typically, larger probes (> 25 bp) provide the strongest signal with large amplicons (> 100 bp). Peak height also depends on the concentration of the probe and amount of competing DNA (Zhou et al., 2004; Zhou et al., 2005). The probe is subject to more destabilization when the mismatch is in the center, rather than at the extremities (Erali et al., 2008).

Melting analysis is altered when the region to which the probe anneals contains polymorphisms. To overcome this problem, a number of modifications can be introduced into the probe.

- Incorporation of a *mismatch* at a site that interacts with a polymorphic base can bypass the affects of the polymorphism. As a consequence of the mismatch, the wild-type and polymorphic probe-amplicon duplexes contain one mismatch, while the mutant sequences harbour two mismatches (Margraf et al., 2007; Margraf et al., 2006).

- A *deletion* of one to three problematic polymorphic bases in a probe can be incorporated. Upon formation of the probe-target duplex, the unmatched base or bases of the target ssDNA bulge out. Thus regardless of the base/s at the polymorphic site, both wild-type and polymorphic amplicons will have the same T_m.

- The incorporation of a *universal base* into a probe can bypass polymorphisms as these bases pair indiscriminately with any DNA nucleotide (Margraf et al., 2007; Margraf et al., 2006; Zheng et al., 2008). Hypoxanthine and its universal base analogue, inosine, are produced by RNA editing and are found in transfer RNA. However inosine is strictly not a universal base, as it does not pair indiscriminately; despite this inosine is widely used and has proved useful in primer, probe and micro-array design (Watkins Jr and SantaLucia Jr, 2005). Alternatively, 3-nitropyrrole can be used, which pairs indiscriminately and the duplexes formed are less stable than the natural base pairs (Loakes, 2001; Loakes and Brown, 1994).

- *Locked nucleic acids* (LNAs) are stable in the presence of polymorphisms. LNAs are nucleotide analogues which contain a methylene linkage connecting the 2' and 4' carbons of the ribose ring. By restricting the conformation of the nucleotide the LNAs are optimized for base pairing (Kaur et al., 2006). Consequently, LNAs have a high affinity for their

complementary base and the T_m is higher than that of unmodified bases (> 3-8 °C) (Koshkin et al., 1998). The inclusion of locked nucleic acids (LNA) improves variant discrimination with short probes (< 15 bp) because of the higher thermal stability (Chou et al., 2005; Simeonov and Nikiforov, 2002; Ugozzoli et al., 2004).

1.4.2.6.2 HRMA Applications

Due to its simplicity, cost effectiveness, accuracy and flexibility HRMA is widely used. Besides for homozygotic and heterozygotic variant screening and typing, HRMA has been applied to methylation and quantification studies (Rouleau et al., 2009; Vossen et al., 2009b; Wojdacz and Dobrovic, 2007). Mutation scanning HRMA assays have been setup to type clinically relevant bacterial and viral species (Cheng et al., 2006; Giglio et al., 2005; Hewson et al., 2009; Jeffery et al., 2007; Lin et al., 2008; Nakagawa et al., 2009; Odell et al., 2005; Price et al., 2007; Sabol et al., 2009; Steer et al., 2009; Tajiri-Utagawa et al., 2009; Toi and Dwyer, 2008). In addition, HRMA assays have been setup to detect mutations associated with somatic diseases in human genetic material (Grievink and Stowell, 2008; Hill et al., 2006; Krenková et al., 2009; Krypuy et al., 2006; Liew et al., 2004; Nguyen-Dumont et al., 2009; Nienke van der Stoep et al., 2009; Poláková et al., 2008; Poulson and Wittwer, 2007; Reed and Wittwer, 2004; Simi et al., 2008; Vandersteen et al., 2007; Willmore-Payne et al., 2005; Zhou et al., 2004; Zhou et al., 2005). HRMA has not been applied to the detection of drug resistance mutations in HIV.

1.5 Study Objectives

HRMA is a useful platform for SNP detection and typing. Assays can be designed to rapidly and accurately detect genotypes at selected loci (Zhou et al., 2005). HIV-1 drug resistance mutations

typically consist of SNPs and many of these mutations have clinically relevant implications (Shafer and Schapiro, 2008). While Sanger population sequencing is expensive, time-consuming and insensitive it is the gold standard for HIV drug resistance mutation detection (Hanna and D'Aquila, 2001). Consequently the development of new and refinement of current HIV SNP detection methodologies is desirable.

1.5.1 Research Question

Can high resolution melting analysis (HRMA) assays be designed to detect HIV-1 resistance-related mutation codons?

1.5.2 Main Objectives

The main objective of this study is to determine whether HRMA incorporating probes is a feasible approach for accurately and rapidly identifying HIV-resistance-related mutation codons in HIV-1 patient samples. The optimal size and design of probes for use in an HRMA assay applied to highly polymorphic genetic material will be established. Additionally, the possibility that this method can be used as a mutation screening tool for large numbers of samples will be investigated.

1.5.3 Specific Objectives

- Specific HIV-1 RT drug resistance mutations will be introduced into plasmids by site-directed mutagenesis.
- Primers will be designed and asymmetric PCRs setup to amplify these codons in the plasmids.

- Short, unlabelled, 3' blocked oligonucleotide probes will be designed to genotype the mutation sites during HRMA following PCR.
- Thermocycling and HRMA will be carried out on the LightCycler 480 Real-Time PCR machine (Roche Applied Science, GmbH, Germany).
- The LightCycler HRM Master (Roche Applied Science, GmbH, Germany), which contains a saturating dsDNA binding fluorescent dye will be utilized.
- After optimization on the plasmids the assays will be applied to the same mutation codons in the HIV-1 *p66/p51* gene in previously genotyped patient samples.
- Patient HIV-1 RNA will be isolated and amplified by a nested RT-PCR for use in HRMA
- A number of masking techniques will be utilized in order to minimize the effect that polymorphisms have on HRMA.
- Clonal analysis and serial dilutions will be setup to establish the limit of detection of the assays.
- Validation of successful assays, which includes sensitivity, specificity, repeatability, reproducibility and limit of detection will be completed.

Chapter 2: Materials and Methods

2.1 RNA Isolation

HIV-1 RNA was isolated from 200 µL of stored patient plasma using the MagNA Pure LC Instrument and the MagNA Pure LC Total Nucleic Acid Isolation Kit (Roche Applied Science, GmbH, Germany) according to the manufacturers' instructions. In total 116 patient samples were utilized and details are in section 3.2 (page 40). The kit contains three Wash Buffers, a Lysis/Binding buffer, Proteinase K, Magnetic Glass Particles and an Elution Buffer. The Lysis/Binding buffer contains a chaotropic salt which disrupts the cell membrane leading to lysis. The Proteinase K digests the released proteins and nucleases and the Binding buffer allows for the binding of the nucleic acid to positively charged Magnetic Glass Particles.

2.2 cDNA Construction by Reverse Transcription

Complementary DNA (cDNA) was synthesized with Thermoscript RT (Invitrogen, USA) as per the manufacturers' instructions. The reagents for the reactions were added in the following final concentrations: 10 pmol/µL IN3 primer, 1 mM dNTPs, 1x cDNA synthesis buffer, 5 mM DTT, 20 U RNaseOUT (Invitrogen, USA) and 7.5 U Thermoscript RT. The IN3 (Appendix A, Table A1) primer amplified HIV-1 from nucleotide 3757 (HXB2 Genbank accession number AF033819).

Four microlitres of purified RNA was added to the primer/dNTP mix, and then denatured at 65 °C for 5 minutes. Thereafter the tubes were placed on ice for one minute and the master mix was added. The mixture was incubated for one hour at 55 °C to allow for cDNA synthesis; thereafter

the enzyme was deactivated by heating to 85 °C for five minutes. The tubes were cooled on ice for one minute before 1 U of RNase H was added. The reaction was incubated at 37 °C for 20 minutes to degrade the RNA. The cDNA was stored at -20 °C.

2.3 RT-PCR of the *p66/p51* Fragment of the *pol* Gene

A 986 bp region spanning amino acids 1 to 321 of HIV-1 RT was amplified with an in-house, two stage nested reverse transcription PCR (RT-PCR) (Loubser et al., 2006). For the outer reaction, the forward and reverse primers, pFor-out and pRev-out (Appendix A, Table A1) were utilized at final concentrations of 20 pmol/µL per primer. The amplified region spanned nucleotides 1,951 to 3,037 of HIV-1 *p66/p51* (HXB2 Genbank accession number AF033819). The final concentrations of the reagents were: 1.4 mM $MgCl_2$, 160 µM dNTP, 4 U/µL AMV RT (Roche Applied Science, GmbH, Germany), 1.25 U/µL Super-Therm enzyme (Southern Cross Biotechnology (Pty.) Ltd., South Africa), 10 U/µL RNase Inhibitor (Roche Applied Science, GmbH, Germany), and 1 x for the ammonium sulphate based buffer. With the addition of 5 µL of RNA, the total volume was 50 µL. The RT-PCR conditions for the first reaction were 42 °C for 60 minutes, 95 °C for seven minutes and 35 cycles of 92 °C for 20 seconds, 50 °C for 30 seconds and 72 °C for 90 seconds and a final ten minutes at 72 °C.

The second round of the PCR procedure amplified nucleotides 2,056 to 3,004 (HXB2 Genbank accession number AF033819) and was performed using the pFor-in and pRev-in forward and reverse primers (Appendix, Table A1). The Taq polymerase, primers, $MgCl_2$, dNTP and buffer were added to the same final concentrations as before. The total volume was 100 µL with 10 µL of first round PCR product added. The cycling conditions were the same as above, excluding the

initial 42 °C for 60 minutes. The PCR products were visualized on 1% agarose gels and the products were stored at -20 °C.

2.4 Purification of PCR Products

PCR samples were purified using the High Pure PCR Product Purification Kit (Roche Applied Science, GmbH, Germany) according to the manufacturers' protocol. Purification was required to remove excess primers, salts, dNTPs and enzymes to prevent inhibition of downstream reactions. Five hundred microlitres of Binding Buffer was mixed with each PCR reaction and placed into a filter tube and centrifuged for one minute at 13 000 g. The chaotropic salt guanidine thiocyanate in the Binding Buffer causes the DNA to bind to glass fibers within the filter tube. This allows contaminant removal during the ensuing wash steps. The flow through was discarded from the collection tubes and 500 µL of Wash Buffer was added prior to re-centrifugation. This step was repeated with 200 µL of Wash Buffer. The PCR DNA was eluted in 50 µL of the Elution Buffer by one minute of centrifugation at 13 000 g. The samples were quantified using the NanoDrop1000 spectrophotometer (Thermo Fisher Scientific Inc, USA) at 260 nm. The DNA was diluted (1:100) in Tris-HCl pH 8, and stored at -20 °C.

2.5 High Resolution Melting Analysis (HRMA)

2.5.1 Primer Design for HRMA

An HIV-1 South African based consensus sequence, using 648 subtype C sequences was assembled using Sequencher version 4.5 (Gene Codes Corporation, USA). The sequences were downloaded from the Los Alamos HIV Database (http://www.hiv.lanl.gov), and primers and probes were designed using this consensus sequence (Tables 3.2 and 3.3, page 45). Six PCRs

(Table 3.2), spanning the mutations of interest, were designed encompassing amino acids 37–44 (nucleotides 2,203–2,227), 60–74 (nucleotides 2,272–2,317), 100–108 (nucleotides 2,391–2,421), 146–154 (nucleotides 2,529–2,557), 181–191 (nucleotides 2,636–2,668) and 212–229 (nucleotides 2,729–2,783) of the HIV-1 *p66/p51* gene (HXB2 Genbank accession number AF033819). Including the primer, the amplicon length ranged from 72 bp to 100 bp.

In addition, "altered" primers were designed to anneal to the sites directly adjacent the 103, 151, 184 and 190 mutation codons (Table 3.3, page 45). These primers produced a PCR product of 3 bp (excluding the primer) which would mask the polymorphisms flanking the codons of interest, preventing erroneous HRMA. The T_m of each primer, after salt adjustment, was between 58 °C and 62 °C (Kibbe, 2007). The primers were diluted in dH_2O pH 7.4 and stored at -20 °C.

2.5.2 Unlabelled Probe Design for HRMA

Short probes of 11, 15 and 16 bp in length were designed for codon genotyping during HRMA. Probes were designed to be complementary to the wild-type and mutant codons at each position of interest. The probe length was minimized to prevent hybridization to polymorphic flanking regions and to allow for simple melt curve interpretation. The mutation of interest was in the center of the probe to maximize probe instability when melting (Naiser et al., 2008). Each probe was designed to hybridize to the sense strand. In order to prevent probe extension during thermocycling, the probes were blocked at the 3' end by phosphorylation. The probes were manufactured by Inqaba Biotec, South Africa.

To facilitate polymorphism masking in the event that polymorphisms disrupted HRMA, a number of modifications were introduced into the probes (Margraf et al., 2006). Probes containing LNAs, ambiguous, universal, deleted and mismatched bases at selected polymorphic regions were tested. Ambiguous bases incorporated a mixture of each base at the selected region. Universal bases included inosine at the polymorphic region. Deleted bases consisted of a complementary probe with a missing nucleotide/s at the polymorphic site. An extra base/s was added onto the probe to maintain the 15 bp length. Deliberate mismatches were incorporated to the ensure instability of the probe-amplicon interaction in cases of non-specific binding.

2.5.3 HRMA-PCR

The real-time PCRs were performed using the ready-to-use master mix, LightCycler HRM Master (Roche Applied Science, GmbH, Germany). The mix contains LightCycler 480 High Resolution Melting Dye (Roche Applied Science, GmbH, Germany) which intercalates with dsDNA, allowing for HRMA.

Asymmetric PCRs were designed to ensure the visibility of the weaker probe signal. The optimal concentration of the reagents for each assay was determined using the wild-type HIV-1 plasmid as the template molecule. The final concentrations of the reagents for the HRM-PCR were 1x LightCycler HRM Master, 2.5 mM $MgCl_2$, 10 pmol/µL of the forward primer and 2.5 ng of template DNA. The optimal concentrations for the reverse primers and probes were 0.3–1 pmol/µL and 2 µM, respectively. The final volume of the reactions was 10 µL. The real-time PCRs were carried out in 96 multi-well plates, sealed with LightCycler Sealing Foil (Roche Applied Science, GmbH, Germany) and centrifuged for one minute at 150 rpm.

The LightCycler 480 Real-Time PCR conditions were: 94 °C for five minutes with a ramp rate of 4.4 °C/s; 45 cycles at 95 °C for 10 seconds at 4.4 °C/s, 55 °C for 15 seconds at 2.2 °C/s and 72 °C for 15 seconds at 4.4 °C/s; high resolution melting at 95 °C for one minute at 4.4 °C/s, 40 °C for one minute at 2.2 °C/s, then a temperature increase from 40 °C to 95 °C at 1-3 °C/s, followed by 40 °C for ten seconds at 2.2 °C/s. During PCR optimization, the products were run on 2% agarose gels, to test for specific and successful amplification.

2.6 HRM Data Analysis

The melting data was analyzed (Figure 2.1) using the LightCycler 480 Gene Scanning Software version 1.2.0.0625 (Roche Applied Science, GmbH, Germany). For data normalization, fluorescence base lines were selected before and after the melting transition. The pre-melt fluorescence was adjusted to a relative value of 100%, while the post-melt fluorescence, to 0%. This normalization of the data was required to distinguish homozygous mutants by T_m differences. Negative first derivative (-dF/dT) plots of the normalized data were used to visualize probe and amplicon melting in a single curve. The T_m of the probe and amplicon appear as peaks (Erali et al., 2008; Montgomery et al., 2007b). The assay procedure is diagramed in Figure 2.2.

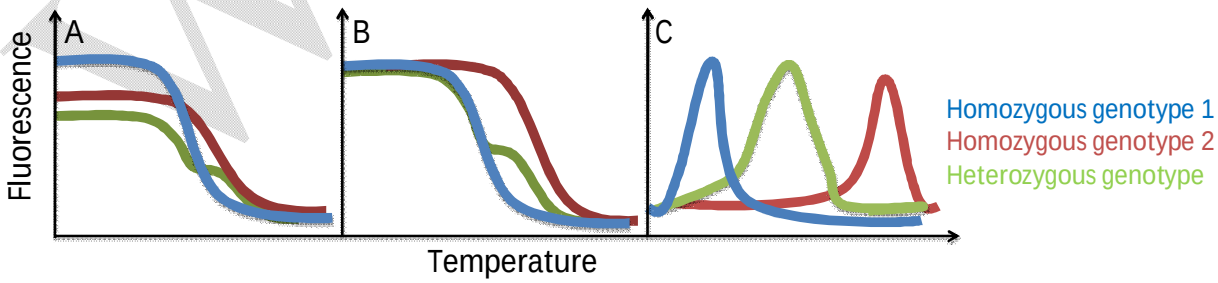

Figure 2.1. Diagram of data formats. (**A**) Raw Data (**B**) Normalization: genotype 1 and genotype 2 are homozygous, differentiated by a SNP. Normalized homozygous mutants are parallel to one another. (**C**) Negative first derivative plots: homozygotes have a sharp melting peak while heterozygotes have a broader peak. The latter is due to the mixture of two genotypes, with two different T_m's (Erali et al., 2008; Montgomery et al., 2007b; Wittwer et al., 2003).

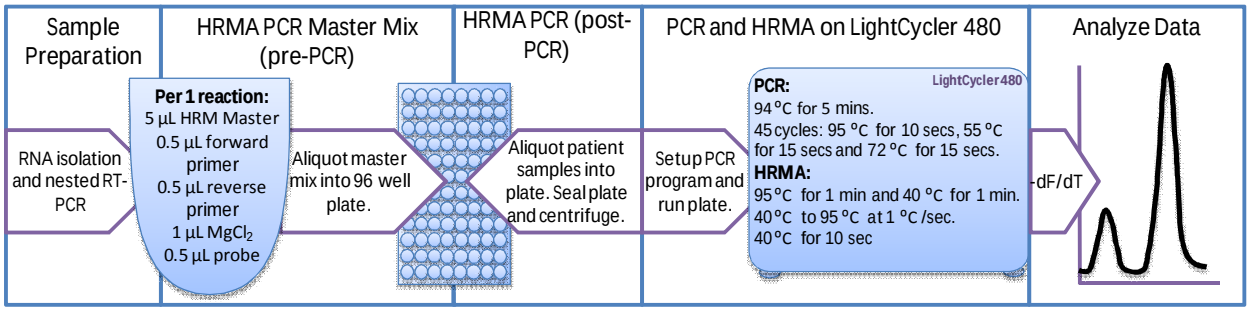

Figure 2.2. Diagrammatic representation of the HRMA assays. Samples were prepared and stored, while master mixes were prepared and used as needed.

2.7 TOPO TA Cloning

Cloning of five HIV-1 patient samples (10b, 26, 47, 73 and 92) was conducted to detect mutations at the 103, 151, 181, 184 and 190 codons present at minority levels. HRMA identified minority resistance populations in these samples which were not detected by population sequencing. The TOPO TA Cloning Kit with the pCR 2.1-TOPO vector (Appendix B, Figure B1) and TOP10 chemically competent cells (Invitrogen, USA) were utilized for cloning according to the manufacturer's guidelines. Four microlitres of PCR product from the second round nested PCR were mixed with 1 µL of the vector and 1 µL of the supplied salt solution (200 mM NaCl and 10 mM $MgCl_2$). The solution was gently mixed and incubated at room temperature for 30 minutes. The salt solution increases the number of transformants as it prevents topoisomerase I from rebinding and nicking the DNA after ligation. After incubation, 5 µL of the cloning reaction was added to a vial of TOP10 cells thawed on ice. This mixture was incubated on ice for 20 minutes; thereafter the cells were heat-shocked at 42 °C for 30 seconds. The cells were placed on ice and 250 µL of room temperature SOC medium was added. The vials were incubated at 37 °C with horizontal shaking (200 rpm) for one hour. Before the cells were spread onto selective agar plates (100 mg/ml ampicillin), 40 µl of X-gal (40 mg/ml) was spread onto the plates for blue-white screening. A third of the cell mixture was spread onto the

selective plates and incubated at 37 °C for 16 hours. Positive colonies (white) were selected by blue-white screening.

Colony PCR was performed using inner primers for the RT-PCR as per section 2.3 page 30. Following PCR the products were diluted (1:100) in Tris-HCl pH 8 and used as template for HRMA. HRMA was performed on 100 colonies per patient sample to detect mutations present at minority levels.

2.8 Site-Directed Mutagenesis

Plasmids containing each mutation under analysis were required for HRM-PCR optimization and for serial dilutions. Site-directed mutagenesis was performed on a previously engineered plasmid which contained 1,129 bp of the *p66/p51* gene of the HIV-1 subtype C CM9 virus (CM9 Genbank accession number AF411967), cloned into the pCR 2.1 vector (Invitrogen, USA) (Cilliers et al., 2005; Loubser et al., 2006). Mutagenesis was performed using the QuikChange® II Site-Directed Mutagenesis Kit (Stratagene, USA). The oligonucleotide primers for site-directed mutagenesis were designed according to the manufacturer's instructions (Appendix A, Table A2). In addition a full length (9,913 bp) recombinant subtype C HIV-1 clone, MJ4 (MJ4 Genbank accession number AF321523), was utilized for the 181 and 184 assay optimization and serial dilutions (Ndung'u et al., 2001). CM9 plasmid containing K65R and K103N and PMJ4 containing Y181C and M184V were previously engineered in our laboratory by Shayne Loubser and Visva Pillay. The author introduced the HIV-1 resistance related mutations M41L, D67N, K70R, Q151M, G190A, T215F, T215Y and P225H into the CM9 plasmid.

For side-directed mutagenesis the reagents were prepared to the following final concentrations, according the manufacturer's guidelines: 1 x reaction buffer, 125 ng for both primers, 1 mM dNTP and 50 ng of template DNA in 50 µL reactions. PCR conditions were 95 °C for 30 seconds, 20 cycles of 95 °C for 30 seconds, 55 °C for one minute and 68 °C for six minutes. As the wild-type parental strand is methylated, it is digested by the methylation specific endonuclease *Dpn* I. One microlitre of *Dpn* I was added following the PCR and the mixture was incubated for one hour at 37 °C.

To transform the mutated plasmids, 1 µL of the restricted DNA was added to 50 µL of thawed XL1-Blue supercompetent cells (Stratagene, USA). After incubation on ice for 30 minutes, the cells were heat-shocked at 42 °C for 45 seconds and placed on ice for two minutes. The cells were then incubated in 0.5 mL of non-selective SOC medium for one hour at 37 °C with horizontal shaking at 230 rpm. Thereafter, 150 µL of the mixture was spread onto ampicillin (amp)-containing agar plates (100 mg/mL) and incubated for 16 hours at 37 °C. As the pCR 2.1 vector contains a gene for ampicillin resistance, only transformed cells grew on the amp+ plates.

2.9 Isolation of Plasmids

The GenElute HP Plasmid Midiprep Kit (Sigma-Aldrich, GmbH, Germany) was used to isolate the plasmid DNA from the transformed *Escherichia coli* cells. Following the manufacturer's protocol, a single colony from each plate was used to inoculate 5 mL of lysogeny broth (LB)-amp+ (100 mg/mL). After an eight hour incubation at 37 °C with horizontal shaking at 230 rpm, the cells were diluted to 1:1000 in 15 mL of LB-amp+. The cells were again incubated, under the same conditions for 16 hours.

Following incubation the cells were collected by centrifugation at 5000 g for ten minutes. The supernatant was discarded and 4 mL of the Resuspension/RNase A Solution was added and the bacterial pellet was resuspended by vortexing. Four millilitres of Lysis Solution was added and the cells were gently mixed, allowing cell lysis and a pH increase. The increase in pH leads to denaturation of the chromosomal DNA, while the covalently closed circular plasmid DNA remains renatured. After five minutes the cell lysate was neutralized by the addition of 4 mL of Neutralization Solution. Neutralization leads to the formation of an insoluble network of chromosomal DNA while the plasmid DNA remains in solution (Birnboim and Doly, 1979). The solution was gently mixed and 3 mL of Binding Solution was added. Following further gentle mixing the cell lysate was poured into the barrel of a filter syringe. Binding columns were placed into collection tubes, 4 mL of Column Preparation Solution was added, and the tubes centrifuged. The centrifugation during the preceding and proceeding wash steps occurred at 3000 g for two minutes. The eluate, containing cell debris, lipids and chromosomal DNA, was discarded each time. The cleared lysate in the filter syringe was emptied into the binding column, to which it absorbed, and was then centrifuged. Four millilitres of Wash Solution 1 was added and the column centrifuged. Four millilitres of Wash Solution 2 was added and the column centrifuged for five minutes. Following the final wash step the binding column was placed into a new collection tube and 1 mL of the Elution Solution was added. The tube was centrifuged for five minutes and the eluate saved. The purified plasmids were quantified on a NanoDrop1000 spectrophotometer (Thermo Fisher Scientific Inc, USA) at 260 nm, diluted in Tris-HCl pH 8, and stored at -20 °C.

2.10 Population Sequencing

Sanger population sequencing reactions were setup according to the BigDye Terminator v3.1 Cycle Sequencing Kit guidelines (Applied Biosystems, USA). This reagent contains fluorescently labeled ddNTPs required sequencing. The reaction mix consisted of 0.5 x Sequencing Buffer, 3.2 pmol/µL primer, 60-300 ng of template DNA and 2 µL of the Ready Reaction Mix, to a total of 10 µL. The forward primers pFor-in and LC-outF (Appendix A, Table A1) amplified nucleotides 2,056 and 2,344, respectively (Loubser et al., 2006). The reverse primers pRev-in and M8 (Appendix A, Table A1) amplified from nucleotides 3,004 and 2,847, respectively (HXB2 Genbank accession number AF033819) (Loubser et al., 2006). Thermocycling was performed under the following conditions: 96 °C for one minute followed by 25 cycles of 96 °C for ten seconds, 50 °C for five seconds and 60 °C for four minutes.

The products were purified by alcohol precipitation. Fifty microlitres of 3 M pH 4.6 sodium acetate and ethanol (1:25) mixture was added to each tube. After vortexing, the strips were centrifuged at room temperature for 30 minute at 2000 g. The supernatant was decanted and the pellet was spun upside-down for one minute at 150 g. Seventy micolitres of ice-cold ethanol was then added and the tubes spun for five minutes at 2000 g, and the supernatant discarded. The pellet was spun upside-down again for one minute at 150 g. The wash steps remove excess ddNTPs and other contaminants. Following drying at 65 °C for three minutes, the pellets were resuspended in 10 µL of Formamide and loaded onto 96 well plates (Applied Biosystems, USA) for sequencing. The sequencing was carried out on an ABI 3100 Genetic Analyzer (Applied Biosystems, USA). The sequences were analyzed on Sequencher version 4.5 (Gene Codes Corporation, USA).

Chapter 3: Results

3.1 Selection of Mutations for HRMA

The current South African Department of Health treatment guidelines for HIV infected adults recommends a first-line ARV combination of two NRTIs and one NNRTI and a second-line combination of two NRTIs and one boosted PI (National Department of Health South Africa 2010, 2010). To date, three studies have shown the predominance of the M184V/I (64%-78%), K103N (39%-55%), TAMs (23%-32%), V106M (19%-31%), G190A/S (16%-20%), P225H (7%-14%), Y181C (10%), K65R (3%-9%) and Q151M (1%-3%) mutations in South African patients failing first- or second-line treatment (Marconi et al., 2008; Orrell et al., 2009; Wallis et al., 2009). Consequently, these mutations were selected for investigation in this project.

3.2 Selection of HIV-1 Patient Samples

Previously sequenced, stored plasma (n=116) from HIV-1 patients (n=103) were selected for analysis. The patient samples were obtained from four previously established cohorts. Samples were selected to ensure the presence of a variety of HIV-1 *p66/p51* genotypes, both wild-type and mutant. Ethics clearance (M090360) was received from the Human Research Ethics Committee in order to utilize the samples (Appendix E).

Samples 1 to 9 were selected from a longitudinal study of HIV-1 mutations in mothers and infants following exposure to single-dose NVP (sd-NVP) for the prevention of mother-to-child transmission of HIV. Maternal plasma from two different time-points were analyzed. The first time-point was drawn during patient enrolment (designated ‘a’) and the second time-point was six weeks post-exposure to sd-NVP, (‘b’) (Martinson et al., 2007). Samples 10 to 20 were

selected from a longitudinal study of two groups of pregnant woman: one exposed to sd-NVP during a previous pregnancy and one drug naïve cohort (Martinson et al., 2009). Maternal plasma was utilized and four of the ten samples had two time-points; enrolment ('a') and six weeks post sd-NVP exposure ('b'). In both studies the principal maternal drug resistance mutation was K103N. Samples 21 to 62 were selected from a cross-sectional study of HIV infected patients on ART. The most common drug resistance mutations in these patients were M184V and K103N (El-Khatib et al., 2009). The remaining samples, 63 to 103, were selected from a random group of patients failing first- and second-line ARV drug regimens (Pillay et al., 2008). In total, 13 of the patients had two time-points and the remaining 90 were single time-point. In each of these cohorts, patients were enrolled at South African hospitals and 97% of the patients were subtype C and the remaining were subtype B.

The following Table shows the genotypes of the relevant codons of the patient samples utilized in this study. The genotypes were previously determined by Sanger population sequencing. The most common mutations were K103N (n=43) and M184V (n=40).

Table 3.1. *p66/p51* sequences of 116 samples from 103 patients at selected mutation codons.

		Codon												
Patient sample	Drugs	41	65	67	70	103	106	151	181	184	190	215	225	Subtype
Sample 1a	naïve	ATG	AAG	GAC	AAG	AAA	GTG	CAG	TAT	ATG	GGA	ACC	CCC	C
Sample 1b	sd-NVP	ATG	AAG	GAC	AAG	**AAM**	GTG	CAG	**TRT**	ATG	GGA	ACC	CCC	C
Sample 2a	naïve	ATG	AAG	GAC	AAG	AAA	GTG	CAG	TAT	ATG	GGA	ACC	CCC	C
Sample 2b	sd-NVP	ATG	AAG	GAC	AAG	**AAM**	**RTG**	CAG	TAT	ATG	GGA	ACC	CCC	C
Sample 3a	naïve	ATG	AAG	GAC	AAG	AAA	GTT	CAG	TAT	ATG	GGA	ACC	CCC	C
Sample 3b	sd-NVP	ATG	AAG	GAC	AAG	AAA	GTT	CAG	**TRT**	ATG	GGA	ACC	CCC	C
Sample 4a	naïve	ATG	AAG	GAC	AAR	AAA	GTG	CAG	TAT	ATG	GGA	ACC	CCC	C
Sample 4b	sd-NVP	ATG	AAG	GAC	AAG	**AAM**	GTG	CAG	TAT	ATG	**GSA**	ACC	CCC	C
Sample 5a	naïve	ATG	AAG	GAC	AAG	AAA	GTG	CAG	TAT	ATG	GGA	ACC	CCC	C
Sample 5b	sd-NVP	ATG	AAG	GAC	AAG	AAA	**RTG**	CAG	TAT	ATG	GGA	ACC	CCC	C
Sample 6a	naïve	ATG	AAG	GAC	AAG	AAA	GTG	CAG	TAT	ATG	GGA	ACC	CCC	C
Sample 6b	sd-NVP	ATG	AAG	GAC	AAG	**AAC**	GTG	CAG	TAT	ATG	GGA	ACC	CCC	C
Sample 7a	naïve	ATG	AAG	GAC	AAG	AAA	GTG	CAA	TAT	ATG	GGA	ACT	CCC	C
Sample 7b	sd-NVP	ATG	AAG	GAC	AAG	**AAM**	GTG	CAA	TAT	ATG	GGA	ACT	CCC	C
Sample 8a	naïve	ATG	AAG	GAC	AAG	AAA	GTG	CAA	TAT	ATG	GGA	ACY	CCC	C
Sample 8b	sd-NVP	fail†	AAA	**AAH**	AGT	**AAH**	TCC	CAA	TAT	GGA	**ACA**	fail	fail	C
Sample 9a	naïve	ATG	AAG	GAC	AAG	AAA	GTG	CAG	TAT	ATG	GGA	ACC	CCC	C

Patient sample	Drugs	Codon												Subtype
		41	65	67	70	103	106	151	181	184	190	215	225	
Sample 9b	sd-NVP	ATG	AAG	GAC	AAG	AAA	GTG	CAG	TAT	ATG	GGA	ACC	CCC	C
Sample 10a	naïve	ATG	AAG	GAC	AAG	AAA	GTG	CAA	TAT	ATG	GGA	ACC	CCC	C
Sample 10b	sd-NVP	ATG	AAG	GAC	AAG	AAM	GTG	CAA	TRT	ATG	GGA	ACC	CCC	C
Sample 11a	naïve	ATG	AAG	GAY	AAG	AAA	GTG	CAG	TAT	ATG	GGA	ACC	CCC	C
Sample 11b	sd-NVP	ATG	AAG	GAC	AAG	AAA	GTA	CAG	TAT	ATG	GGA	ACC	CCC	C
Sample 12a	naïve	ATG	AAG	GAC	AAG	AAA	GTG	CAG	TAT	ATG	GGA	ACC	CCC	C
Sample 12b	sd-NVP	ATG	AAG	GAC	AAG	AAM	RTG	CAG	TRT	ATG	GSA	ACC	CCC	C
Sample 13a	naïve	ATG	AAG	GAC	AAG	AAA	GTG	CAA	TAT	ATG	GGA	ACC	CCC	C
Sample 13b	naïve	ATG	AAG	GAC	AAG	AAM	GYG	CAA	TAT	ATG	GGA	ACC	CCC	C
Sample 14	naïve	ATG	AAG	GAC	AAG	AAA	GTG	CAG	TAT	ATG	GGA	ACC	CCC	C
Sample 15	naïve	ATG	AAG	GAC	AAG	AAA	GTG	CAG	TAT	ATG	GGA	fail	fail	C
Sample 16	naïve	ATG	AAG	GAC	AAG	AAA	GTG	CAG	TAT	ATG	GGA	ACC	CCC	C
Sample 17	naïve	ATG	AAG	GAC	AAG	AAA	GTG	CAG	TAT	ATG	GGA	ACC	CCC	C
Sample 18	sd-NVP	ATG	AAG	GAC	AAA	AAA	GTA	CAG	TAT	ATG	GGA	ACC	CCC	C
Sample 19	sd-NVP	ATG	AAG	GAC	AAR	AAM	GTG	CAG	TRT	ATG	GGA	ACC	CCC	C
Sample 20	naïve	ATG	AAG	GAC	AAG	AGA	GTG	CAG	TAT	ATG	GGR	ACC	CCC	C
Sample 21	d4T/3TC/EFV	ATG	AAG	AAC	AAG	AAA	ATG	CAG	TAT	GTG	GGA	ACC	CCC	C
Sample 22	d4T/3TC/EFV	ATG	AAG	GAC	AAG	AAC	GTG	CAG	TAT	GTG	GGA	ACC	CCC	C
Sample 23	d4T/3TC/NVP	ATG	AAG	GAC	AAG	AAA	ATG	CAG	TAT	GTG	GGA	ACC	CCC	C
Sample 24	d4T/3TC/EFV	ATG	AAG	GAT	AAG	AAC	GTG	CAG	TAT	GTG	GGA	ACC	CCC	C
Sample 25	d4T/3TC/KAL	ATG	AAG	GAC	AAG	AAA	GTT	CAG	TAT	RTG	GGA	ACC	CCC	C
Sample 26	d4T/3TC/EFV	ATG	AAG	GAC	AAA	AAA	GTA	CAG	TAT	GTG	GGA	ACC	CCC	C
Sample 27	AZT/3TC/KAL	ATG	AAG	GAC	AAG	AAA	GTG	CAG	TAY	ATG	GGR	ACC	CCC	C
Sample 28	d4T/3TC/EFV	ATG	AAG	GAC	AAG	AAA	ATG	CAG	TAT	GTR	GGA	TTC	CAC	C
Sample 29	d4T/3TC/EFV	ATG	AAG	GAC	AAG	AAC	GTG	CAA	TAT	GTG	GGA	ACC	CCC	C
Sample 30	AZT/3TC/EFV	TTG	AAG	GAT	AAG	AAT	GTG	CAA	TAT	GTG	GGA	TAC	CCC	C
Sample 31	AZT/3TC/EFV	ATG	AAG	GAC	AAG	AAA	GTG	CAG	TAT	ATG	GGA	ACC	CCC	C
Sample 32	AZT/ddI/KAL	ATG	AAG	GAC	AAG	AGA	ATG	CAA	TAT	ATG	GGA	ACC	CCC	C
Sample 33	d4T/3TC/EFV	ATG	AAG	AAT	AAG	AGA	ATG	CAG	TAT	GTG	GCA	ACC	CCC	C
Sample 34	AZT/ddI/KAL	ATG	AAG	GAC	AAR	AAC	GTG	CAG	TAT	ATG	GGA	ACC	CCC	C
Sample 35	AZT/3TC/EFV	ATG	AAG	GAC	AAG	AAA	ATG	CAG	TAT	RTR	GSA	ACC	CCC	C
Sample 36	d4T/3TC/EFV	ATG	AAG	GAC	AAG	AAC	GTG	CAG	TAT	GTG	GGC	TAC	CCC	C
Sample 37	d4T/3TC/EFV	ATG	AAG	GAC	AAG	AAA	GTG	CAG	TAT	ATG	GSA	ACC	CCC	C
Sample 38	AZT/3TC/KAL	ATG	AAG	GAC	AAA	AAC	GTG	CAG	TAT	ATG	GGA	ACC	CCC	C
Sample 39	d4T/3TC/EFV	ATG	AAG	GAC	AAG	AAG	GTG	CAG	TAT	ATG	GGA	ACC	CCC	C
Sample 40	d4T/3TC/EFV	ATG	AAG	RAC	AAG	AAC	ATG	CAG	TAT	GTG	GGA	ACC	CCC	C
Sample 41	AZT/3TC/NVP	ATG	AAG	GAC	AAG	AAC	GTG	CAA	TAT	GTG	GGA	ACC	CCC	C
Sample 42	AZT/ddI/KAL	ATG	AAG	GAC	AAG	AAA	GTG	CAG	TAT	ATG	GGA	ACC	CCC	C
Sample 43	d4T/3TC/EFV	ATG	AAG	GAC	AAG	AAC	GTG	CAA	TAT	ATG	GGA	ACC	CCC	C
Sample 44	AZT/3TC/EFV	ATG	AAG	GAC	AAG	AAT	GTG	CAA	TAT	GTG	GGA	ACC	CAC	C
Sample 45	AZT/3TC/EFV	ATG	AAG	GAC	AAA	AAA	GTG	CAG	TAT	ATG	GGA	ACC	CCC	C
Sample 46	d4T/3TC/EFV	ATG	AAG	GAC	AAG	AAA	GTG	CAG	TAT	RTG	GGA	ACC	CCC	C
Sample 47	d4T/3TC/EFV	ATG	AAG	GAC	AAG	AAG	GTG	CAG	TAT	GTG	GGA	ACC	CCC	C
Sample 48	d4T/3TC/EFV	ATG	AAG	GAC	AAG	AAC	GTG	CAA	TAT	GTG	GGA	ACC	CCC	C
Sample 49	d4T/3TC/EFV	ATG	AAG	GAC	AAA	AAR	GTG	CAG	TAT	GTG	GGA	ACC	CCC	C
Sample 50	d4T/3TC/EFV	ATG	AAG	GAC	AAG	AAA	GTG	CAG	TAT	ATG	GGA	ACC	CCC	C
Sample 51	d4T/3TC/EFV	ATG	AAG	GAC	AAG	AAA	ATG	CAG	TAT	RTG	GGA	ACC	CCC	C
Sample 52	d4T/3TC/NVP	ATG	AAA	GAC	AAA	AAC	GTA	CAA	TAT	GTA	GGA	ACC	CCT	C
Sample 53	d4T/3TC/EFV	ATG	AAG	GAC	AAG	AAA	ATG	CAG	TAT	GTG	GGA	ACC	CCY	C
Sample 54	AZT/ddI/KAL	ATG	AAG	GAC	AAG	AGT	GTG	CAG	TAT	GTG	GCA	ACT	CCC	C
Sample 55	d4T/3TC/EFV	ATG	AAG	GAC	AAG	AAA	GTG	CAG	TAT	ATG	GGA	ACC	CCC	C
Sample 56	d4T/3TC/EFV	ATG	AAG	GAC	AAG	AAC	GTG	CAG	TAT	ATG	GGA	ACC	CCC	C
Sample 57	d4T/3TC/EFV	ATG	AAG	GAC	AAG	AAC	GTA	CAG	TAT	GTG	GGA	ACC	CAC	C
Sample 58	AZT/ddI/KAL	ATG	AAG	GAC	AAG	AAA	GTG	CAG	TAT	ATG	GGA	ACC	CCC	C
Sample 59	d4T/3TC/KAL	ATG	AAG	GAC	AAG	AAA	GTG	CAG	TAT	ATG	GGC	CCC	CCC	C
Sample 60	AZT/ddI/KAL	ATG	AAG	GAC	AAG	AAM	GTG	CAG	TAT	ATG	GGA	ACT	CCC	C

Patient sample	Drugs	Codon												Subtype
		41	65	67	70	103	106	151	181	184	190	215	225	
Sample 61	AZT/3TC/EFV	ATG	AAG	GAC	AAG	AAA	GTG	CAG	TAT	**GTG**	GGA	ACC	CCC	C
Sample 62	d4T/3TC/EFV	ATG	AAG	GAC	AAG	AAA	**ATG**	CAG	TAT	GTG	GGA	ACC	CCT	C
Sample 63	AZT/EFV/SQV	ATG	AAG	**AAC**	**AGG**	**AAT**	GTA	CAA	TAT	ATG	GGA	ACC	CCC	C
Sample 64	naïve	ATG	AAG	GAC	AAG	AAA	GTA	CAG	TAT	ATG	GGA	ACC	CCC	C
Sample 65	AZT/3TC/ABC	**TTG**	AAG	**AAC**	AAG	AAA	GTG	CAG	TAT	**GTR**	GGA	ACC	CCC	C
Sample 66	AZT/ddI	ATG	AAG	GAC	AAG	AAA	GTA	CAG	TAT	ATG	GGA	ACC	CCC	C
Sample 67	d4T/ddI/EFV	ATG	AAA	**RAC**	**ARG**	**AGA**	**ATG**	CAG	TAT	ATG	GGA	ACC	CCC	C
Sample 68	AZT/ddI/EFV	**TTG**	AAG	**AAC**	AAG	AAA	**ATG**	CAG	TAT	ATG	**GCA**	**TAC**	CCC	C
Sample 69	d4T/3TC/NFV	ATG	AAG	GAC	AAG	AAA	GTA	CAG	TAT	**GTR**	GGR	ACC	CCT	C
Sample 70	AZT/3TC/NVP	ATG	AAA	GAC	**ARA**	AAA	GTA	CAG	TAT	**GTG**	GGA	ACC	CCC	B
Sample 71	AZT/3TC/ABC	ATG	AAG	**AAC**	**AGG**	**AGC**	GTG	CAG	TAT	**GTA**	GGA	AYC	CCC	C
Sample 72	AZT/3TC/EFV	ATG	AAG	GAC	AAG	**AAC**	GTG	CAA	TAT	ATG	GGA	TAT	CCC	C
Sample 73	AZT/3TC/NFV	ATG	AAG	**AAC**	**AGG**	**AAT**	GTG	CAA	TAT	ATG	**GCA**	ACC	CCC	C
Sample 74	d4T/ddI/HU	ATG	AAG	GAC	AAG	AAG	GTG	CAG	TAT	ATG	GGA	TAC	CCC	C
Sample 75	d4T/3TC/NVP	ATG	AAG	GAT	AAG	AAA	GTG	CAG	TAT	**GTG**	**GCA**	ACC	CCT	C
Sample 76	d4T/3TC/LPV	ATG	AAG	**AAC**	**ARA**	**AAT**	GTG	CAG	TAT	ATG	**GCA**	TAC	CCC	C
Sample 77	d4T/ddI/HU	ATG	AAG	GAC	AAG	AAA	GTG	CAA	TAC	ATG	GGA	ACC	CCC	C
Sample 78	AZT/3TC/NVP	ATG	AAG	**AAT**	**AGG**	**AAC**	GTG	CAG	TAT	**GTG**	GGA	AYC	CCC	C
Sample 79	AZT/3TC/NVP	ATG	AAG	**AAC**	**AGG**	AAA	GTG	CAG	TAT	**GTG**	**GCA**	ACC	CCC	C
Sample 80	ddI/ABC/NFV	ATG	AAG	**AAC**	**AGG**	AAA	GTG	CAG	TAT	**GTG**	GGA	ACC	CCC	C
Sample 81	d4t/ddI/EFV	ATG	AAG	**GRC**	AAG	AAA	**ATG**	CAG	TAT	ATG	GGA	ACC	CCC	C
Sample 82	d4T/ddI	ATG	AAG	GAC	AAG	AAA	GTG	**ATG**	TAT	ATG	GGA	ACC	CCC	C
Sample 83	d4T/ddI/RTV	ATG	**ARG**	GAC	AAG	AAA	GTG	CAG	TAT	ATG	GGA	ACC	CCC	C
Sample 84	d4T/ddI/EFV	ATG	**ARG**	TAC	AAG	**AAC**	**ATG**	**ATG**	TAT	ATG	GGA	ACT	CCT	C
Sample 85	d4T/ddI/EFV/NFV	**CTG**	AAR	**AAC**	**AGA**	AAA	GTA	**ATG**	**TRT**	ATG	**AGC**	**TAC**	CCT	B
Sample 86	AZT/3TC/NVP	ATG	AAG	GAC	AAA	AAG	GTA	CAG	**TGT**	**GTG**	GGA	ACC	CCC	C
Sample 87	EFV/3TC/AZT	ATG	AAG	GAC	AAG	**AAC**	**ATG**	CAG	TAT	**GTG**	GGA	ACC	CCC	C
Sample 88	d4T/3TC/EFV	ATG	AAG	GAC	AAG	AAA	**ATG**	CAA	TAT	**GTG**	GGA	ACT	TCC	C
Sample 89	d4T/3TC/RTV	ATG	AAG	GAC	AAG	AAG	GTG	CAG	TAT	ATG	GGA	ACC	CCC	C
Sample 90	AZT/3TC/RTV	ATG	AAG	GAC	AAG	AAA	GTG	CAG	TAC	**GTG**	GGA	ACC	CCC	C
Sample 91	d4T/3TC/RTV	ATG	AAG	GAC	AAG	AAG	GTG	CAG	TAT	**GTG**	GGA	ACC	CCC	C
Sample 92	d4T/ddI/EFV	ATG	AAG	GAC	AAG	**AAC**	GTA	CAG	TAT	ATG	GGA	ACC	CCC	C
Sample 93	AZT/3TC/NVP	ATG	AAG	GAC	AAG	AAA	GTG	CAG	**TRT**	**GTG**	**GSA**	ACY	CCC	C
Sample 94	d4T/ddI/EFV	ATG	AAG	GAC	AAG	**AAC**	GTG	CAG	TAT	**GTG**	GGA	**TAC**	CCC	C
Sample 95	AZT/3TC/NVP*	ATG	AAG	GAC	AAG	AAA	GTG	CAG	TAT	ATG	GGA	ACC	CCC	C
Sample 96	d4T/ddI/RTV	ATG	AAG	GAC	AAG	AAA	GTG	CAG	TAT	ATG	GGA	ACC	CCC	C
Sample 97	d4T/ddI/EFV	ATG	**ARG**	GAC	**ARG**	AAA	**ATG**	**MTG**	TAT	ATG	GGA	ACC	CCC	C
Sample 98	d4T/ddI	ATG	AAG	GAT	AAG	AAA	GTG	CAG	TAT	ATG	GGA	**WMC**	CCC	C
Sample 99	d4T/ddI	**YTG**	AAG	GAC	AAG	AAA	GTA	CAG	TAT	ATG	GGA	**TAC**	CCC	C
Sample 100	d4T/ddI	**MTG**	AAA	GAC	AAA	AAA	GTA	**ATG**	TAT	ATG	GGA	ACC	CCT	B
Sample 101	d4T/EFV/LPV	**TTR**	AAG	**AAC**	**AGG**	AAA	**ATG**	CAG	TAT	ATG	**GSA**	TGT	CCC	C
Sample 102	AZT/3TC/EFV	ATG	AAG	GAC	AAG	**AAC**	GTG	CAG	TAT	**GTG**	GGA	ACC	**CAC**	C
Sample 103	d4T/ddI/EFV	**TTG**	AAG	GAC	AAG	**AAC**	**ATG**	CAG	TAT	ATG	GGA	**TAC**	CCC	C
Total mutations		8	3	17	12	43	23	5	8	40	14	9	4	

Genotypes in blue indicate drug resistance mutations. † Fail indicates failure of population sequencing. * Previous regimen (current not available). Hydroxyurea (HU) reduces dNTP production and is rarely used for ARV therapy (Lori and Lisziewicz, 1999).

3.3 Design and Optimization of HRMA-PCR

Plasmids were required for assay optimization and for use in serial dilutions. The *p66/p51* fragment from the CM9 HIV-1 subtype C clinical isolate (Genbank accession number

AF411967) was previously cloned into the pCR 2.1 vector (Appendix B, Figure B1). The K65R, K103N and V106M mutations had been previously introduced into the wild-type plasmid by site-directed mutagenesis. Due to mismatches the 181F and 181R primers could not be used to amplify the CM9 plasmid. The sequence of the subtype C pMJ4 plasmid (Genbank accession number AF321523) better matched the 181F/R primers and so was utilized for 181 and 184 assay optimization. The Y181C and M184V mutations had been previously introduced in pMJ4.

The author utilized the QuikChange® II Site-Directed Mutagenesis Kit (Stratagene, USA) to introduce the M41L, D67N, K70R, Q151M, G190A, T215F, T215Y and P225H mutations into the CM9 plasmid (primer sequences Appendix A, Table A2). The plasmids were isolated with the GenElute HP Plasmid Midiprep Kit (Sigma-Aldrich, GmbH, Germany) and genotyped by population sequencing to confirm the presence of the mutations.

3.3.1 HRMA-PCR Primers

The HRMA-PCR primers (Tables 3.2 and 3.3) were designed using a South African HIV consensus sequence (SAC) constructed with 648 HIV sequences from South African patients, downloaded from the Los Alamos HIV Database (http://www.hiv.lanl.gov). Six PCRs, spanning the mutations of interest were designed encompassing amino acids 37–44, 60–74, 100–108, 146–154, 181–191 and 212–229 of the HIV-1 *p66/p51* fragment. Asymmetric and short PCRs (72 bp-100 bp) were setup to minimize the size of the larger amplicon-amplicon peak (Figure 3.1). A gradient (0.1-1 pmol/µL) with the limiting reverse primer for the HRMA-PCR was tested (Figure 3.2) to determine the optimal primer concentrations. Altered primers, which directly flanked the codons of interest, were designed for polymorphism masking (Table 3.3).

Table 3.2. Primer sequences for the HRMA-PCR assays.

Codon/s	Template	Name	Primer sequence (5' - 3')	Concentration (pmol/µL)	T_m (°C)	Product length (bp)
41	CM9	41F 41R	AAGAGAAAATAAAAGCATTAACAGC AGGCCCAATTTTTGTAATTTTTCC	10 0.4	58	74
65, 67, 70	CM9	62F 62R	GCCTGAAAATCCATATAACACTCC TCTTTTATTGAGTTCCCTGAAATCTAC	10 0.5	62	97
103, 106	CM9	100F 100R	AGGAATACCACACCCAGCAG AAATATGCATCCCCCACATCC	10 0.4	60	72
151	CM9	151F 151R	TGAAACACCAGGGATTAGATATC CTGGAATATTGCTGGTGATCC	10 0.4	59 60	73
181, 184, 190	MJ4	181F 181R	AGCAAAAAATCCAGAAATAGTCATC CTATGTTGCCCTATTTCTAAGTC	10 0.6	59	81
215, 225	CM9	215F 215R	GGAGTTAAGAGAACATCTATTAAAG AGGATGGAGTTCATACCCCA	10 0.4	59 58	100

Table 3.3. Sequences for the altered primers for the HRMA-PCR assays.

Codon	Template	Name	Primer sequence (5' - 3')	Concentration (pmol/µL)	Tm (°C)	Product length (bp)
103	CM9	ap103F ap103R	CACCCAGCAGGGTTAAAAAAG ACATCCAGTACTGTCACTGATTT	10 1	60 59	47
151	CM9	ap151F ap151R	TAGATATCAATATAATGTGCTTCCA GCTGGTGATCCTTTCCATCC	10 1	58 60	48
184	MJ4	ap184F ap184R	AATCCAGAAATAGTCATCTATCAATAT TCAGATCCTACATACAAGTCATC	10 1	59 59	53
190	MJ4	ap190F ap190R	CAATATATGGATGACTTGTATGTA TGTTGCCCTATTTCTAAGTCAGA	10 1	57 59	50

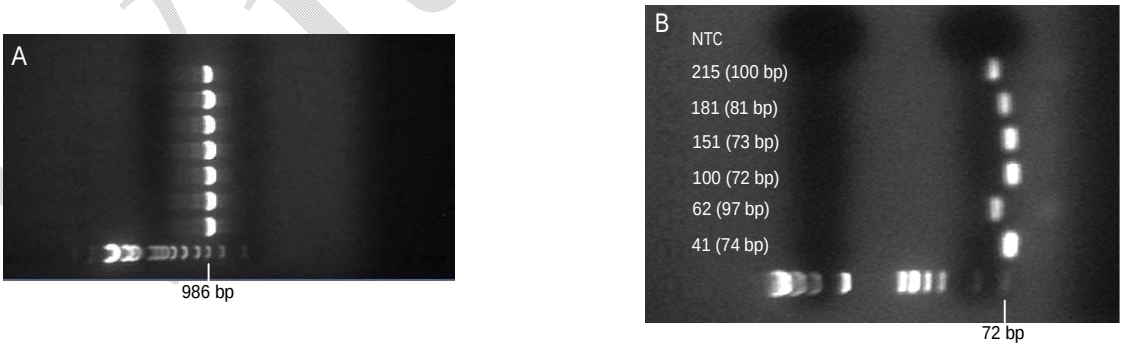

Figure 3.1. Agarose gels of the PCR products following RT-PCR and HRMA. (**A**) PCR products from patient samples were run on 1% agarose gels for one hour at 80 volts (an example shown in **A**). The fragment length of the second round PCR, shown here, was 986 bp. The Roche molecular weight marker IV (Roche Applied Science, GmbH, Germany) was utilized for size comparison (**B**) The HRMA-PCR products were run on 2% agarose gels for one hour at 80 volts (an example shown in **B**). The products ranged from 72 bp to 100 bp in length. The Roche molecular weight marker IX (Roche Applied Science, GmbH, Germany) was utilized. The no template control (NTC) is on the right side of each gel.

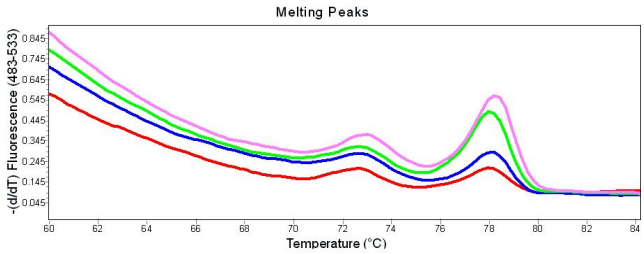

Figure 3.2. Optimization of the reverse primer for HRMA-PCR. A range of concentrations for each reverse primer was tested. From top to bottom, 0.4 (pink), 0.3 (green), 0.2 (blue) and 0.1 (red) pmol/µl of the 100R primer with the wild-type (AAA) 103 plasmid. Optimal reverse primer concentrations are in Tables 3.2 and 3.3.

3.3.2 HRMA Template

RNA was isolated with the MagNA Pure LC Instrument (Roche Applied Science, GmbH, Germany) from stored patient plasma. The nucleic acid was amplified by a nested RT-PCR and the products run on agarose gels (Figure 3.1 A) (Loubser et al., 2006). Amplified samples were purified with the High Pure PCR Product Purification Kit (Roche Applied Science, GmbH, Germany) and diluted 1:100 in Tris HCl pH 8.

DNA from different stages of the amplification process was used as template for HRMA. cDNA, first-round and second-round RT-PCR products were tested. The cDNA was too dilute as the crossing point for the PCR was ~40 cycles. First- or second-round PCR products, purified and diluted to 2.5 ng/reaction provided a suitable template for HRMA-PCR. The crossing point of the assays was ~10-20 cycles (data not shown).

3.3.3 HRMA-PCR Conditions

The optimal cycling conditions for HRMA-PCR on the LightCycler 480 Real-Time PCR were: 94 °C for 5 minutes with a ramp rate of 4.4 °C/s; 45 cycles at 95 °C for 10 seconds at 4.4 °C/s, 55 °C for 15 seconds at 2.2 °C/s and 72 °C for 15 seconds at 4.4 °C/s followed by HRM melting program.

3.3.4 HRM Melting Program

The melting program, which allows for HRMA, directly followed the real-time PCR. Melting from 40 °C to 95 °C, at 1°C/second, with 25 points of data/°C, produced the most distinct melting peaks (Figure 3.3). The high resolution melting began with 95 °C for one minute at 4.4 °C/s, 40 °C for one minute at 2.2 °C/s, then a temperature increase from 40 °C to 95 °C at 1 °C/s, followed by 40 °C for ten seconds at 2.2 °C/s.

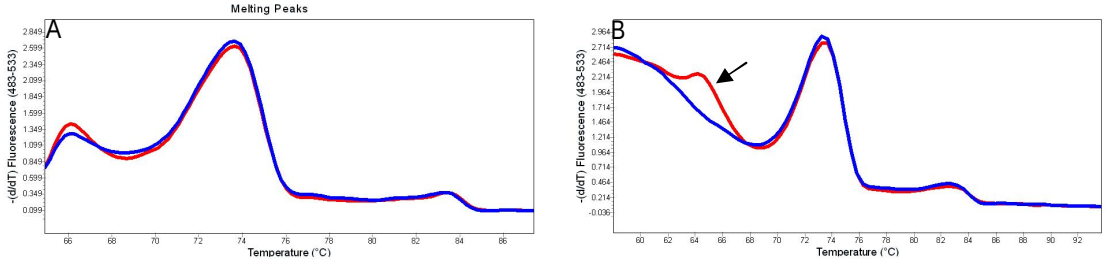

Figure 3.3. Optimization of the melt for HRMA. (**A**) The probe melting peak was absent when the melting step began at 65 °C. (**B**) When the melting began at 40 °C, a probe peak was present (arrow).

3.4 HRMA Probe Design and Optimization

3.4.1 HRMA Probes

Unlabeled probes are incorporated into HRMA assays to enhance detection of specific alleles (Zhou et al., 2004). A minimum of two probes per mutation site was designed; one complementary to the wild-type and the other complementary to the mutant sequence at the site of interest. Genotype detection occurs by means of an additional melting peak to the left of the amplicon melting peak. Ideally, if probes are short (< 21 bp), the non-corresponding probe does not bind and no probe peak is generated (Zhou et al., 2004). For optimal probe-target destabilization in the presence of a non-corresponding mutation, the variable base is placed in the

center of the probe (Erali et al., 2008; Montgomery et al., 2007b). Probe and amplicon melting peaks were required to fall within a defined temperature range, specific to each assay. Probes of 15 bp were designed on a South African consensus sequence and each probe was blocked by 3' phosphorylation. A concentration gradient (0.5-10 µM) was tested with each probe and the optimal concentration, which generated the most distinct peaks was 2 µM (Figure 3.4, green curve).

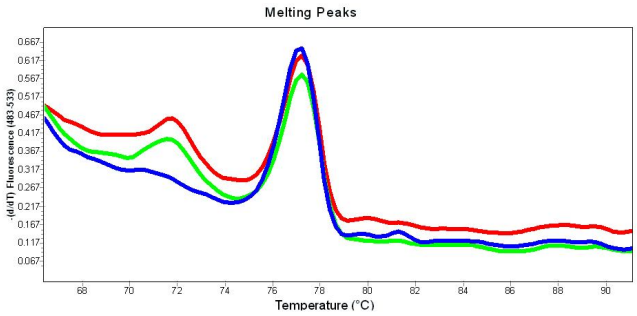

Figure 3.4. Optimization of probe concentration for HRMA. A concentration gradient with the probes was tested on the respective plasmids; from top to bottom, 5 (red), 2 (green) and 0.5 µM (blue) of the 103A (Table 3.4) probe with wild-type (AAA) 103 plasmids.

3.4.2 HRMA Probe Polymorphism Masking

The heterogeneous nature of HIV led to differences in the results generated upon application of the probes to plasmids and patient samples. As benign polymorphisms can disrupt accurate HRMA, a number of probe and primer modifications were introduced to mask the affects of the polymorphisms (Margraf et al., 2006). These alterations include incorporation of universal, ambiguous, mismatched or deleted bases, or locked nucleic acids (LNAs). Universal and ambiguous bases pair indiscriminately despite sequence variation. Mismatched bases are intentionally inserted in order to prevent base pairing with either the conserved or polymorphic base; thus masking the melting effects of the polymorphism. A deletion of a base in the probe causes the polymorphic or conserved base in the amplicon to bulge out, preventing participation

during HRMA (Margraf et al., 2006). LNAs are modified nucleic acids that have a higher binding affinity to their target and this may increase the binding affinity in the presence of destabilizing polymorphisms (Kaur et al., 2006; Koshkin et al., 1998). In addition PCRs using altered primers were designed (Table 3.3). In these assays the primers directly flank the mutation codon, thereby preventing polymorphic bases from interacting with the complementary probes.

3.5 Interpretation and Validation of HRMA Results

Three possible outcomes were generated, a correct genotype prediction, a discordant genotype prediction or no genotype prediction. Concordance between the HRMA result and the population sequencing result was considered a correct prediction. In addition to this, the probe and amplicon melting peaks had to fall within defined temperature intervals. When the genotypes by population sequencing and HRMA did not match, the result was considered discordant. In these cases HRMA on discordant samples was repeated and the patient samples were re-sequenced. No result occurred if no probe melting peaks were produced, if the melting peaks were small, if the melting peaks fell outside the defined melting intervals or if atypical curve shapes were generated. HRMA was repeated three times on these samples. In the Tables that follow the centre of the probe (red base) binds to the wild-type or mutant nucleotide of interest.

3.5.1 K103N Assay

K103N results in high level resistance to NVP and EFV (Ren and Stammers, 2008). Probes were designed to genotype the common wild-type (AAA/G) and mutant (AAC/T) sequences at codon 103. The probes designed for the K103N assay included complementary probes (15 bp), complementary short probes (11 bp), complementary short probes with LNAs and ambiguous

probes (Table 3.4). Altered primers were also designed to facilitate polymorphism masking (Table 3.3).

Table 3.4. Probe sequences for the K103N assay.

Codon (sequence)	Name	Sequence (5' -3')	Modification	Length (bp)	G+C (%)
K103 (AAA)	103A	CTGATTT**T**TTCTTTT	-	15	20
K103 (AAG)	103G	CTGATTT**C**TTCTTTT	-	15	27
K103N (AAC)	103C	CTGATTT**G**TTCTTTT	-	15	27
K103N (AAT)	103T	CTGATTT**A**TTCTTTT	-	15	20
K103 (AAA)	103A.S	GATTT**T**TTCTT	Short	11	18
K103 (AAG)	103G.S	GATTT**C**TTCTT	Short	11	27
K103N (AAC)	103C.S	GATTT**G**TTCTT	Short	11	27
K103N (AAT)	103T.S	GATTT**A**TTCTT	Short	11	18
K103 (AAA)	103A.LNA	GATTT**T**TTCTT	LNA	11	18
K103 (AAG)	103G.LNA	GATTT**C**TTCTT	LNA	11	27
K103N (AAC)	103C.LNA	GATTT**G**TTCTT	LNA	11	27
K103N (AAT)	103T.LNA	GATTT**A**TTCTT	LNA	11	18
K103 (AAA)	N103A	CTGAT**N**T**T**TTCTT**N**T	Ambiguous base	15	20-33
K103 (AAG)	N103G	CTGAT**N**T**C**TTCTT**N**T	Ambiguous base	15	27-40
K103N (AAC)	N103C	CTGAT**N**T**G**TTCTT**N**T	Ambiguous base	15	27-40
K103N (AAT)	N103T	CTGAT**N**T**A**TTCTT**N**T	Ambiguous base	15	20-33

Ambiguous base (N) is in green and locked nucleic acids (LNAs) are shown underlined.

The complementary probes accurately genotyped all four plasmids and 93 (80%) of the 116 samples. No probe melting peak was generated with 21 (18%) of the samples and two (1.7%) predictions were discordant with the population sequencing result (Table 3.5). The T_m of the amplicon-amplicon duplexes was 78 ± 2 °C and the T_m of the probe-amplicon duplexes was 72 ± 2 °C. Representative melting plots are shown in Figure 3.5. The genotype and HRMA results for the K103N assay are summarized in Appendix D, Table D2.

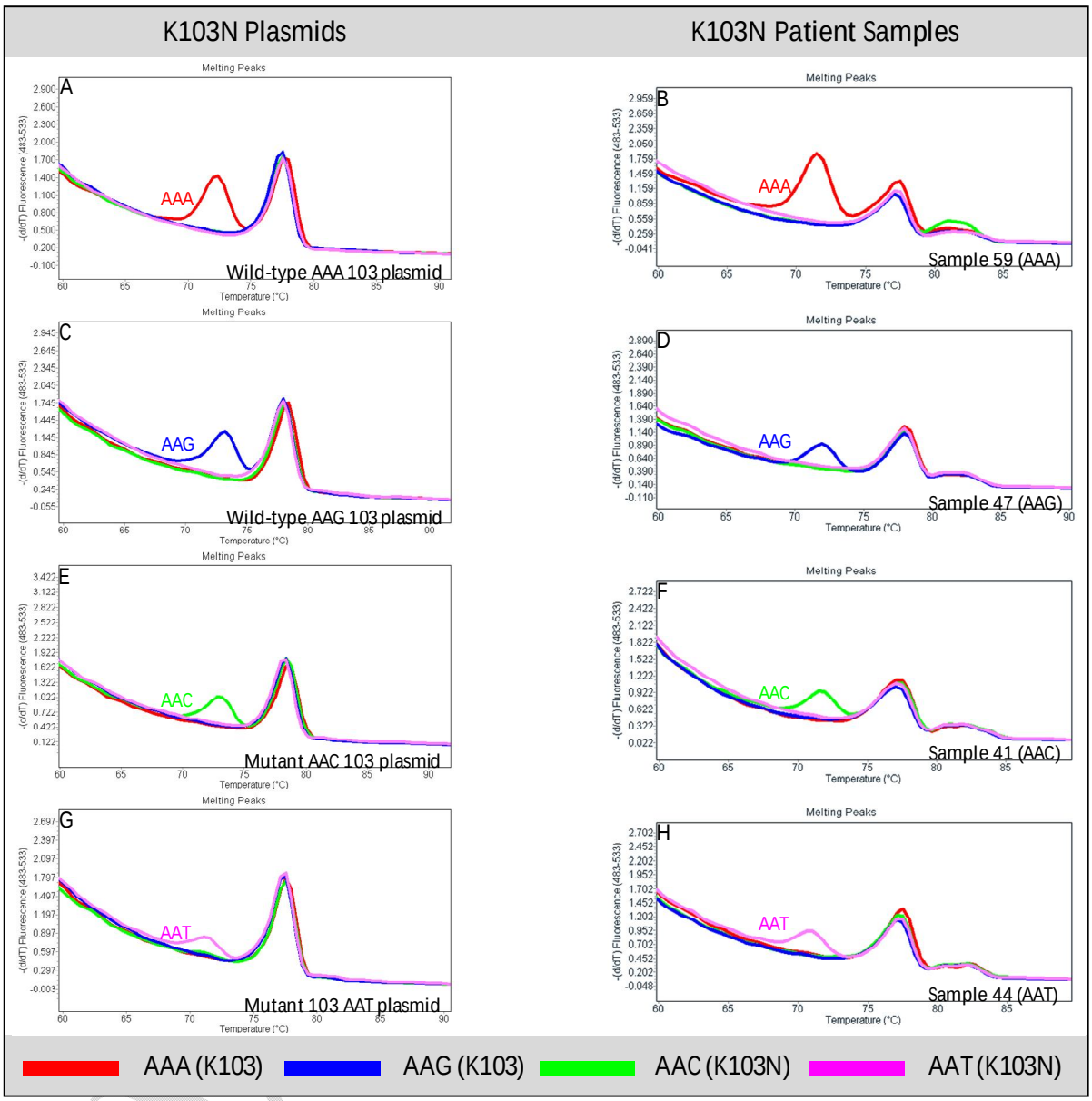

Figure 3.5. **Application of 103 HRMA assay to plasmids and patient samples.** Negative first derivative (-dF/dT) plots of the common SNP genotypes at position 103, obtained by using either engineered plasmids (left panels) or patient samples (right panels) and complementary probes. The presence of a probe peak alongside the amplicon peak indicates successful probe binding, allowing for the allocation of a 103 genotype to the sample. (**A**) Wild-type (AAA) plasmid and (**B**) wild-type (AAA) patient sample. (**C**) Wild-type (AAG) plasmid and (**D**) wild-type (AAG) patient sample. (**E**) Mutant (AAC) plasmid and (**F**) mutant (AAC) patient sample. (**G**) Mutant (AAT) plasmid and (**H**) mutant (AAT) patient sample.

HRMA incorporating polymorphism masking probes and altered primers was performed on the 21 samples that did not generate codon 103 genotype predictions when using the complementary probes. Ambiguous bases were incorporated at two polymorphic sites in the long probes (Table 3.4) as determined by analysis of the patient samples sequences (Table 3.6). Of the 21 samples to which these probes were applied, five genotypes were correctly predicted, five had discordant results and 11 samples did not generate a result (examples are shown in Figure 3.6). The short probes (illustrated in Figure 3.7) and probes incorporating LNAs (data not shown) did not generate probe melting peaks.

Using altered primers with the complementary probes, 10 genotypes of the 21 samples were correctly identified, while nine samples did not generate a result and two predictions were discordant (examples are shown in Figure 3.6). The K103N assay results for each primer and probe are summarized in the following Table.

Table 3.5. Summary of K103N assay results.

Assay	Correct	Discordant	No result
Complementary probes	93 (80%)	2 (1.7%)	21 (18%)
Of the 21 samples with no result:			
Complementary short probes	0	0	0
Complementary short probes with LNAs	0	0	0
Ambiguous bases	5	5	11
Altered primers	10	2	9
Total*	103 (89%)	9 (7.8%)	4 (3.4%)

* Calculated from Table D2 (Appendix D).

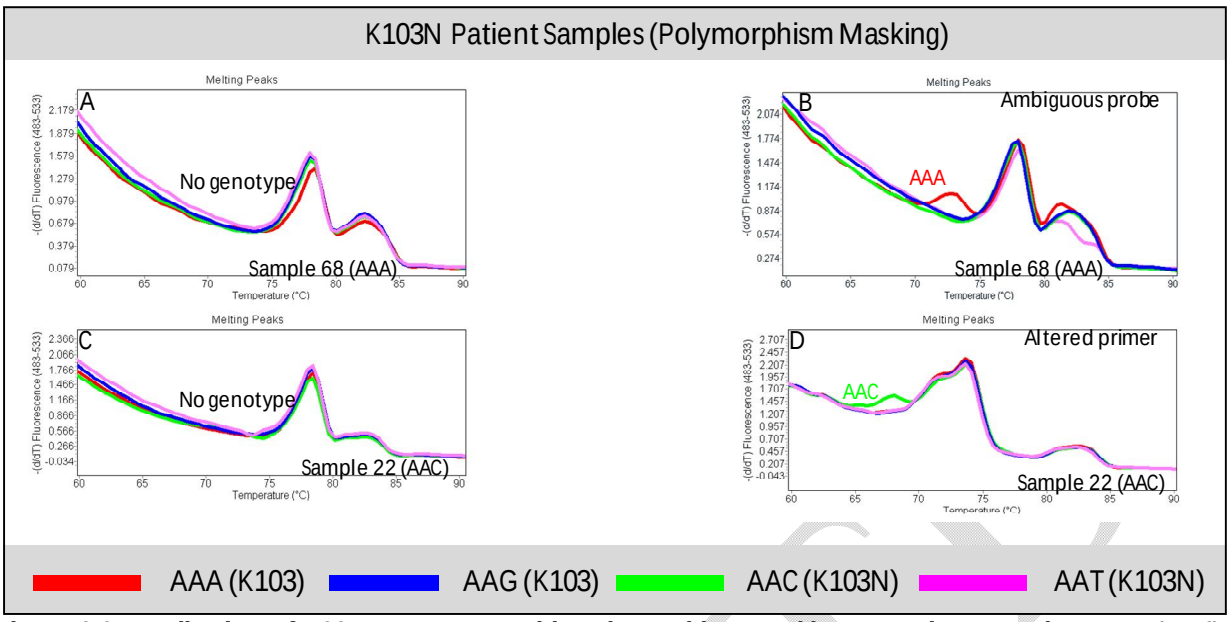

Figure 3.6. **Application of 103 HRMA assay with polymorphism masking to patient samples.** Negative first derivative (-dF/dT) plots of possible SNP genotypes at position 103, obtained by using patient samples and complementary probes, ambiguous probes and altered primers. A wild-type (AAA) patient sample with (**A**) complementary and (**B**) ambiguous probes. A mutant (AAC) patient sample with (**C**) regular and (**D**) altered primers with the same complementary probes.

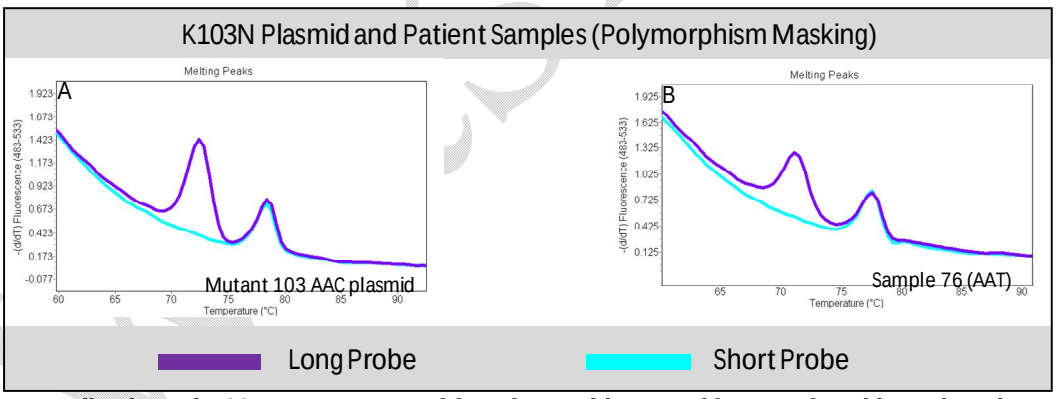

Figure 3.7. **Application of 103 HRMA assay with polymorphism masking to plasmids and patient samples.** Negative first derivative (-dF/dT) plots of common SNP genotypes at position 103, obtained by using either (**A**) engineered mutant (AAC) plasmid and (**B**) mutant (AAT) patient sample with complementary long probes (purple) or complementary short probes (turquoise).

To investigate reasons for discordant (n=2) or no results (n=21, Table 3.5), the patient sequences corresponding to the region of probe binding were examined (Table 3.6). In all cases where no

polymorphisms were present (n=93), the complementary probes were capable of accurately genotyping codon 103. However the presence of polymorphisms in the probe binding region appeared to interfere with HRMA. Polymorphisms in the patient samples clustered in three groups, two and seven bases upstream, and six bases downstream from the central base of the probe. The variation at the seventh base upstream from the probe center was due to the presence of the V106M NNRTI mutation; however this mutation did not seem to disrupt HRMA. Polymorphisms at the other two sites appeared to disrupt HRMA and the ambiguous nucleotides were incorporated at these sites (Tables 3.4 and 3.6).

Table 3.6. No result and discordant patient sequences with polymorphisms within the binding region of the K103N assay probes. Correctly genotyped samples without polymorphisms were excluded.

Wild-type sequence	A	A	A	A	G	A	A	A	A	A	A	T	C	A	G	
Patient Sample																
Sample 1b			W					M								
Sample 2b								M							R	
Sample 10a	G									R						
Sample 21															A	
Sample 23															A	
Sample 26								A			G					
Sample 35															A	
Sample 41		G						C								
Sample 43								C		G						
Sample 51															A	
Sample 53															A	**Modification:** None
Sample 56	M	G						C								**Result:** Correct prediction
Sample 62		G													A	
Sample 78								C			R					
Sample 81															A	
Sample 84		G						C							A	
Sample 87								C							A	
Sample 88															A	
Sample 92	M							C								
Sample 99	C															
Sample 101															A	
Sample 103								C							A	
Sample 5a										G						
Sample 22								C			G					
Sample 28		C													A	
Sample 40				G				C							A	**Modification:** Altered primers and/ or
Sample 50		G									G					ambiguous probe
Sample 60								M		G						**Result:** Correct prediction
Sample 68		G													A	
Sample 79											G					
Sample 94			C					C								
Sample 20							G									**Modification:** None
Sample 54							G	T								**Result:** Discordant prediction
Sample 5b										G					R	
Sample 10b	G							M		R						
Sample 11b								W								**Modification:** Altered primers and/or
Sample 12b								M		G					R	ambiguous probe
Sample 32							G								A	**Result:** Discordant prediction
Sample 46		G														
Sample 67			C				G								A	
Sample 33							G								A	**Modification:** Altered primers and ambiguous
Sample 71				G			G	C								probe
Sample 77											G					
Sample 97															A	**Result:** No prediction

The purple indicates the sites where ambiguous bases were incorporated. The samples in blue (AGA/C) did not generate a peak, samples in red (AGA/T) generated a discordant prediction.

Six patient samples carried the unusual AGA/T/C (K103N/S) drug resistance mutations, of which four could not be genotyped with the complementary probes. These four samples (samples 32, 33, 67 and 71 in blue in Table 3.6) had additional polymorphisms within the probe binding

region other than these rare codon 103 mutations. The combination of sequence variation adjacent the center of the probe and additional polymorphisms probably prevented probe binding due to thermal instability. The remaining samples (samples 20 and 54 in red in Table 3.6) did not carry any other polymorphism besides the rare AGA/T and generated discordant results. These two (1.7%) discordant predictions were wild-type (AAA and AAG) by HRMA but drug resistant by population sequencing (AGA and AGT).

To determine the limit of detection of the K103N assay using complementary probes, sample 47 was selected for clonal analysis. This sample generated a large probe peak which corresponded to the presence of the AAG genotype at 103. In addition a very small peak, representing AAA was also formed (Figure 3.8 A). This sample was selected for clonal analysis, which detected the presence of the AAA genotype in 3 of 100 clones (3%).

The complementary probes were applied to a serial dilution of K103N diluted in K103 and the limit of detection was ~5% of mixed species (Figure 3.8 B).

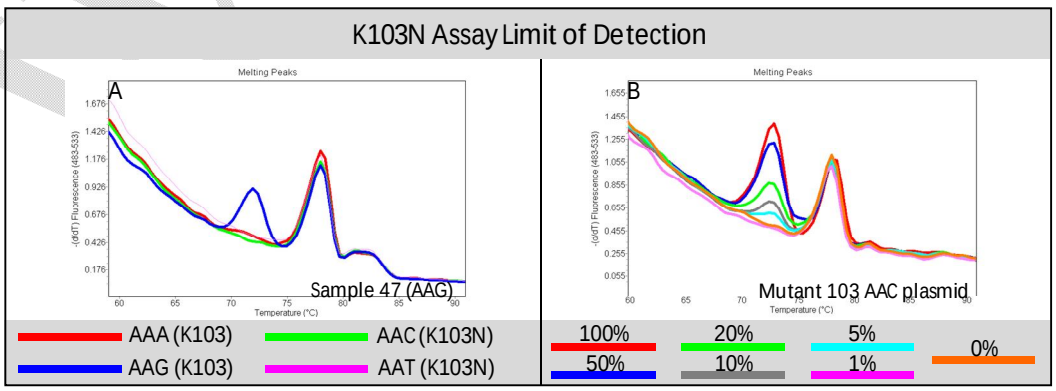

Figure 3.8. **103 HRMA assay and analytical sensitivity.** Negative first derivative (-dF/dT) plots of SNP genotypes at position 103, obtained by using a (**A**) patient sample and (**B**) engineered plasmids and complementary probes. (**A**) Wild-type (AAG) patient sample; a small peak corresponding to the AAA genotype is visible and was confirmed by clonal analysis (3%). (**B**) Dilution series of mutant AAC plasmid diluted in wild-type AAA plasmid.

In summary the complementary probes accurately genotyped the majority of the patient samples (n=93), with two discordant predictions (Table 3.5 and Appendix D, Table D2). The discordant samples carried unusual drug resistance mutations and were identified as wild-type by HRMA. The various polymorphism masking techniques had some success as ten of the 21 samples with no result were genotyped. Seven additional discordant results arose from the application of the altered primers and probes incorporating ambiguous bases. The short probes and those incorporation LNAs did not increase the success of the 103 assay. Despite this, with the unmodified probes and primers, 80% of the patient samples were accurately genotyped with two discordances and so this assay is useful for genotyping the clinically important 103 codon in HIV-1 samples.

3.5.2 Y181C Assay

Y181C (TAT → TGT) is a NNRTI mutation that is associated with strong NVP and moderate EFV resistance (Ren and Stammers, 2008). The probes designed for the Y181C assay included complementary probes and probes incorporating universal bases and deletions (Table 3.7).

Table 3.7. Probe sequences for the Y181C assay.

Codon (sequence)	Name	Sequence (5' -3')	Modification	Length (bp)	G+C (%)
Y181 (TAT)	wt181	ATATTGATAGATGAC	-	15	27
Y181C (TGT)	mut181	ATATTGACAGATGAC	-	15	33
Y181 (TAT)	wt181.univ	ATAITGATAGATGAC	Inosine	15	33
Y181C (TGT)	mut181.univ	ATAITGACAGATGAC	Inosine	15	40
Y181 (TAT)	wt181.del	ATA_TGATAGATGACT	Deletion	15	27
Y181C (TGT)	mut181.del	ATA_TGACAGATGACT	Deletion	15	33

The inosine (I) is in pink, the deletion is represented by the orange underscore and the additional base is in purple.

The complementary probes were applied to the wild-type and Y181C plasmids and 116 HIV-1 samples. The assay successfully genotyped the plasmids and 102 samples (88%), 11 samples

(9.5%) produced no probe melting peaks and three (2.6%) genotypes were discordant with the sequencing results (Table 3.8). While the other assays reported here required one melting program, the HRMA for codon 181 required two successive melts for optimal results. The T_m of the amplicon-amplicon duplexes was 75.8 ± 1 °C and the T_m of the probe-amplicon duplexes was 65 ± 2 °C. Representative melting plots are shown in Figure 3.9. The genotype and HRMA results for the Y181C assay are summarized in Appendix D, Table D3.

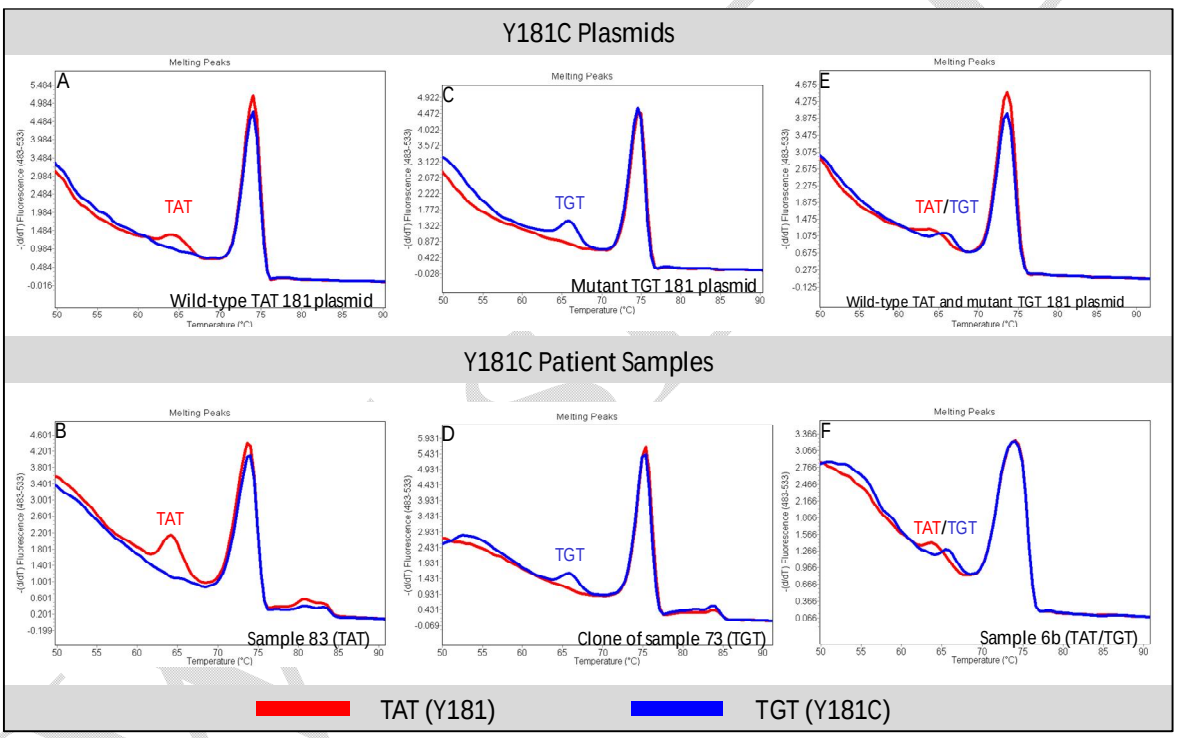

Figure 3.9. **Application of 181 HRMA assay to plasmids and patient samples.** Negative first derivative (-dF/dT) plots of common SNP genotypes at position 181, obtained by using either engineered plasmids (top box) or patient samples (bottom box) and complementary probes. The smaller probe peak at a lower T_m indicates successful probe binding, allowing for the allocation of a 181 genotype to the sample. (**A**) Wild-type (TAT) plasmid and (**B**) wild-type (TAT) patient sample. (**C**) Mutant (TGT) plasmid and (**D**) mutant (TGT) patient sample. (**E**) Mixture of wild-type and mutant plasmid and (**F**) patient sample.

Table 3.8. Summary of Y181C assay results.

Assay	Correct	Discordant	No result
Complementary probes	102 (88%)	3 (2.6%)	11 (9.5%)
Of the 11 samples with no result:			
Probe with inosine	3	0	8
Probe with deletion	7	0	4
Total*	109 (94%)	3† (2.6%)	4 (3.4%)

* Calculated from Table D3 (Appendix D).

† The discordance arose due to the increased analytical sensitivity of HRMA.

Discordance arose as HRMA identified wild-type Y181 (TAT) as well as minority Y181C (TGT) populations in three samples (6b, 69 and 73) which were determined to be completely wild-type (TAT) by population sequencing. One of these samples (73) was selected for clonal analysis and Y181C was detected in 33% of the 100 clones. This indicates that the 181 HRMA assay is more sensitive than population sequencing and so identifies minority resistant populations.

The limit of detection of the Y181C assay was determined by serial dilutions to be ~5% of mixed species (Figure 3.8). Therefore the extra limit of detection accounts for the 2.6% discordance as the HRMA assays can detect minority populations that sequencing cannot.

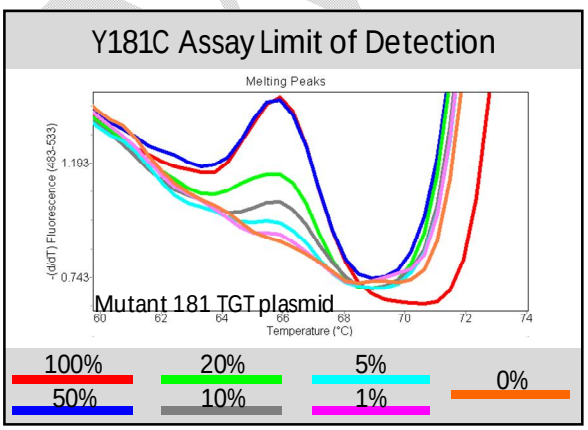

Figure 3.10. Determination of 181 HRMA assay limit of detection. Negative first derivative (-dF/dT) plot of a dilution series of mutant (TGT) at position 181 diluted in wild-type (TAT) obtained by using engineered plasmids and complementary probes for the determination of analytical sensitivity. The amplicon melting peaks have been cropped for increased visibility of the probe melting peaks.

To investigate reasons for discordant or no results, the patient sample sequences corresponding to the region of probe binding were examined (Table 3.9). Polymorphism that clustered at the 5' end of the probe binding region and five bases upstream from the center of the probe did not appear to interfere with HRMA, in that melting peaks were formed. However sequence variation in the middle of the probe did appear to prevent probe melting peak formation, which cannot be masked (Margraf et al., 2006). A guanine located four bases downstream from the probe center was present in six samples and in five of these samples no probe melting peaks were formed (example is shown in Figure 3.11 A). This polymorphism was then selected for masking as it is further from the center of the probe. Two types of masking techniques were attempted; incorporation of a universal base and the deletion of the polymorphic base (Table 3.7). The modified probes were applied to the 11 samples which generated no result with the complementary probes.

Table 3.9. No result and discordant patient sequences with polymorphisms within the binding region of the Y181C assay probes. Correctly genotyped samples without polymorphisms were excluded.

Wild-type sequence	G	T	C	A	T	C	T	A	T	C	A	A	T	A	T	
Patient Sample																
Sample 5a			T													
Sample 5b			T													
Sample 6a			T													
Sample 8a															C	
Sample 8b															C	
Sample 9a			T													
Sample 9b			T													
Sample 10a			Y													
Sample 19			A					R								
Sample 20						Y										
Sample 25			Y													
Sample 27									Y							
Sample 30			T													
Sample 32		A	T													
Sample 35			T													
Sample 36			T													
Sample 38			T													
Sample 45			T												C	
Sample 48						T										
Sample 50	A		T													
Sample 52			G												C	**Modification:** None
Sample 57						T										**Result:** Correct prediction
Sample 60			T			T						R				
Sample 63															C	
Sample 64			T												C	
Sample 65			T												C	
Sample 66			T												C	
Sample 67		A	T													
Sample 70			T												C	
Sample 71	R															
Sample 74			T													
Sample 84												G				
Sample 85						T		R							C	
Sample 87			T			T										
Sample 89															C	
Sample 91			T												C	
Sample 92						Y										
Sample 95			G												Y	
Sample 96			T													
Sample 99			T												C	
Sample 100			Y									R			C	
Sample 103						T										
Sample 15												G				
Sample 34												G				**Modification:** Deletion probe
Sample 49			M									G				**Result:** Correct prediction
Sample 58						Y						G				
Sample 6b*			T													**Modification:** None
Sample 69*																**Result:** Discordant prediction
Sample 73*																
Sample 26			T													**Modification:** None and/ or deletion probe
Sample 62		A	A									G				**Result:** No prediction
Sample 77									C							
Sample 90									C							

* The discordance arose due to the increased sensitivity of HRMA as compared to population sequencing.

A deletion of the polymorphic site (guanine) was introduced at this position (Table 3.7), which causes the polymorphic base to bulge out during base pairing thereby preventing destabilization. In order to maintain the 15 bp probe length an extra nucleotide was added. These probes were applied to the 11 polymorphic patient samples, previously with no result, and the correct genotype was predicted with seven samples (example is shown in Figure 3.11 B).

Inosine is a base that pairs indiscriminately and was incorporated at the same polymorphic position within the probes (Table 3.7). These probes were applied to the same 11 polymorphic patient samples. While small peaks were generated, three genotypes were correctly predicted and eight could not be genotyped (illustrated in Figure 5.11 C).

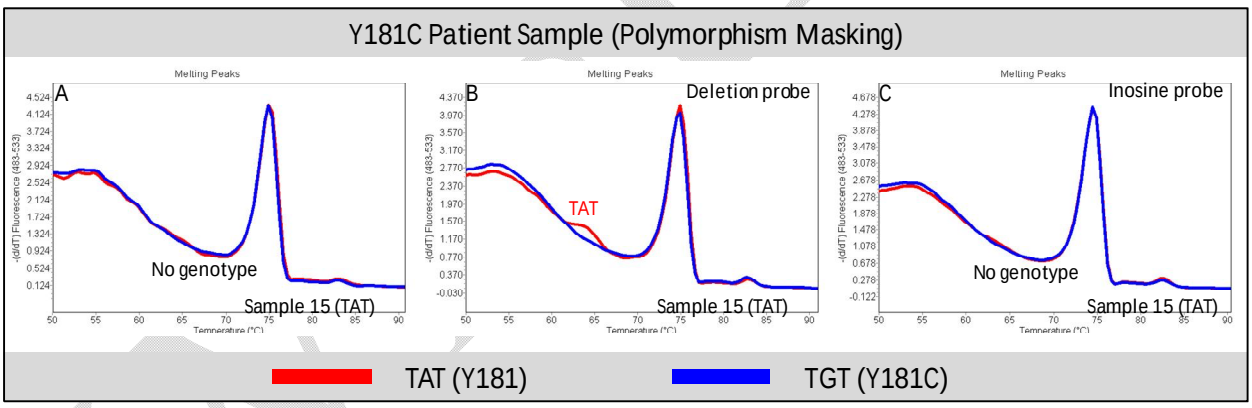

Figure 3.11. **Application of 181 HRMA assay with polymorphism masking to patient samples.** Negative first derivative (-dF/dT) plots of wild-type (TAT) at position 181, obtained by using a wild-type patient sample and (**A**) complementary probes, (**B**) deletion probes and (**C**) universal probes.

In summary the complementary probes and probes incorporating a deletion successfully genotyped most samples (n=109) at position 181, with only four samples without a result (Table 3.8 and Appendix D, Table D3). The 181 HRMA assay was more sensitive (~5%) than

population sequencing and so the assay error rate may be zero for the samples selected. Thus this assay can be used to accurately genotype the 181 codon in most HIV-1 samples.

3.5.3 M184V Assay

M184V (ATG → GTG) is a NRTI mutation that results in high level resistance to 3TC, low level resistance to ddI and ABC, but increased susceptibility to ZDV, d4T and TDF (Shafer and Schapiro, 2008). Complementary probes (Table 3.10) and altered primers (Table 3.3) were utilized for the M184V HRMA assay.

Table 3.10. Probe sequences for the M184V assay.

Codon (sequence)	Name	Sequence (5' -3')	Modification	Length (bp)	G+C (%)
M184 (ATG)	wt184V	TCATCCA**T**ATATTGA	-	15	33
M184V (GTG)	mut184V	TCATCCA**C**ATATTGA	-	15	27

The genotypes of the wild-type and mutant plasmids and 92 of 116 patient samples (79%) were correctly predicted, 20 samples (17%) could not be genotyped and four (3.4%) genotypes were discordant with the sequencing results (Table 3.11). The T_m of the amplicon-amplicon duplexes was 75.5 ± 1 °C and the T_m of the probe-amplicon duplexes was 67 ± 1 °C. Representative melting plots are shown in Figure 3.12. The genotype and HRMA results for the M184V assay are summarized in Appendix D, Table D4.

Table 3.11. Summary of M184V assay results.

Assay	Correct	Discordant	No result
Complementary long probes	92 (79%)	4 (3.4%)	20 (17.2%)
Of the 20 samples with no result:			
Altered primers	10	0	10
Total*	102 (88%)	4† (3.4%)	10 (8.6%)

* Calculated from Table D4 (Appendix D).

† Three discordance arose due to the increased analytical sensitivity of HRMA.

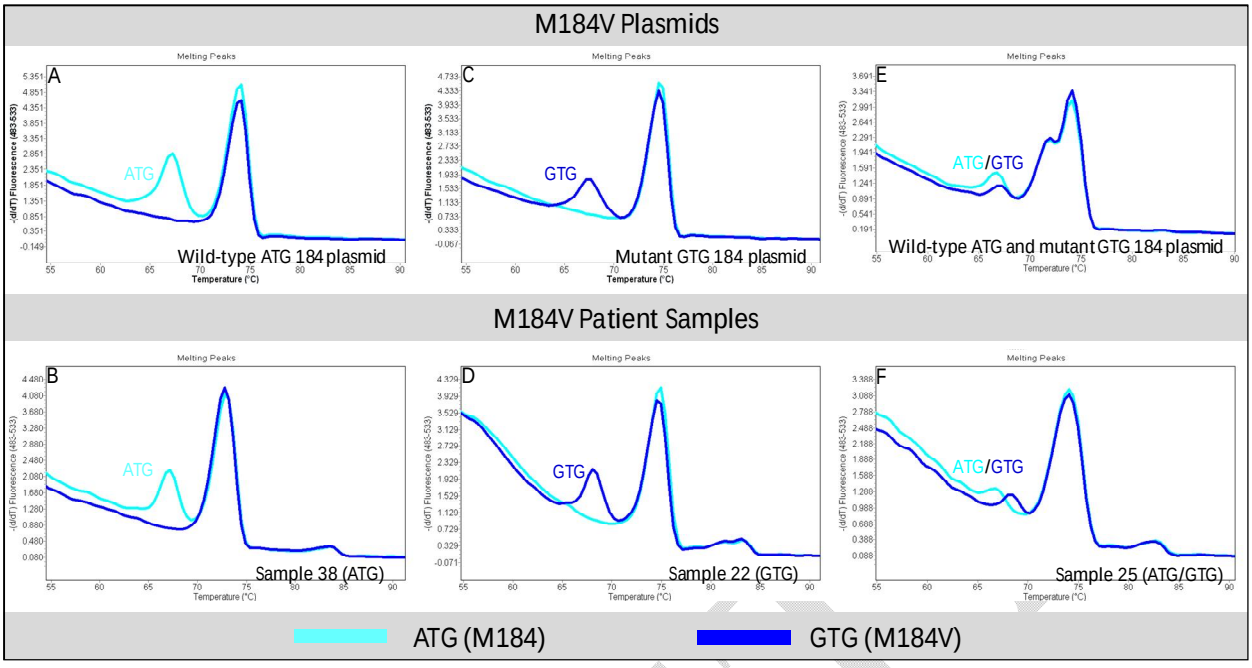

Figure 3.12. **Application of 184 HRMA assay to plasmids and patient samples.** Negative first derivative (-dF/dT) plots of the common SNP genotypes at position 184, obtained by using either engineered plasmids (top box) or patient samples (bottom box) and complementary probes. The presence of a probe peak alongside the amplicon peak indicates successful probe binding, allowing for the allocation of a 184 genotype to the sample. (**A**) Wild-type (ATG) plasmid and (**B**) wild-type (ATG) patient sample. (**C**) Mutant (GTG) plasmid and (**D**) mutant (GTG) patient sample. (**E**) Mixture of wild-type and mutant plasmids and (**F**) patient sample.

Altered primers were designed (Table 3.3) and applied with the complementary probes to the 20 patient samples that could not be genotyped. Ten of the 20 genotypes could be correctly determined while the remaining samples could not be genotyped as no melting peaks were produced (example in Figure 3.13). Analysis of the sequences corresponding to the probe binding region indicated that sequence variation directly adjacent to the mutation site of interest usually prevented melting peak formation (Table 3.12). In addition, guanine four bases downstream from the probe center did appear to prevent probe curve formation.

Table 3.12. No result and discordant patient sequences with polymorphisms within the binding region of the M184V assay probes. Correctly genotyped samples without polymorphisms were excluded.

Wild-type sequence	T	C	A	A	T	A	T	A	T	G	G	A	T	G	A	
Patient Sample																
Sample 27	Y															**Modification:** None **Result:** Correct prediction
Sample 28								G		R						
Sample 60				R												
Sample 65								G		R						
Sample 69								G		R						
Sample 70							C	G								
Sample 77	C															
Sample 90	C							G								
Sample 95							Y									
Sample 34				G												**Modification:** Altered primers **Result:** Correct prediction
Sample 49				G				G								
Sample 58				G												
Sample 62				G				G								
Sample 63							C									
Sample 84				G												
Sample 89							C									
Sample 91							C	G								
Sample 99							C									
Sample 100				R			C									
Sample 10b*																**Modification:** None **Result:** Discordant prediction
Sample 35								R		R						
Sample 55*																
Sample 92*																
Sample 8a							C									**Modification:** Altered primers **Result:** No prediction
Sample 8b								G	G	A						
Sample 15				G												
Sample 45							C									
Sample 52							C									
Sample 64							C									
Sample 66							C									
Sample 71										A						
Sample 85							C									

* The discordance arose due to the increased sensitivity of HRMA as compared to population sequencing.

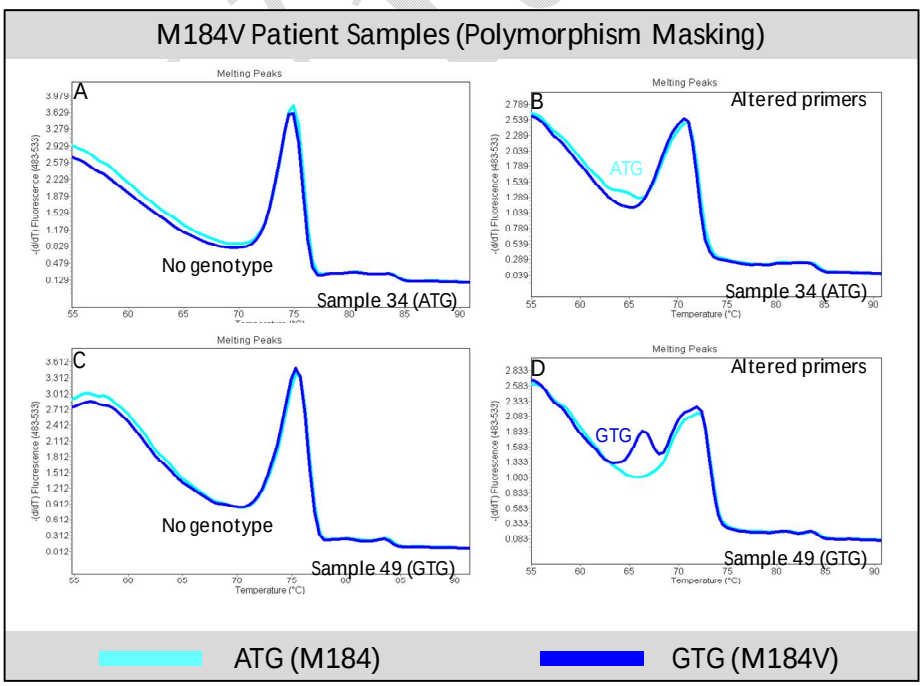

Figure 3.13. Application of 184 HRMA assay with polymorphism masking to patient samples. Negative first derivative (-dF/dT) plots of position 184, obtained by using a wild-type (ATG) patient sample and (**A**) normal and (**B**) altered primers; and a mutant (GTG) patient sample with (**C**) normal and (**D**) altered primers.

The limit of detection was ~20% of mixed species, as determined by serial dilutions with the wild-type and M184V plasmid (Figure 3.14). This assay is slightly more sensitive than population sequencing but is less sensitive than the HRMA assays for codons 103 and 181.

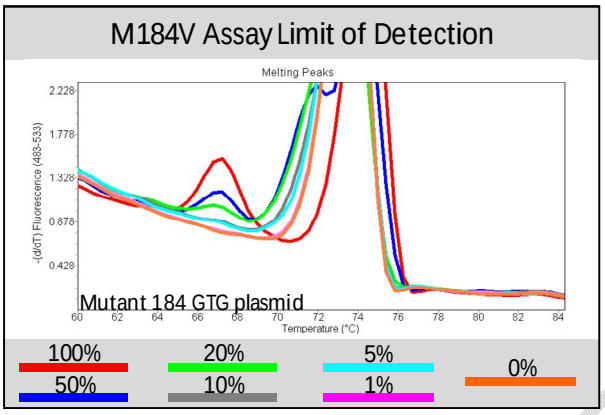

Figure 3.14. Determination of 184 HRMA assay limit of detection. Negative first derivative (-dF/dT) plot of a dilution series of mutant (GTG) at position 184 diluted in wild-type (ATG) obtained by using engineered plasmids and complementary probes for the determination of analytical sensitivity. The amplicon melting peaks have been cropped for increased visibility of the probe melting peaks.

Discordance arose as HRMA identified wild-type M184 (ATG) as well as minority M184V (GTG) populations in three samples (10b, 55 and 92) which were determined to be completely wild-type (ATG) by population sequencing. Two of these samples (10b and 92) were selected for clonal analysis and M184V (GTG) was detected in 25% and 20% of the 100 clones, respectively. Consequently, the increased sensitivity of HRMA in comparison with population sequencing accounts for these three discordances.

One sample (35) was identified as mutant M184V (GTG) by HRMA but wild-type (ATG) by population sequencing. The sample was resequenced and the reason for this discordance is unknown but it may be due to the unique A/GTA/G sequence at codon 184 of this sample.

Excluding the samples which were discordant due to the extra analytical sensitivity of the M184V assay, the error rate of the assay is probably ~0.9%.

In summary the complementary probes and altered primers accurately genotyped (n=102) most patient samples (Table 3.11 and Appendix D, Table D4). Similar to the assay for codon 181, the error rate is probably lower than that calculated due to the extra sensitivity of the HRMA assays. As with the preceding assays, at the respective sites (103 and 181), this assay can be utilized to accurately genotype the codon 184 in most HIV-1 patient samples.

3.5.4 Q151M Assay

Q151M (CAA/G → ATG) results in high level resistance to the NRTIs ZDV, d4T, ddI and ABC (Shafer and Schapiro, 2008). The probes designed for the Q151M assay included complementary probes and probes incorporating mismatches (Table 3.13). Altered primers were also designed to facilitate polymorphism masking (Table 3.3)

Table 3.13. Probe sequences for the Q151M assay.

Codon (sequence)	Name	Sequence (5' -3')	Modification	Length (bp)	G+C (%)
Q151 (CAA)	wt151A	TCCATCC**T**TGTGGAA	-	15	47
Q151 (CAG)	wt151G	TCCATCC**C**TGTGGAA	-	15	53
Q151M (ATG)	mt151	CCATCC**CAT**TGGAAG	-	15	53
Q151 (CAA)	wt151A.mm	TCCATCC**T**TG**A**GGAA	Mismatch	15	47

Mismatched base is in blue.

When applied to plasmids and patient samples, the complementary probes often produced inconclusive results. Specifically, the wt151A probe, designed to signal the presence of the wild-type CAA genotype, produced a melting peak when bound to either the CAA or CAG sequence, indicating limited non-specific binding at this position (Figure 3.15A). The wt151G probe,

designed to signal the wild-type CAG genotype, correctly produced a melting peak in the presence of the CAG sequence only; however the curve was shifted on the –dF/dT rather than the temperature axis (Figure 3.15B). Lastly, the mt151 probe, designed to indicate the mutant ATG sequence, did not generate a melting peak when applied to the Q151M (ATG) plasmids (Figure 3.15C). However the mt151 probe was still applied to patient samples, with which it generated accurate melting peaks. The reason for the inconsistent performance of this probe, which was dependent on the genetic material, is unknown. The T_m of the amplicon-amplicon duplexes was 76.5 ± 2 °C and the T_m of the probe-amplicon duplexes was 71 ± 2 °C. Representative melting plots are shown in Figures 3.15 and 3.16. The genotype and HRMA results for the Q151M assay are summarized in Appendix D, Table D5.

To compensate for the limited non-specific binding of the wt151A probe, a deliberate mismatch (T→A) was incorporated to destabilize the probe binding (Table 3.13). The wt151A.mm, wt151G and mt151 probes were then applied to 116 patient samples. Eighty-one samples (69.8%) were correctly genotyped and four predictions (3.4%) were discordant with the population sequencing result. The remaining 31 (26.7%) samples could not be genotyped as small or no probe melting peaks were generated (Table 3.14).

Table 3.14. Summary of Q151M assay results.

Assay	Correct	Discordant	No result
Complementary probes with mismatch	81 (70%)	4 (3.4%)	31 (27%)
Of the 32 samples with no result:			
Altered primers	17	0	14
Total*	98 (85%)	4 (3.4%)	14 (12%)

* Calculated from Table D5 (Appendix D).

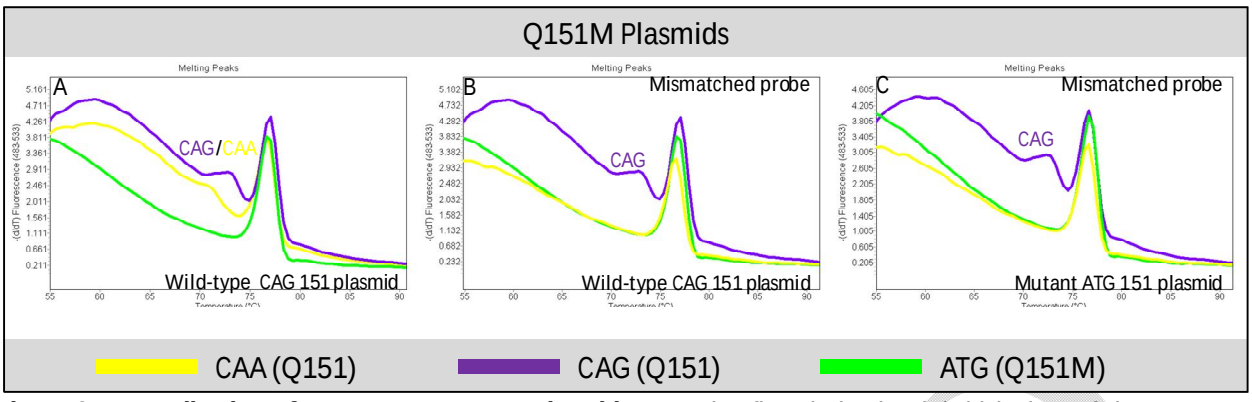

Figure 3.15. Application of 151 HRMA assay to plasmids. Negative first derivative (-dF/dT) plots of the common SNP genotypes at position 151, obtained by using engineered plasmids and probes. The presence of a probe peak alongside the amplicon peak indicates successful probe binding, allowing for the allocation of a 151 genotype to the sample. (**A**) Wild-type (CAG) plasmid with a complementary probe and (**B**) wild-type (CAG) plasmid with the wt151A.mm mismatched probe. This mismatch was introduced to prevent the non-specific binding of the wt151A probe. (**C**) Mutant (ATG) plasmid with the complementary and mismatched probes.

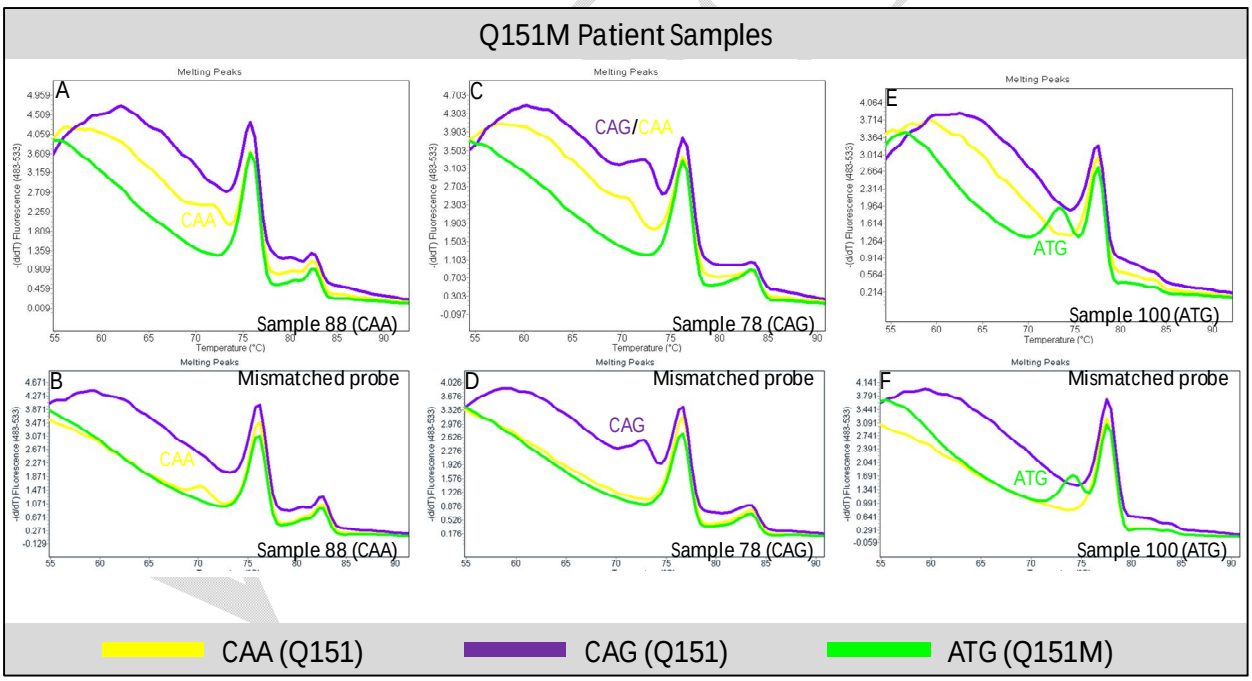

Figure 3.16. Application of 151 HRMA assay to patient samples. Negative first derivative (-dF/dT) plots of the common SNP genotypes at position 151, obtained by using patient samples and probes. (**A**) Wild-type (CAA) patient sample with complementary and (**B**) mismatched probes. (**C**) Wild-type (CAG) patient sample with complementary and (**D**) mismatched probes. (**E**) Mutant (ATG) patient sample with complementary and (**F**) mismatched probes.

To determine reasons for the discordant or no results, the patient sequences corresponding to the region of probe binding were examined (Table 3.15). The majority of the polymorphisms clustered four bases upstream from codon 151.

Table 3.15. No result and discordant patient sequences with polymorphisms within the binding region of the Q151M assay probes. Correctly genotyped samples without polymorphisms were excluded.

Wild-type sequence	C	T	T	C	C	A	C	A	G	G	G	A	T	G	G	A	
Patient Sample																	
Sample 6a			Y														
Sample 11a												R					
Sample 11b												R					
Sample 23						W						G					
Sample 27			Y														
Sample 36												M					
Sample 41						R											
Sample 51												G					**Modification:** None
Sample 54			G														**Result:** Correct prediction
Sample 66			A														
Sample 69			G														
Sample 71						M											
Sample 81												K					
Sample 84			C				A	T									
Sample 87												R					
Sample 97			C				M	T									
Sample 102												G					
Sample 34			G									G					
Sample 40			G														
Sample 42	T		G														
Sample 45			G														
Sample 58			G														
Sample 59			G														**Modification:** Altered primers
Sample 64			A														**Result:** Correct prediction
Sample 65			A														
Sample 75			G														
Sample 76			A														
Sample 95			R														
Sample 99	T		G														
Sample 10b									A								**Modification:** None
Sample 14			A														**Result:** Discordant prediction
Sample 67																	
Sample 7a			K						A								
Sample 7b			K						A								
Sample 13a			G						A			G					
Sample 13b			G						A			G					
Sample 18			G														**Modification:** Altered primers
Sample 20			G														
Sample 21			G									G					**Result:** No prediction
Sample 38			C			T											
Sample 44			C						A								
Sample 52						C			A								
Sample 90			A														

PCRs using altered primers were designed to mask polymorphisms (Table 3.3) and were applied with the complementary probes to the 31 patient samples with no result. Seventeen genotypes were correctly predicted and 14 samples could not be genotyped (Table 3.14). However the melting peaks that were generated were small (examples are shown in Figure 3.17).

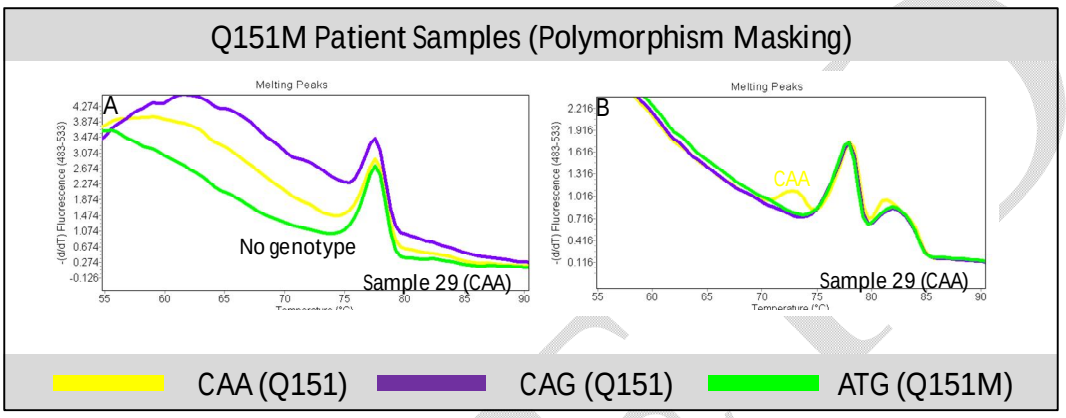

Figure 3.17. Application of 151 HRMA assay with polymorphism masking to patient samples. Negative first derivative (-dF/dT) plots of wild-type (CAA) at position 151, obtained by using a wild-type patient sample and (**A**) normal primers and (**B**) altered primers.

HRMA did not detect Q151M minority population in any samples and so the limit of detection could not be studied by clonal analysis. However one patient sample (sample 26) which was wild-type by population sequencing and by HRMA was selected for clonal analysis. This confirmed the genotype as the sample was 100% wild-type by analysis of 100 clones. A dilution series could not be performed as the mt151 probe could not detect the Q151M plasmid.

The Q151M assay generated four discordant results (samples 10b, 14, 67, 70). The discordant predictions occurred between the wild-type genotypes CAA and CAG, rather than mutant ATG genotype. This discordances did not have clinical relevance as wild-type samples of one genotype were incorrectly predicted to be wild-type with the other 151 wild-type genotype.

In summary the two complementary probes and one probe incorporating a mismatch accurately genotyped most of the samples (n=81) with a small discordance (n=4). Despite the generation of small peaks when the altered primers were utilized, polymorphism masking was successful with half (n=17) of the polymorphic samples (Table 3.14 and Appendix D, Table D5) and so the total number of samples genotyped was 98. While not as reliable or accurate as the preceding assays this assay did genotype most wild-type and all mutant 151 codons in the patient samples.

3.5.5 G190A Assay

G190A is a NNRTI mutation conferring resistance to NVP (Boyer et al., 1998). Complementary probes were designed to hybridize to the common GGA wild-type sequence and GCA mutant sequence (Table 3.16). In addition altered primers were designed for the purposes of polymorphism masking (Table 3.3).

Table 3.16. Probe sequences for the G190A assay.

Name (sequence)	Sequence (5' -3')	Modification	Length (bp)	G+C (%)
wt190 (GGA)	ATCAGATCCTACATA	-	15	33
mut190A (GCA)	ATCAGATGCTACATA	-	15	33

The 190 assay was applied to the wild-type and mutant G190A plasmids and patient samples. Large probe peaks were generated that were partially merged with the amplicon melting peaks, however these probe peaks were consistent and could be used to successfully genotype position 190 in 73 (63%) of the 116 patient samples. No clear probe peak was present in 41 samples (35%) and two (1.7%) samples generated discordant genotype predictions (Table 3.17). The T_m of the amplicon-amplicon duplexes was 73.9 ± 1 °C and the T_m of the probe-amplicon duplexes

was 71.5 ± 1 °C. Representative melting plots are shown in Figures 3.18 and 3.19. The genotype and HRMA results for the G190A assay are summarized in Appendix D, Table D6.

Table 3.17. Summary of G190A assay results.

Assay	Correct	Discordant	No result
Complementary long probes	73 (63%)	2 (1.7%)	41 (35%)

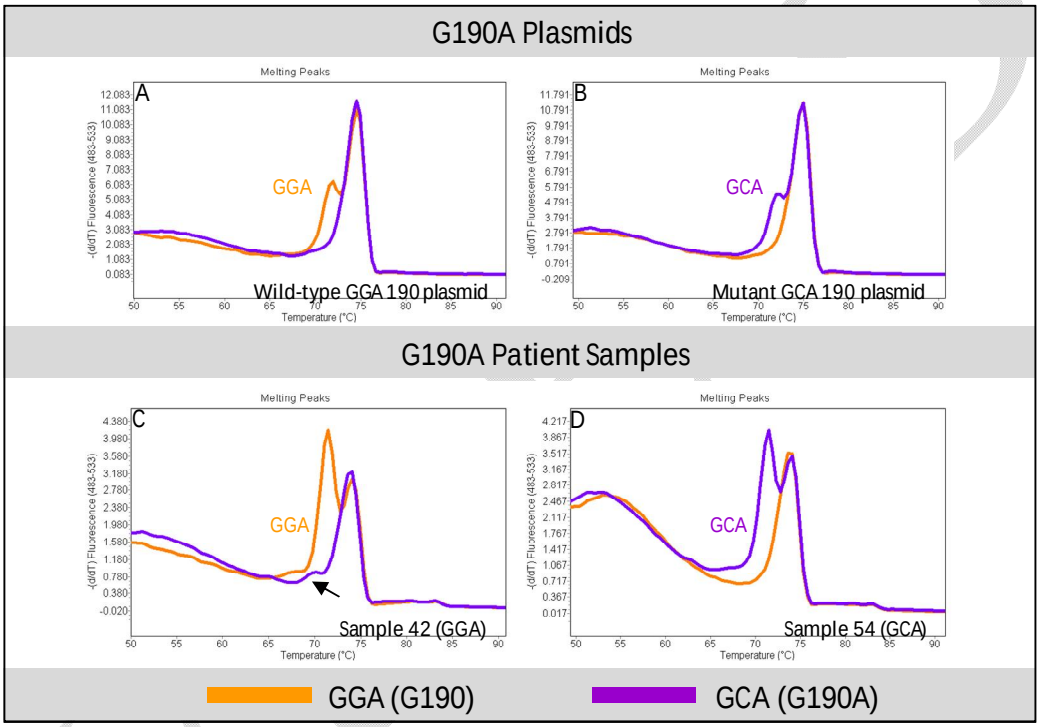

Figure 3.18. **Application of 190 HRMA assay to plasmids and patient samples.** Negative first derivative (-dF/dT) plots of the common SNP genotypes at position 190, obtained by using either engineered plasmids (top box) or patient samples (bottom box) and complementary probes. The probe peak at a lower T_m indicates successful probe binding, allowing for the allocation of a 190 genotype to the sample. (**A**) Wild-type (GGA) and (**B**) mutant (GCA) plasmid; (**C**) wild-type (GGA) and (**D**) mutant (GCA) patient sample. The mut190A probe usually produced a small peak in the presence of the GGA sequence (arrow).

Altered primers (Table 3.3) were designed and applied with the complementary probes to the 41 samples that could not be genotyped. In most of these samples, probe peaks corresponding to both the wild-type and mutant genotypes were generated, regardless of the sample genotype

(examples are shown in Figure 3.19). Consequently the altered primers could not be used to genotype any patient samples.

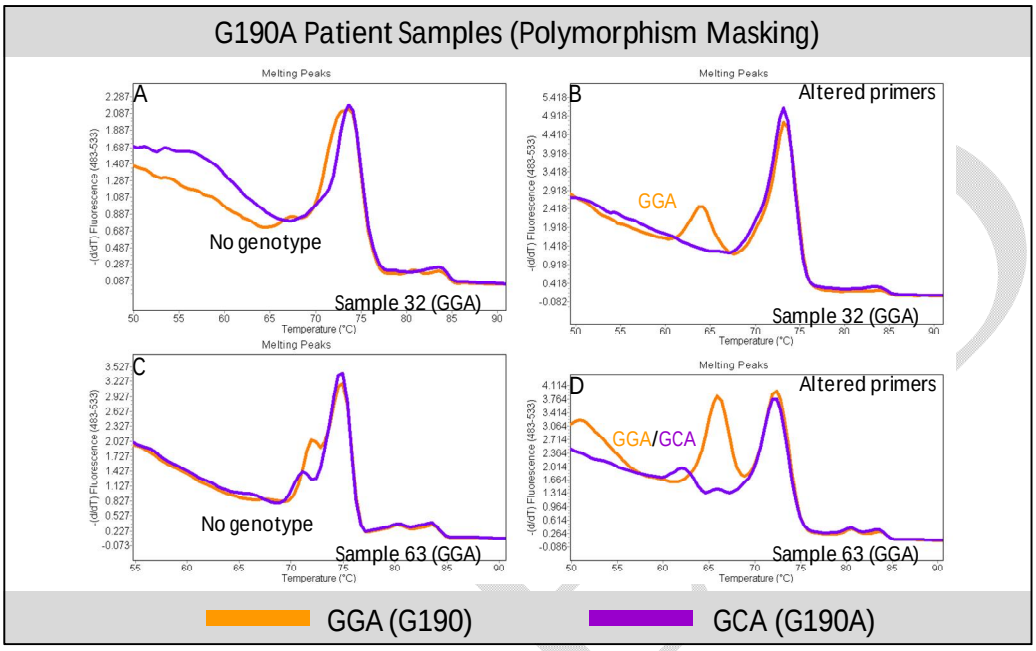

Figure 3.19. **Application of 190 HRMA assay with polymorphism masking to patient samples.** Negative first derivative (-dF/dT) plots of possible SNP genotypes at position 190, obtained by using patient samples and complementary probes with normal or altered primers. Wild-type (GGA) patient sample with (**A**) normal and (**B**) altered primers. Wild-type (GGA) patient sample with (**C**) normal and (**D**) altered primers.

A 190 genotype could not be allocated to samples with no melting peaks, small melting peaks or peaks that lacked sharp boundaries (illustrated in Figure 3.19 A and C). Samples generating small peaks and those with indistinct boundaries introduced ambiguity to the genotype interpretation. The sequences of the patient samples corresponding to the probe binding region were investigated to determine the affects of polymorphisms on melt curve generation (Table 3.18). Similar to the preceding assays the presence of sequence variation directly adjacent to the mutation codon appeared to prevent probe melting peak formation. Polymorphisms at the 5' end of the probe did not appear to disrupt HRMA as did base changes in most other locations.

Table 3.18. No result and discordant patient sequences with polymorphisms within the binding region of the G190A assay probes. Correctly genotyped samples without polymorphisms were excluded.

Wild-type sequence	T	A	T	G	T	A	G	G	A	T	C	T	G	A	C	
Patient Sample																
Sample 4a				R												
Sample 7b		R														
Sample 9a						G										
Sample 10b															T	
Sample 11a															Y	
Sample 12a															T	
Sample 18															T	
Sample 23															T	
Sample 24															T	
Sample 27			Y						R							
Sample 29															T	
Sample 33								C			Y					
Sample 38															T	**Modification:** None
Sample 46	Y	W													Y	**Result:** Correct prediction
Sample 52															T	
Sample 55															T	
Sample 56															T	
Sample 58															T	
Sample 64															T	
Sample 66															T	
Sample 72															T	
Sample 77															T	
Sample 94															T	
Sample 96															T	
Sample 97									K						T	
Sample 99															T	
Sample 103															T	
Sample 8b							A									**Modification:** None
Sample 12b		R						S							T	**Result:** Discordant prediction
Sample 4b				R				S								
Sample 5a											W					
Sample 9b		R				G										
Sample 10a															T	
Sample 11b		R													Y	
Sample 20						Y			R							
Sample 21	Y	W				G										
Sample 25															T	
Sample 28															T	
Sample 32									G						T	
Sample 36									C		A					
Sample 37								S							T	
Sample 44						G										
Sample 47	C	T													T	**Modification:** None
Sample 50						K										**Result:** No prediction
Sample 53		R														
Sample 59						T			C							
Sample 61	C															
Sample 62						G										
Sample 65															T	
Sample 69									R							
Sample 75								C							T	
Sample 78						G										
Sample 81		G														
Sample 84															T	
Sample 85							A		C						Y	
Sample 101		R						S								
Sample 102											Y				T	

Discordance arose with sample 8b which had the G190T (AGA) mutation and was identified as wild-type by HRMA. The other discordant prediction, with sample 12b, was identified as wild-type (GGA) by HRMA but GGA/C by population sequencing. The 1.7% error rate does not reflect the insensitivity of population sequencing but rather the inaccuracy of the 190 HRMA assay.

HRMA did not detect G190A minority population in any samples and so the limit of detection could not be studied by clonal analysis. However a patient sample (10b) which was wild-type by population sequencing and by HRMA was selected for clonal analysis. One of the 100 (1%) clones harboured G190A which were not detected by HRMA or population sequencing.

In summary the G190A assay is not as useful as the preceding assays in genotyping the respective mutation codons as only 73 samples could be genotyped (Table 3.17 and Appendix D, Table D6). Despite this, the discordance was low as only two samples generated incorrect genotypes. Polymorphism severely affected the 190 assay and the altered primers did not allow for accurate masking in 41 samples. No particular sequence appeared to generate the aberrant melting peaks for assay G190A and so additional polymorphism masking techniques were not attempted.

3.5.6 K65R Assay

K65R (AAG → AGG) is a multi NRTI resistance mutation selected for by TDF, ABC, ddI, and d4T (Xu et al., 2009). The probes designed for the K65R assay included complementary probes and probes incorporating mismatches and deletions (Table 3.19).

Table 3.19. Probe sequences for K65R assay.

Codon (sequence)	Name	Sequence (5' -3')	Modification	Length (bp)	G+C (%)
K65 (AAG)	wt65G	TGTCCTTCTTTTTTA	-	15	27
K65R (AGG)	mt65	GTCCTTCCTTTTTAT	-	15	33
K65 (AAG)	wt65G.MM	TGTCATTCTTTTTTA	Mismatch	15	20
K65R (AGG)	mt65.MM	GTCATTCCTTTTTAT	Mismatch	15	27
K65 (AAG)	wt65.del	AC___CCTTCCTTTTTAT	Deletion	15	20
K65R (AGG)	mt65.del	AC___CCTTCCTTTTTAT	Deletion	15	27

Mismatched base is in blue, the extra nucleotides are in purple and the deleted bases are represented by the orange underscores.

The wild-type (AAG) and mutant (AGG) plasmids were accurately genotyped with the complementary probes. When applied to the patient samples, multiple indistinct melting peaks were generated (examples are shown in Figure 3.20). A C→A transversion was introduced into the probes to destabilize the probe-target interaction. The plasmids were accurately genotyped with these mismatched probes; however the majority of wild-type patient samples produced multiple, small or no melting peaks (illustrated in Figure 3.20). Three samples harboured K65R, and the complementary and mismatched probes correctly identified these clinically relevant mutations. The T_m of the amplicon-amplicon duplexes was 74.5 ± 2 °C and the T_m of the probe-amplicon duplexes was 70 ± 2 °C. Representative melting plots are shown in Figures 3.20 and 3.21. Selected genotype and HRMA results for the K65R assay are summarized in Appendix D, Table D7.

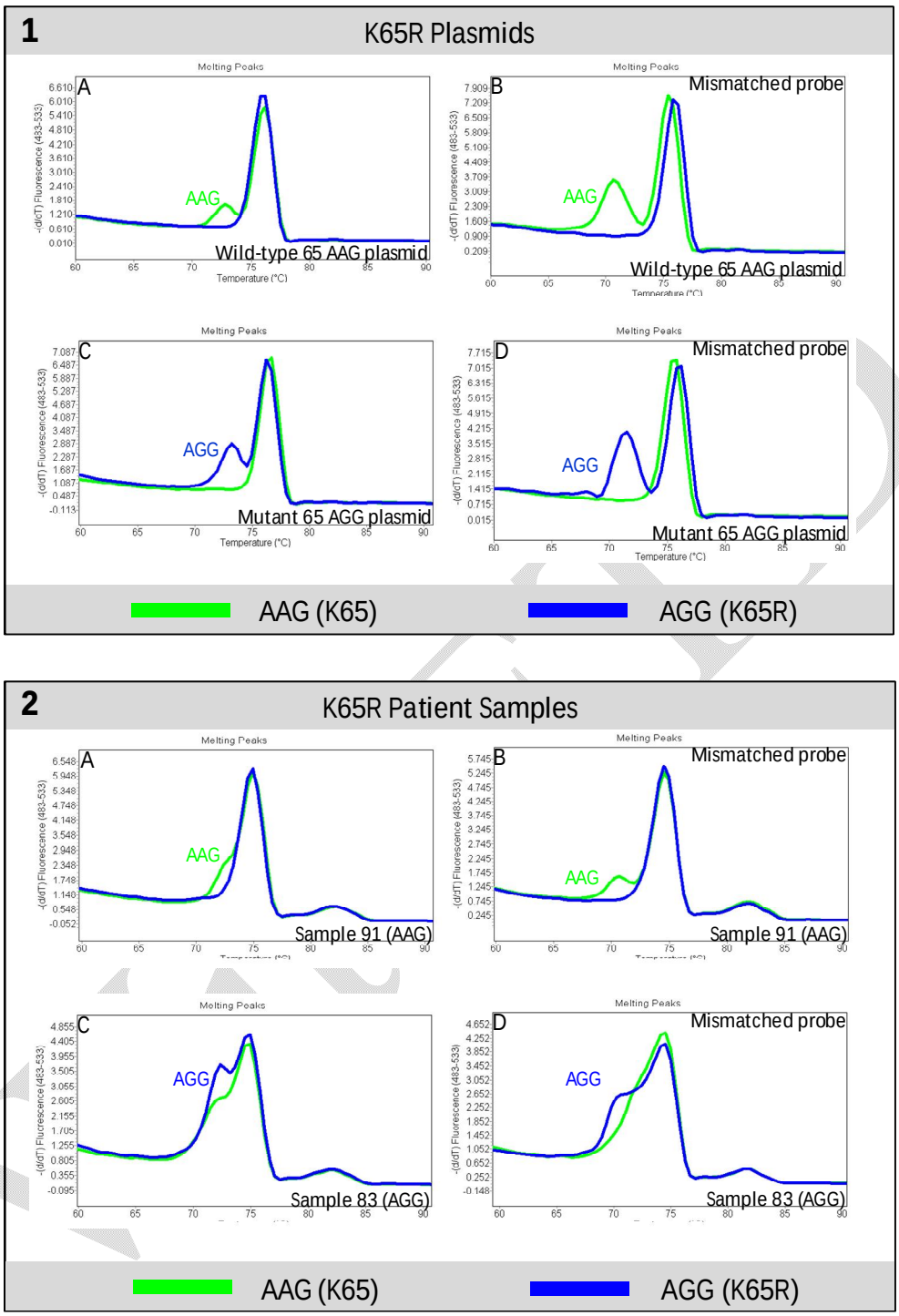

Figure 3.20. **Application of 65 HRMA assay to plasmids and patient samples.** Negative first derivative (-dF/dT) plots of common SNP genotypes at position 65, obtained by using either engineered plasmids (**1**) or patient samples (**2**) and complementary probes (left panels) or mismatched probes (right panels). The smaller probe peak at a lower T_m indicates successful probe binding, allowing for the allocation of a 65 genotype to the sample. Wild-type (AAG) plasmid with (**1A**) complementary and (**1B**) mismatched probes. Mutant (AGG) plasmid with (**1C**) complementary and (**1D**) mismatched probes. Wild-type (AAG) patient sample with (**2A**) complementary and (**2B**) mismatched probes. Mutant (AGG) patient sample with (**2C**) complementary and (**2D**) mismatched probes.

As the complementary probes were 15 bp long, the region of binding intersected with both codon 65 and the highly polymorphic codon 67 (Kuiken et al., 2009). Probes were then designed lacking the bases complementary to position 67. Three additional bases were included to maintain the optimal 15 bp probe length (Table 3.19). The deletion probes produced melting peaks when applied to the plasmids, but not when applied to the patient samples (examples are shown in Figure 3.21).

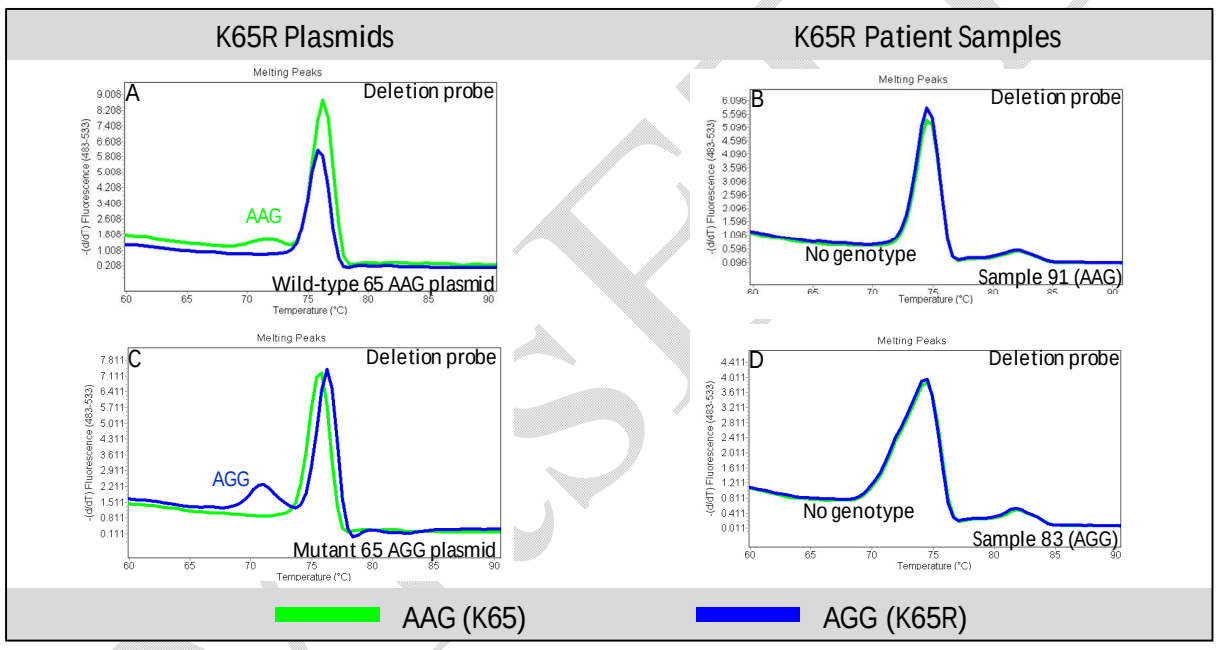

Figure 3.21. Application of 65 HRMA assay with polymorphism masking to plasmids and patient samples. Negative first derivative (-dF/dT) plots of the common SNP genotypes at position 65, obtained by using either engineered plasmids (left panels) or patient samples (right panels) and deletion probes. (**A**) Wild-type (AAG) plasmid and (**B**) wild-type patient sample. (**C**) Mutant (AGG) plasmid and (**D**) mutant patient sample.

In summary the complementary, mismatched and deletion probes were unsuitable to genotype the wild-type codon 65. However, the complementary and mismatched probes were able to genotype K65R in the patient samples (n=3) that harboured this mutation (Appendix D, Table D7).

3.5.7 V106M Assay

V106M (GTA/G → ATG) is selected for by EFV but is associated with broad NNRTI resistance (Brenner et al., 2003). The probes designed for the V106M assay included complementary probes and probes incorporating mismatches at selected sites (Table 3.20).

Table 3.20. Probe sequences for V106M assay.

Codon (sequence)	Name	Sequence (5' -3')	Modification	Length (bp)	G+C (%)
V106 (GTA)	wt106A	GTACTGTTACTGATT	-	15	33
V106 (GTG)	wt106G	GTACTGTCACTGATT	-	15	40
V106M (ATG)	mt106	ACTGTCATTGATTTT	-	15	27
V106 (GTA)	wt106A.mm	GTACTATTACTGATT	Mismatch	15	27
V106 (GTG)	wt106G.mm	GTACTATCACTGATT	Mismatch	15	33
V106M (ATG)	mt106.mm	ACTGTCATTAATTTT	Mismatch	15	20

Mismatched base is in blue.

When applied to the wild-type (GTG) plasmid each of the three complementary probes generated a peak, indicating non-specific binding (examples are shown in Figure 3.22). However the T_m of the mt106 probe melting peak differed when the probe was applied to wild-type (GTG) and mutant (ATG) plasmids or patient samples. Specifically, the T_m of the melting peak was ~2 °C lower than the T_m when applied to wild-type as compared to mutant samples (illustrated in Figure 3.23C and E).

By noting the differences in the T_m, the V106M samples could be identified. Of the 15 samples harbouring V106M, 13 (87%) were correctly genotyped, while two could not be genotyped probably due the presence of an G→A transition five bases upstream from the probe center. The wt106A probe, in some cases, generated an accurate small peak when applied to wild-type GTA patient samples (Figure 3.23A). The T_m of the amplicon-amplicon duplexes was 77 ± 1 °C and the T_m of the probe-amplicon duplexes was 72.5 ± 1 °C. Representative melting plots are shown

in Figures 3.22 and 3.23. Selected genotype and HRMA results for the V106M assay are summarized in Appendix D, Table D8.

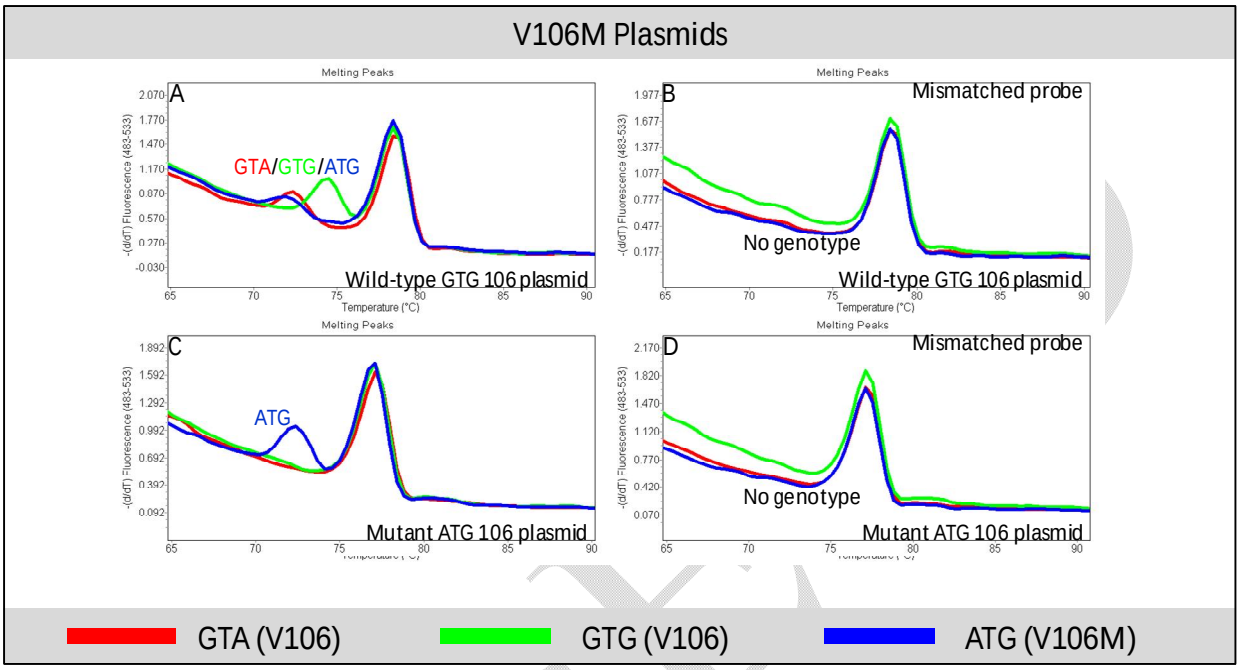

Figure 3.22. **Application of 106 HRMA assay to plasmids.** Negative first derivative (-dF/dT) plots of common SNP genotypes at position 106. The presence of a probe peak alongside the amplicon peak indicates successful probe binding, allowing for the allocation of a 106 genotype to the sample. The curves were obtained by using wild-type (GTG, top panels) and mutant (ATG, bottom panels) engineered plasmids and complementary probes (left panels) or mismatched probes (right panels). No wild-type GTA plasmid was constructed.

As the complementary probes were stable in the presence of a central mismatch, an A→G transition was introduced in order to destabilize non-specific probe-target interactions (Table 3.20). This mismatch was one base pair upstream from the central nucleotide of the probe. The mismatch (A→G) in the mt106.mm probe was in a different location to the wild-type probes in order to ensure that the type and position of the mismatch was the same in each of the probes. The wt106G.mm mismatched probe rarely generated a peak when applied to wild-type GTG patient samples. The remaining mismatched probes did not generate melting peaks when applied to the plasmids or patient samples (examples are shown in Figure 3.23).

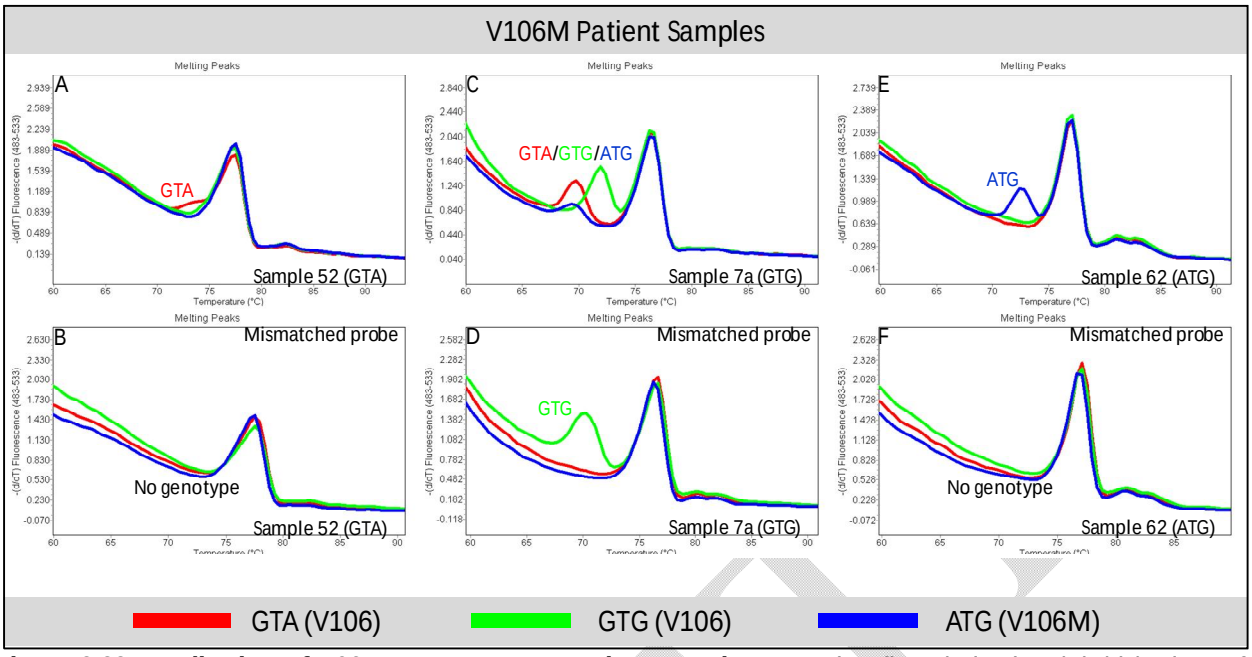

Figure 3.23. **Application of 106 HRMA assay to patient samples.** Negative first derivative (-dF/dT) plots of common SNP genotypes at position 106, obtained by using patient samples and complementary probes (top panels) and mismatched probes (bottom panels). Wild-type (GTA) patient sample with the (**A**) complementary and (**B**) mismatched probes. Wild-type (GTG) patient sample with the (**C**) complementary and (**D**) mismatched probes. Mutant (ATG) patient sample with the (**C**) complementary and (**D**) mismatched probes.

In summary the wild-type complementary and mismatched probes did not produce accurate melting peaks. While the complementary mutant probe produced a melting peak in the absence of a mutant sequence, the T_m of the peak differed from that generated with a mutant sample. In this way the clinically relevant mutant patient samples (n=15) were identified (Appendix D, Table D8).

3.5.8 M41L Assay

M41L (ATG → C/TTG) is a type I thymidine analogue mutation (TAM) that confers resistance to the thymidine analogues (ZDV and d4T) in the presence of K70R, M184V and T215Y/F

(Garcia-Lerma, 2005). The probes designed for the M41L assay included complementary probes and probes incorporating mismatches (Table 3.21).

Table 3.21. Probe sequences for M41L assay.

Codon (sequence)	Name	Sequence (5' -3')	Modification	Length (bp)	G+C (%)
M41 (ATG)	wt41A	TTCTCCATTTCTTCA	-	15	33
M41L (TTG)	mt41T	TTCTCCAATTCTTCA	-	15	33
M41L (CTG)	mt41C	TTCTCCAGTTCTTCA	-	15	40
M41 (ATG)	wt41A.mm	TTTTCCATTTCTTCA	Mismatch	15	27
M41L (TTG)	mt41T.mm	TTTTCCAATTCTTCA	Mismatch	15	27
M41L (CTG)	mt41C.mm	TTTTCCAGTTCTTCA	Mismatch	15	33

Mismatched base is in blue.

When the probes were applied to plasmids or patient samples, multiple melting peaks where generated (examples are shown in Figure 3.24). Consequently, a C→T transition was introduced in order to destabilize non-specific probe binding. This modification allowed for accurate genotyping of the wild-type (ATG) and mutant (C/TTG) plasmids. However, the masking did not allow genotyping of the patient samples as multiple peaks were still generated. However, in some cases the wt41A.mm probe did generate accurate melting peaks (Figure 3.24 2B). The T_m of the amplicon-amplicon duplexes was 73.5 ± 2 °C and the T_m of the probe-amplicon duplexes was 69 ± 2 °C. Representative melting plots are shown in Figure 3.24.

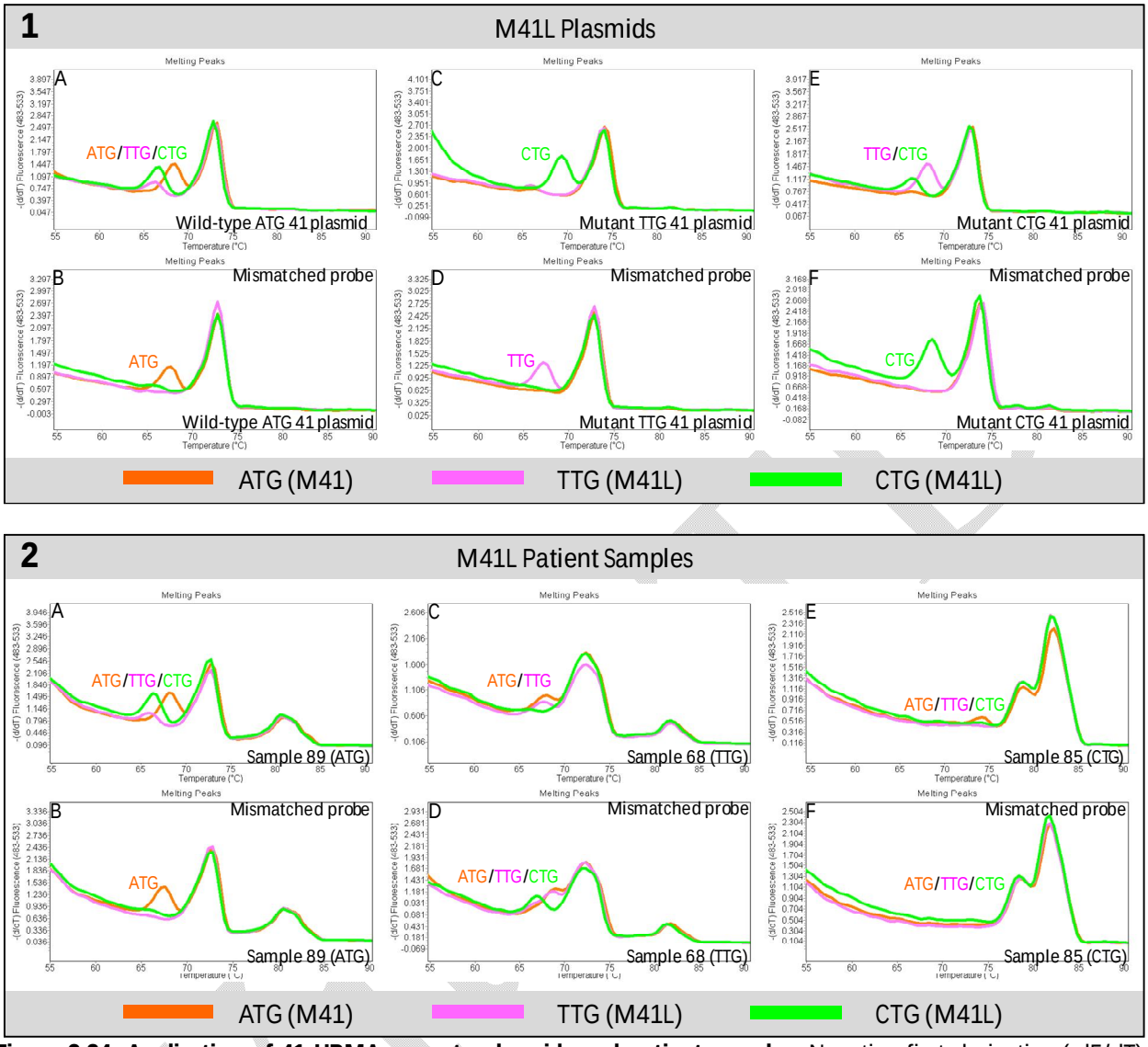

Figure 3.24. **Application of 41 HRMA assay to plasmids and patient samples.** Negative first derivative (-dF/dT) plots of the common SNP genotypes at position 41, obtained by using either engineered plasmids (**1**) or patient samples (**2**) and complementary probes (top panels of each box) or mismatches probes (bottom panels of each box). The presence of a probe peak alongside the amplicon peak indicates successful probe binding, allowing for the allocation of a 41 genotype to the sample. Wild-type (ATG) plasmid with the (**1A**) complementary and (**1B**) mismatched probes. Mutant (TTG) plasmid with the (**1C**) complementary and (**1D**) mismatched probes. Mutant (CTG) plasmid with the (**1E**) complementary and (**1F**) mismatched probes. The same combination of probes in (**1**) are contained in (**2**) but applied to patient samples.

In summary the complementary probes were unable to genotype codon 41 in plasmids or patient samples. The introduction of a mismatch allowed genotyping of the plasmids but not the patient samples.

3.5.9 D67N Assay

D67N (GAC/T → AAC) is a type II TAM and is associated with ZDV and d4T resistance when present with particular combinations of type I and II TAMs (Garcia-Lerma, 2005; Menendez-Arias, 2008). Complementary probes were designed to identify the common wild-type and mutant genotypes. Additionally, a mismatch was introduced into the mutant probe (Table 3.22).

Table 3.22. Probe sequences for D67N assay.

Codon (sequence)	Name	Sequence (5' -3')	Modification	Length (bp)	G+C (%)
D67 (GAC)	wt67C	TAGTACT**G**TCCTTCT	-	15	40
D67 (GAT)	wt67T	TAGTACT**A**TCCTTCT	-	15	33
D67N (AAC)	mt67C.mm	GTACT**T**T**T**CTTCTTT	Mismatch	15	27

Mismatched base is in blue.

Due to the high G+C content, a G→T transversion was introduced into the mutant mt67.mm probe to reduce the binding affinity of the probe to its target. When the two wild-type complementary probes and the mismatched mutant probe were applied to the wild-type (GAC/T) and mutant (AAC) plasmids, small and indistinct melting peaks were formed when the G/AAC sequences were present. No probe melting peak was formed when the complementary probes were applied to the wild-type GAT sequence. Upon application of the probes to patient samples, inconsistent and indistinct peaks were generated with the GAC sequence, while no peaks formed with GAT and AAC. The T_m of the amplicon-amplicon duplexes was 74.3 ± 1 °C and the T_m of the probe-amplicon duplexes was 72 ± 1 °C. Representative melting plots are shown in Figure 3.25.

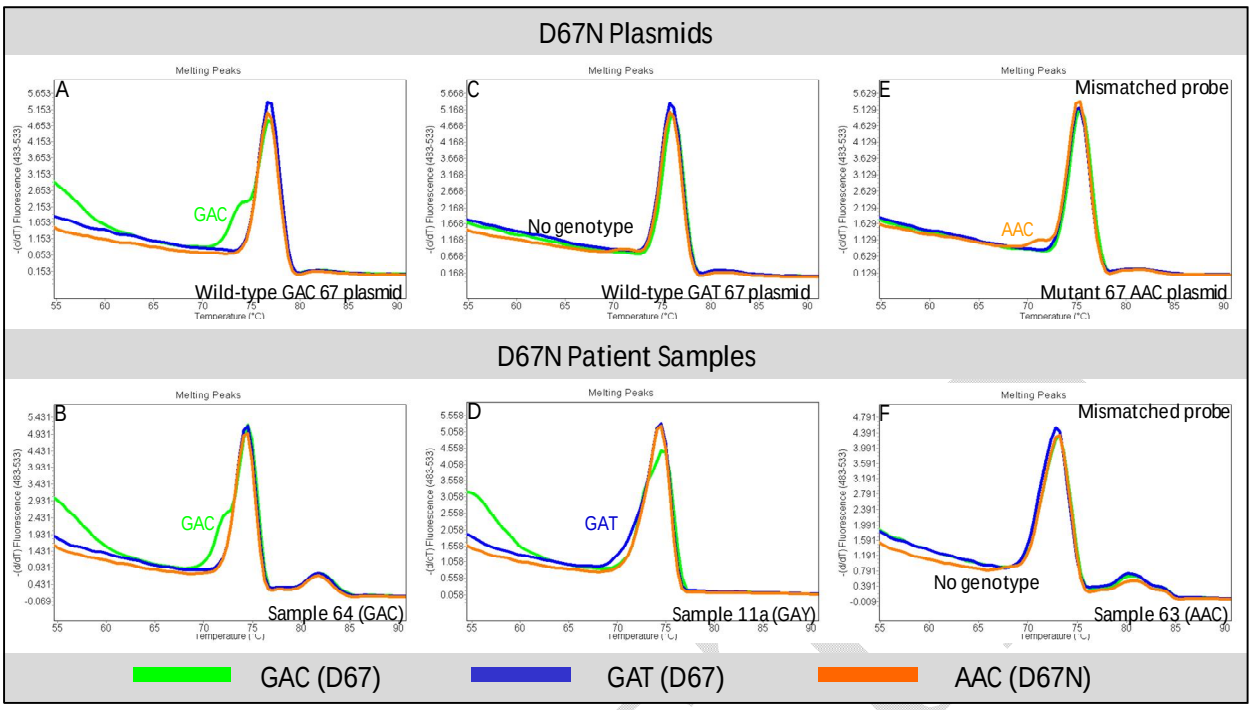

Figure 3.25. **Application of 67 HRMA assay to plasmids and patient samples.** Negative first derivative (-dF/dT) plots of the common SNP genotypes at position 67, obtained by using either engineered plasmids (top panels) or patient samples (bottom panels) and probes. The presence of a smaller probe peak at a lower T_m indicates successful probe binding, allowing for the allocation of a 67 genotype to the sample. (**A**) Wild-type (GAC) plasmid and (**B**) wild-type (GAC) patient sample. (**C**) Wild-type (GAT) plasmid and (**D**) wild-type (GAT) patient sample. (**E**) Mutant (AAC) plasmid and (**F**) mutant (AAC) patient sample. Each probe was complementary besides for the mt67C.mm mismatched probe

In summary the complementary and mismatch probes had very limited success in genotyping position 67 in the plasmids. The probes performed poorly when applied to patient samples.

3.5.10 K70R Assay

K70R (AAA/G → AGG) is a type II TAM and is associated with strong thymidine analogue resistance when present with particular combinations of type I and type II TAMs (Garcia-Lerma, 2005; Menendez-Arias, 2008). Complementary probes were designed to genotype 70 codon (Table 3.23).

Table 3.23. Probe sequences for K70R assay.

Codon (sequence)	Name	Sequence (5' -3')	Modification	Length (bp)	G+C (%)
K70 (AAA)	wt70A	TTCTCCATTTAGTAC	-	15	33
K70 (AAG)	wt70G	TTCTCCACTTAGTAC	-	15	40
K70R (AGG)	mt70	TCTCCACCTAGTACT	-	15	47

Representative melting plots are shown in Figure 3.26 and 3.27. Non-distinct and small peaks were produced upon melting of the probes with the respective wild-type (AAA/G) and mutant (AGG) plasmids (examples are shown in Figure 3.26). The T_m of the amplicon-amplicon duplexes was 74 ± 2 °C and the T_m of the probe-amplicon duplexes was 72 ± 1 °C. No melting peaks were produced when the probes were applied to patient samples (illustrated in Figure 3.27).

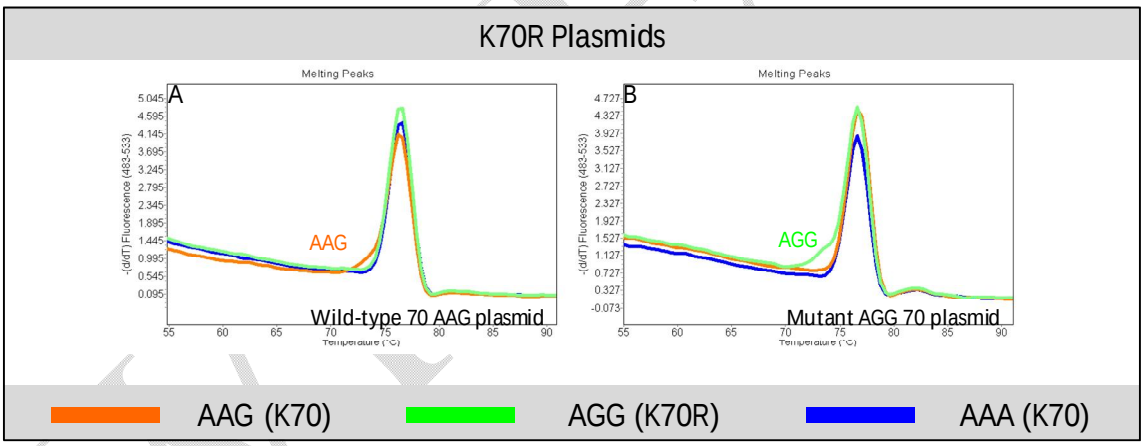

Figure 3.26. Application of 70 HRMA assay to plasmids. Negative first derivative (-dF/dT) plots of the common SNP genotypes at position 70, obtained by using (**A**) wild-type (AAG) and (**B**) mutant (AGG) engineered plasmids and complementary probes. The presence of a smaller probe peak at a lower T_m indicates successful probe binding, allowing for the allocation of a 70 genotype to the sample. No wild-type AAA plasmid was constructed.

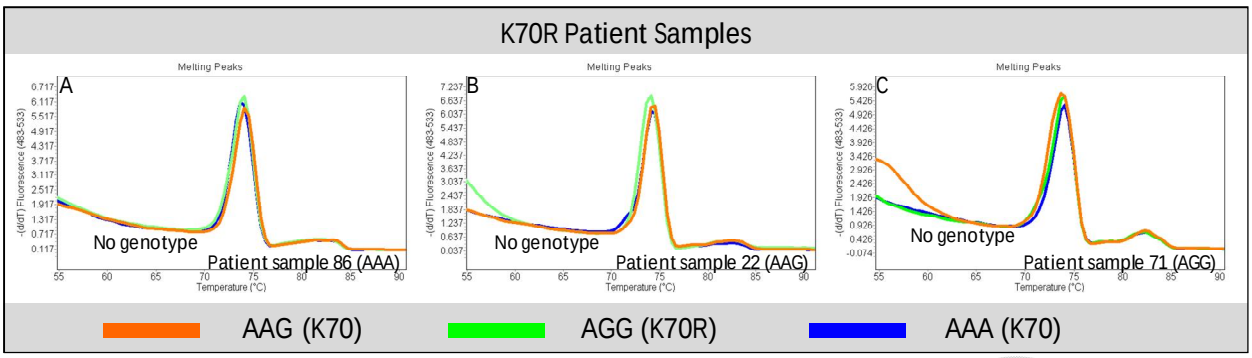

Figure 3.27. **Application of 70 HRMA assay to patient samples.** Negative first derivative (-dF/dT) plots of the common SNP genotypes at position 70, obtained by using a (**A**) wild-type (AAA) patient sample, (**B**) wild-type (AAG) patient sample and (**C**) mutant (AGG) patient sample with complementary probes.

In summary the complementary probes produced small melting peaks when applied to plasmids and no melting peaks upon application to patient samples.

3.5.11 T215F and T215Y Assay

T215Y and T215F are type I and II TAMs, respectively. Similar to D67N and K70R, T215F and T215Y when associated with other TAMs confer ZDV and d4T resistance (Garcia-Lerma, 2005; Menendez-Arias, 2008). ACC is the wild-type sequence at position 215 and so multiple nucleotide changes are required for the mutant T215F (TTC) and T215Y (TAC) to develop. Complementary probes were designed to genotype the 215 codon (Table 3.24).

Table 3.24. Probe sequences for T215F/Y assay.

Codon (sequence)	Name	Sequence (5' -3')	Modification	Length (bp)	G+C (%)
T215 (ACC)	wt215	TGGTGTG**GT**AAATCCC	-	16	47
T215F (TTC)	mt215F	TGGTGTG**AA**AAATCCC	-	16	44
T215Y (TAC)	mt215Y	TGGTGTG**TA**AAATCCC	-	16	44

The probes were designed with the two polymorphic bases in the center. To achieve this, an extra base was added to the probe, bringing the total length to 16 bp (Table 3.24). A single probe melting peak was formed when the probes were applied to wild-type (T215, ACC) plasmids.

However multiple probe melting peaks were generated when the probes were applied to the wild-type (AAC) patient samples (examples are shown in Figure 3.28). The mt215F probe did produce accurate melting peaks with a patient sample and not the plasmids. However only one patient sample in the cohort had TTC at the 215 locus and so the accuracy of this probe cannot be verified. Multiple peaks were generated when the mt215Y probe was applied to plasmids and patient samples. The T_m of the amplicon-amplicon duplexes was 78.5 ± 1 °C and the T_m of the probe-amplicon duplexes was 69.5 ± 1.5 °C. Representative melting plots are shown in Figure 3.28.

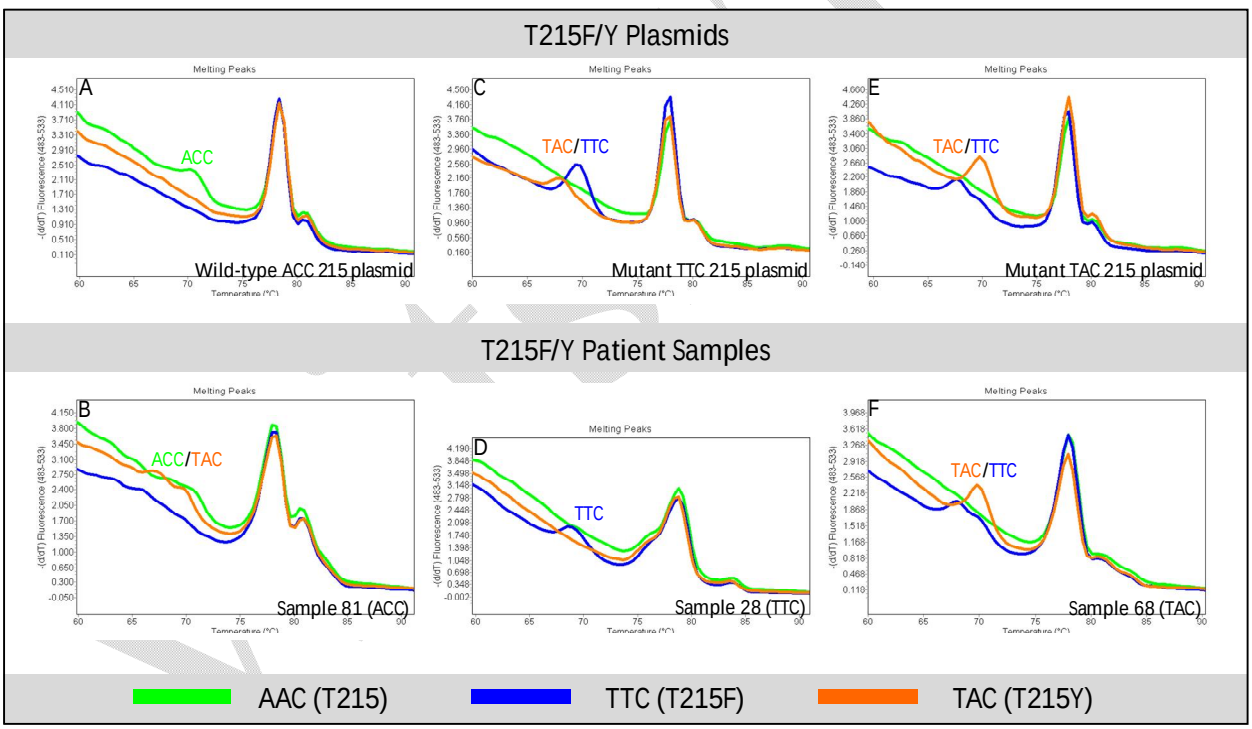

Figure 3.28. **Application of 215 HRMA assay to plasmids and patient samples.** Negative first derivative (-dF/dT) plots of the common SNP genotypes at position 215, obtained by using either engineered plasmids (top panels) or patient samples (bottom panels) and complementary probes. A probe peak alongside the amplicon peak indicates successful probe binding, allowing for the allocation of a 215 genotype to the sample. (**A**) Wild-type (ACC) plasmid and (**B**) wild-type (ACC) patient sample. (**C**) Mutant (TTC) plasmid and (**D**) mutant (TTC) patient sample. (**E**) Mutant (TAC) plasmid and (**F**) mutant (TAC) patient sample.

In summary the complementary probes failed to genotype codon 215 in plasmids or patient samples. The probe complementary to TTC (T215F) was able to genotype this position, however more samples need to be tested.

3.5.12 P225H Assay

P225H (CCC/T → CAC) is a secondary NNRTI mutation that is usually associated with a primary NNRTI mutation to confer NVP and EFV resistance (Shafer and Schapiro, 2008). Complementary probes were designed to genotype the two wild-type and single mutant sequence at this codon (Table 3.25).

Table 3.25. Probe sequences for P225H assay.

Codon (sequence)	Name	Sequence (5' -3')	Modification	Length (bp)	G+C (%)
P225 (CCC)	wt225C	GAAATGG**G**GGTTCTT	-	15	47
P225 (CCT)	wt225T	GAAATGG**A**GGTTCTT	-	15	40
P225H (CAC)	mt225H	AAATGGG**T**GTTCTTT	-	15	40

Representative melting plots are shown in Figures 3.29 and 3.30. No probe melting peaks were generated when the probes were applied to plasmids (examples are shown in Figure 3.29). The probes routinely produced multiple or no melting peaks with the patient samples (example in Figure 3.30). The wt225C probe (Figures 3.29 and 3.30 in red) consistently generated a flat line with each patient sample; the reason for this aberrant melting peak formation is unknown. The T_m of the amplicon-amplicon duplexes was 77.5 ± 1 °C and the T_m of the probe-amplicon duplexes was 75 ± 1 °C.

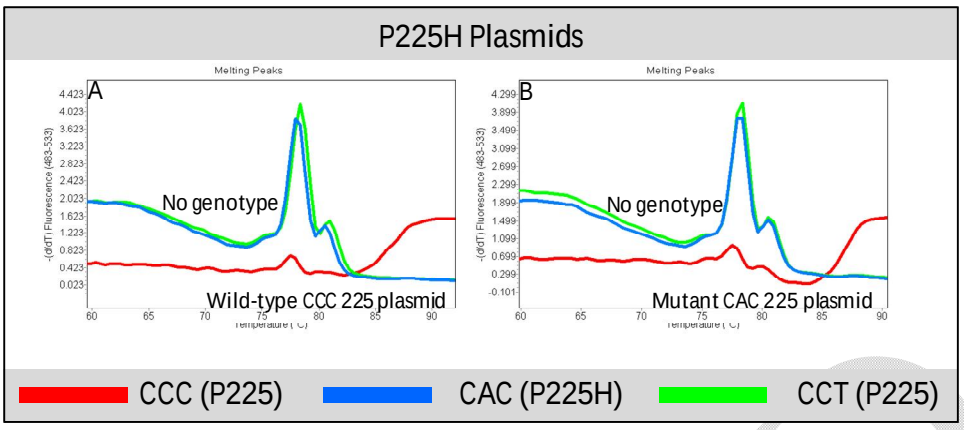

Figure 3.29. **Application of 225 HRMA assay to plasmids.** Negative first derivative (-dF/dT) plots of the common genotypes at position 225, obtained by using (**A**) wild-type (CCC) and (**B**) mutant (CAC) engineered plasmids and complementary probes. A probe peak at a lower T_m indicates successful probe binding, allowing for the allocation of a 225 genotype to the sample. No wild-type CCT plasmid was constructed.

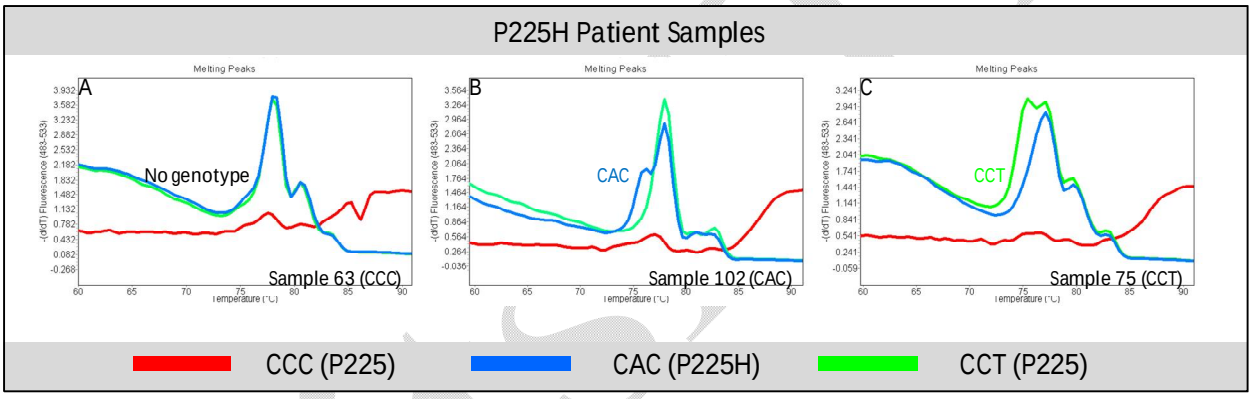

Figure 3.30. **Application of 225 HRMA assay to patient samples.** Negative first derivative (-dF/dT) plots of the common genotypes at position 225, obtained by using patient samples and complementary probes. (**A**) Wild-type (CCC) patient sample, (**B**) mutant (CAC) patient sample and (**C**) mutant (CCT) patient sample.

In summary the complementary probes failed to genotype codon 225 in plasmids and the majority of patient samples.

3.6 HRMA Validation

Validation procedures typically include sensitivity, specificity, repeatability, reproducibility and limit of detection. Sensitivity and specificity are statistical measures of the true positive and true negative test results, respectively (Figure 3.31). Repeatability and reproducibility compares the

intra-run and inter-run precision, respectively. A guideline for HRMA validation, by Norambuena and colleagues was used as a model for the validation of the K103N, Y181C, M184V, Q151M and G190A assays reported here (Norambuena et al., 2009).

3.6.1 Specificity and Sensitivity

$$\text{Specificity} = \frac{\text{number of TN}}{\text{number of TN} + \text{number of FP}} \qquad \text{Sensitivity} = \frac{\text{number of TP}}{\text{number of TP} + \text{number of FN}}$$

Figure 3.31. Formulae for the calculation of specificity and sensitivity*.

True negative (TN) = Wild-type correctly identified as wild-type.
False positive (FP) = Wild-type incorrectly identified as mutant.
True positive (TP) = Mutant correctly identified as mutant.
False negative (FN) = Mutant incorrectly identified as wild-type.

*The genotypes as determined by the complementary probes were used to calculate the specificity and sensitivity for each assay.

3.6.1.1 K103N

Twenty-one samples with no result were removed for the calculations. The specificity was 100% (n=62) and the sensitivity was 94% (n=31) due to two false negatives, samples 20 and 54 (Appendix D, Table D2).

3.6.1.2 Y181C

Eleven samples with no result were removed for the calculations. The specificity (n=95) was 97% due to three false positives (samples 6b, 69 and 73; Appendix D, Table D3). However as the assay has a higher limit of detection than population sequencing the samples may indeed be mutant and so the specificity is probably 100%. The sensitivity was 100% (n=7).

3.6.1.3 M184V

Twenty samples with no result were removed for the calculations. The specificity (n=55) was 95% due to three false positives (samples 10b, 55 and 92; Appendix D, Table D4). However as the assay has a higher limit of detection than population sequencing the specificity is probably 100%. Sample 35 was a false negative and so the sensitivity was 97% (n=37).

3.6.1.4 Q151M

Thirty-one samples with no result were removed for the calculations. Samples 10b, 14, 67 and 70 were identified as wild-type CAA, CAG, CAG and CAG by sequencing, while HRMA identified the codons as CAG, CAA, CAA and CAA, respectively (Appendix D, Table D5). This did not affect the specificity, which was 100% (n=76) and the sensitivity was 100% (n=5).

3.6.1.5 G190A

Fourty-one samples with no result were removed for the calculations. The specificity (n=68) was 100% while the sensitivity (n=5) was 71% due to two false negatives (samples 8b and 12b; Appendix D, Table D6).

3.6.2 Repeatability and Reproducibility

Samples representing each genotype (both wild-type and mutant) of the above mentioned codons were selected. Each reaction was repeated five times during a single PCR run for repeatability and then run five times on different days for reproducibility. The repeatability and reproducibility was 100%

3.7 Summary of HRMA Results

The HRMA assays successfully genotyped most of the wild-type and mutant 103, 181, 184, 151 and 190 codons with a high sensitivity and specificity. The limit of detection for the K103N and Y181C assays were 5% and for the M184V assay, 20%. The probes for assay 151 could not detect Q151M and the G190A plasmids could not be amplified for use in serial dilutions and so the limit of detection for these assays could not be determined. The assays for codons 65 and 106 were not able to genotype the wild-type sequences at the respective sites; however the clinically relevant mutant sequences were genotyped. Table 3.26 (page 95) summarizes these results. The assays for codons 41, 67, 70, 215 and 225 generally were unable to genotype plasmids or patient samples and so were excluded from the Table.

Table 3.26. Summary of the results for the 103, 181, 184, 151, 190, 65 and 106 assays.

Measure	Probe	Primer	Assay						
			103 n (%)	181 n (%)	184 n (%)	151 n (%)	190 n (%)	65 n (%)	106 n (%)
Correct	Complementary	Normal	93 (80)	102 (88)	92 (79)	81 (69)*	73 (63)	3 (100)	13 (87)
Discordant			2 (1.7)	3† (2.6)	4†† (3.4)	4 (3.4)	2 (1.7)	0	0
No result			21 (18)	11 (9.5)	20 (17)	31 (28)	41 (35)	0	2 (13)
Correct	Complementary	Altered	10	-	10	17	0	-	-
Discordant			2	-	0	0	0	-	-
No result			9	-	10	14	0	-	-
	Short	Normal	0	-	-	-	-	-	-
	Short + LNAs	Normal	0	-	-	-	-	-	-
Correct	Ambiguous	Normal	5	-	-	-	-	-	-
Discordant			5	-	-	-	-	-	-
No result			11	-	-	-	-	-	-
Correct	Inosine	Normal	-	3	-	-	-	-	-
Discordant			-	0	-	-	-	-	-
No result			-	8	-	-	-	-	-
Correct	Deletion	Normal	-	7	-	-	-	0	-
Discordant			-	0	-	-	-	0	-
No result			-	4	-	-	-	0	-
Correct	Mismatched	Normal	-	-	-	-	-	3	0
Correct	Any method		103 (89)	109 (94)	102 (88)	98 (85)	73 (63)	3 (100)	13 (87)
Discordant			9 (7.8)	3† (2.6)	4†† (3.4)	4 (3.4)	2 (1.7)	0	0
No result			4 (3.4)	4 (3.4)	10 (8.6)	14 (12)	41 (35)	0	2 (13)
Analytical sensitivity	Complementary	Normal	5%	5%	20%	-	-	-	-
Specificity	Complementary	Normal	100%	97%**	95%**	100%	100%	-	-
Sensitivity			94%	100%	97%	100%	71%		
Repeatability	Complementary	Normal	100%	100%	100%	100%	100%	-	-
Reproducibility			100%	100%	100%	100%	100%		

* Includes mismatched probe. - Experiment not done.

† This discordance can be attributed to the increased analytical sensitivity of HRMA.

†† Three of the four discordant samples can be attributed to the increased analytical sensitivity of HRMA.

** Due to increased analytical sensitivity the specificity is probably 100%.

Chapter 4: Discussion and Conclusion

During HIV infection, quasi-species harbouring drug resistance mutations can expand and become dominant if anti-retroviral (ARV) drug therapy is non-suppressive (Clavel and Hance, 2004). The presence of one or a number of specific mutations in *p66/p51* of *pol* generally has major consequences on the efficacy of the RT inhibitors for the treatment of HIV infection (Shafer and Schapiro, 2008). While Sanger population sequencing is the gold standard for HIV genotyping, it is time-consuming, laborious and costly (Hanna and D'Aquila, 2001). Newly introduced high resolution melting analysis (HRMA) allows for rapid and cost effective closed-tube genotyping and mutation scanning. Accurate genotyping of specific loci by HRMA relies on melting curves generated upon the dissociation of unlabelled probes from a DNA target. The process is monitored in real-time by the fluorescence emitted from a saturating dsDNA binding dye (Zhou et al., 2005). In this study, I showed that HRMA can be used to genotype key HIV-1 drug resistance mutations.

The assays designed to genotype codons 103, 181, 184, 151 and 190 accurately genotyped these loci in 80%, 88%, 79% 69% and 63% of 116 HIV-1 samples from 103 patients. The genotype predictions were discordant in 1.7%, 2.6%, 3.4%, 3.4% and 1.7% of the samples. The K65R and V106M assays genotyped only mutant samples and failed to genotype the wild-type sequences that these positions. The assays for codons 41, 67, 70, 215 and 225 had limited success in genotyping the engineered plasmids and could not genotype the patient samples.

The 1.7% (n=2) discordance for the 103 assay may be bypassed by the design of probes that include a distal mismatch. This may prevent probe melting peak formation in the presence of the rare AGA/T/C 103 genotypes but allow accurate genotyping with AAA/G/C/T at 103. Evidence for this lies in the inaccurate melting patterns generated with the AGA/T/C mutations in the absence of additional polymorphisms (underlined base differs between the common and unusual 103 genotypes). In the presence of additional polymorphisms no melting peaks were formed

The 2.6% (n=3) and 3.4% (n=4) discordance for assays 181 and 184 is probably a function of the limited analytical sensitivity of population sequencing, rather than HRMA inaccuracy. The three Y181C assay discordances and three of the four M184V assay discordances occurred as a result of the detection of minor mutant populations, which were not detected by population sequencing. The HRMA assays have a higher analytical sensitivity and the presence of mutant populations was confirmed by clonal analysis on three discordant samples (Vossen et al., 2009a); consequently the discordance for assays 181 and 184 is likely to be 0% and 0.9%, respectively.

The 3.4% (n=4) discordance between results for the 151 assay involved the wild-type genotypes and not the clinically relevant Q151M mutant. As wild-type samples of one genotype were inaccurately identified as the other wild-type 151 genotype, it would not affect treatment options or drug resistance surveillance.

The G190T (AGA) genotype (n=1) is rare and probes were not designed to genotype this codon. For similar reasons as for the unusual 103 genotypes, a deliberate mismatch may prevent erroneous probe melting peak formation and prevent discordant predictions with G190T samples.

The highly polymorphic nature of HIV probably prevented the genotyping of every patient sample (Preston et al., 1988; Roberts et al., 1988). Despite this, many samples that had polymorphisms within the probe binding region were genotyped. Polymorphisms closer to the extremities of the probes usually did not disrupt HRMA, as did the more destabilizing centralized variation (Naiser et al., 2008; Wu et al., 2009). In contrast, in some instances, no probe melting patterns were generated when the assays were applied to samples with the corresponding genotype. This variation may be a consequence of preferential amplification, of a particular quasi-species, harbouring a different genotype than the predominate species. Alternatively, during melting analysis, as the samples are cooled, secondary structures within the HIV-1 derived amplicons may form which may alter melting results.

Validation of the 103, 181, 184, 151 and 190 HRMA assays was carried out. The specificity of the 103, 151 and 190 assays was 100%. The 181 and 184 assays had a specificity of 97% and 95%, respectively; however due to the increased limit of detection the specificity is probably 100%. The sensitivity was 94%, 100%, 97%, 100% and 71% for the 103, 181, 184, 151 and 190 assays. The repeatability and reproducibility for each assay was 100%. However, the sensitivity for assays 151 and 190 were calculated with five mutant samples and so this may not represent the true sensitivities of the assays, therefore a larger number of mutant samples is required. As the assays were validated on the patient sample cohort on which optimization was performed, the results may be biased and further validation should be performed on a different patient sample set.

There appears to be a loose association between the G+C content adjacent to the target mutant nucleotide and assay success. The assays for codons 103, 181 and 184 produced the most distinct probe melting peaks. Other than identical probe length, the other similarity was the A+T content flanking the mutation sites. The weak A+T interactions in the center of the probe may allow for early dissociation of the mismatched probes, allowing for optimum HRMA. In contrast, the probes for codon 215 and 225 failed to genotype either plasmids or patient samples. The centers of these probes were flanked with, or were rich in G or C. This extra stability appears to have prevented early dissociation of the mismatched probes, leading to extra melting peak formation. Additionally the probes for position 215 were 16 bp in length which would have increased the binding stability (Zhou et al., 2004).

A central distribution of A+T was also found at codons 41, 65, 67 and 70. The use of ZDV and d4T has been widespread amongst South Africa patients receiving HAART, and so the thymidine analogue mutation (TAM) D67N is very common (Wallis et al., 2009). As the probes targeting codon 65 covered the highly polymorphic 67 codon, it probably disrupted successful genotyping of 65. Multiple melting peaks were formed when probes were applied to codon 41. Despite the introduction of a mismatch into the codon 41 probes, which decreased the G+C content to < 33%, multiple peak formation still occurred. In contrast, the probes for codon 70 had a G+C content of > 33%, yet no melting peaks were produced with the patient samples. Additionally, the wt67C probe, with 40% G+C, genotyped plasmids and some patient samples, while the other probes for position 67 (33% and 27% G+C) were unsuccessful. The reasons for this highly unpredictable stability are unknown.

The probes for codon 151 and 190 contained both pyrimidines and purines directly flanking the target mutation at the probe center. While these assays were successful, melting peak formation was not always distinct, which may be due to the extra probe stability. This extra stability may account for the increased atypical melting peak formation generated by the 151 and 190 rather than the 103, 181 and 184 assays.

Various polymorphism masking techniques were applied to samples that could not be genotyped with the unmodified (complementary) probes. The masking techniques included altered primers, short probes, LNAs and ambiguous, mismatched, universal and deleted bases. Polymorphism masking techniques have been reported twice previously (Margraf et al., 2007; Margraf et al., 2006). In both instances the assays were applied to human DNA, probe length varied from 27–33 bp and deleted, mismatched and universal bases were utilized. In these studies, each masking method produced similar, accurate results, save for a deletion adjacent the target site. As with other HRMA assays, the probe length is a significant difference between these assays, and those reported here. The longer probes are steadier in the presence of mismatches or deletions and so generate a signal despite instability. However longer probes will increase the interaction of the probes with polymorphisms. The short probes utilized for HIV-1 HRMA usually did not tolerate mismatches or deletions due to the weaker probe-target interaction, and therefore did not generate a signal. The exceptions were the wt106G.mm, wt151A.mm, the codon 41 mismatched probes and the codon 181 deletion probes. The differences in the response of the mismatched probes may be due to the varying degree of thermal stability of mismatches. Of the mismatches, “A:A” is of the most unstable, and so may account for the success of the wt151A.mm probe (Wu et al., 2009). The mismatches incorporated into the other probes were not as unstable, due to the

presence of G/C and so this may have prevented accurate melting peak generation in patient samples. The codon 181 and 65 deletion probes had one and three deleted bases, respectively. The failure of the latter is probably as a result of the heightened instability of the binding interaction due to the codon deletion. It appears that the small size of the probes for HIV-1 HRMA limits the potential for successful polymorphism masking.

Others have successfully utilized the universal base 5-nitroindole for polymorphism masking (Margraf et al., 2006). Inosine was incorporated into the codon 181 probes but did not mask the polymorphisms efficiently. This is probably because inosine is not truly indiscriminate, with a decreasing binding stability of I·C > I·A > I·T ≈ I· G > I·I (Loakes, 2001; Watkins Jr and SantaLucia Jr, 2005). Moreover a deletion at this site, which is more cost effective than inosine, generated accurate melting peaks. Consequently, deletions, 5-nitroindole or universal bases, other than inosine, should be tested for further HRMA application.

Altered primers, designed to bind directly adjacent to each mutation codon, have not been reported in the literature. These primers were applied to polymorphic samples for codons 103, 184, 151 and 190. The melting peaks generated were difficult to identify and the discordance was high. The low signal, high noise and high discordance may be due to the small amplicons produced. Another drawback is the necessity to design a pair of primers for each mutation codon. Use of these primers is not recommended for future HRMA assays.

The use of ambiguous bases for HRMA is also an unreported masking method. The majority of the polymorphic samples genotyped with these probes did not produce a probe melting signal.

As only a sixteenth of the probe mix participates during HRMA, the fluorescence signal is lower than usual, which probably prevented melting peak formation. Ambiguous bases, comprising of two different bases at the polymorphic site, rather than the tested four, might produce a stronger signal for HRMA.

Short probes of 11 bp and the probes incorporating LNAs did not generate melting peaks. Due to the low thermal stability of these short probes, the probes may have dissociated before the melt program began recording fluorescence changes at 40 °C, the lowest temperature at which the LightCycler 480 Real-Time PCR system (Roche Applied Science, GmbH, Germany) can be set. It has been reported that probes of 10 bases can be detected when the G+C content is 100% (Zhou et al., 2004).

Genotyping by HRMA is limited to the identification of single bases or short stretches of conserved sequences (Vaughn and Elenitoba-Johnson, 2004). Additionally, HRMA assay design relies on sequence information of the target area, which cannot be elucidated by HRMA alone. In contrast, long stretches of a genome can be genotyped *de novo* by population sequencing or pyrosequencing (Ahmadian et al., 2006). Despite these advantages, HRMA can be used in place of *de novo* genotyping if the loci of interest have known genotypes. In this way, HRMA presents a far more rapid genotyping methodology than *de novo* techniques. It is also more cost effective than population sequencing as melting instruments and the required reagents are comparatively less expensive than those required for population and pyrosequencing. The cost of HRM master mix and population sequencing dye is approximately R5 and R33 per reaction, respectively.

An additional shortcoming is the inability of current HRMA software to perform automatic base calling as does the software for population sequencing. As such, traditional HRMA curve interpretation is subjective and lacks statistical interrogation. However a new generation of HRMA software has introduced statistical analysis which allows automated sample genotyping. Currently this software is applicable to normalized melting curve interpretation rather than the negative derivative plots utilized in this study (Reja et al., 2010).

Another marked difference between population sequencing and HRMA, is that the latter is often disrupted by unexpected sequence variation. Consequently, genotyping by HRMA is suited for use with conserved, non-polymorphic genetic material; and so most HRMA studies are conducted on human genetic material. In this setting, genotyping by mutation scanning is possible and most assays designed for human genetic material do not utilize probes (Grievink and Stowell, 2008; Hill et al., 2006; Krenková et al., 2009; Krypuy et al., 2006; Liew et al., 2004; Poláková et al., 2008; Reed and Wittwer, 2004; Simi et al., 2008; Willmore-Payne et al., 2005). Despite the convenience of mutation scanning, assays utilizing unlabeled probes investigating mutations associated with cystic fibrosis, cancer, metabolic diseases and vascular malformations have been designed (Nguyen-Dumont et al., 2009; Poulson and Wittwer, 2007; van der Stoep et al., 2009; Vandersteen et al., 2007; Zhou et al., 2004; Zhou et al., 2005). HRMA assays, with or without probes, show a high concordance with sequence data. In most instances the sensitivity and specificity of the assays ranges from > 95%-100% (Montgomery et al., 2010). As the location, type and prevalence of polymorphisms in human DNA are well established, these sites can be avoided or masked accordingly. In contrast, the number of polymorphism is far higher in HIV and many changes are uncommon, so masking of each polymorphism under the

probe binding region is not feasible. Nevertheless, I show here that selected polymorphisms can be masked to allow successful genotyping.

The limit of detection for the HRMA assays reported here is higher than that of population sequencing and appears to be assay dependent, ranging from ~ 5%-20%. No data on the limit of detection for probe based HRMA assays was found in the literature. However mutation scanning assays have analytical sensitivities of 0.1%-10%. The 0.1% limit of detection is applicable to methylation analysis rather than SNP detection assays. The lower limit of detection of HRMA for SNP detection in mixed species is ~ 3% (Krypuy et al., 2006; Simi et al., 2008; Wojdacz and Dobrovic, 2007). Thus as HRMA is more sensitive than population sequencing, it allows for the detection of clinically relevant drug resistant minority species (Gardner et al., 2009).

When applied to bacteria or viruses, HRMA is usually utilized for subtyping, rather than specific loci genotyping. Mutation scanning assays have been designed to differentiate clinically relevant *Mycobacteria, Campylobacteri, Mycoplasma* and *Legionella* bacterial species or strains (Cheng et al., 2006; Giglio et al., 2005; Jeffery et al., 2007; Odell et al., 2005; Price et al., 2007). Similarly assays have been designed to type DNA viruses (adenoviruses, varicella-zoster and human papillomavirus type 16) and RNA viruses (noroviruses, influenza A/B and infectious bronchitis virus) (Hewson et al., 2009; Lin et al., 2008; Nakagawa et al., 2009; Sabol et al., 2009; Steer et al., 2009; Tajiri-Utagawa et al., 2009; Toi and Dwyer, 2008). Except for the RNA viruses, the mutation rates of these organisms are far lower than that of HIV. Nevertheless, polymorphisms do not exert a strong influence on the outcome of mutation scanning assays for subtyping purposes. Large amplicons, usually > 100 bp are generated and so the distribution and

extent of G+C influences subtyping. To the author's knowledge, only one published paper explores the application of unlabelled probes and HRMA to viral genetic material. Dames and coworkers designed an assay to type herpes simplex virus 1 and 2 (HSV) (Dames et al., 2007). The majority of the samples were correctly classified by mutation scanning, and the use of unlabelled probes increased the success rate to 99%. The higher success rate may be due to the lower mutation rate of HSV and the use of longer probes (> 30 bp), with five mismatches along the probe length. The stronger probe signal decreases the interference that noise introduces into melting peak interpretation and stabilizes the probe in the presence of polymorphisms. Despite the drawbacks the short probes and highly polymorphic genetic material introduce, the success rates of the assays reported here are comparable to that of Dames and colleagues.

While longer probes may tolerate mismatches and deletions for use in polymorphism masking, shorter probes offer certain advantages. The 103, 181, 184, 151 and 190 assays utilize very short probes which do not generate melting peaks when the target sequence is absent. Melting peak identification is simple, as the presence or absence of a peak, at a specific T_m, signals the genotype of the locus. In contrast, long probes generate ≥ 1 melting peak/s, which makes melting curve interpretation difficult, as the number and position of each peak is critical to genotype elucidation (Zhou et al., 2004). A balance between probe length and polymorphism masking robusticity may be a probe of < 21 bp, as probes of this length do not generate a peak when a non-corresponding genotype is present (Zhou et al., 2004). Thus a comparatively longer (< 21 bp) probe than those utilized here may allow for more effective polymorphism masking, while permitting simple curve interpretation.

In addition to short probes, another feature of the assays reported here, which does not usually appear in other probe based HRMA assays is probe redundancy. For the assays reported here, at least one probe was designed to identify the wild-type and at least one other probe, the mutant base at the site of interest. This reduced erroneous base classification as the absence of a peak was not sufficient for genotype prediction. Rather, information from both probes was sufficient to genotype the loci in question. This is important for HIV-1 HRMA, as 10%-30% of the patient samples did not generate melting peaks. If one probe was used to genotype a wild-type location, then the absence of that peak would signal the presence of the mutant genotype. However this result may be a consequence of a polymorphism rather than a mismatch, due the mutant genotype. Thus a peak generated from a wild-type or mutant probe should be used to formulate an accurate base prediction when HRMA is applied to highly polymorphic genetic material.

If the interrogation of a limited number of sites is required then HRMA is an attractive option. While these assays cannot genotype each drug resistance mutation codon in HIV-1 the three most prevalent drug resistance mutations (M184V, K103N and V106M) in South Africa were indentified accurately and with high sensitivity and specificity (Marconi et al., 2008; Orrell et al., 2009; Wallis et al., 2009). Additionally, other major mutations, K65R, Y181C, Q151M and G190A were detected. These assays could not genotype TAMs, which include M41L, D67N, K70R and T215Y/F. TAMs are widespread in resource limited populations as ZDV and d4T are commonly used. Additionally, TAMs are the most commonly transmitted NRTI mutations (Shafer and Schapiro, 2008). While the secondary mutations (M41L, D67N, K70R, T215F/Y and P225H) could not be identified, these mutations are almost exclusively found in the presence of the detectable major NNRTI (K103N, V106M, Y181C and G190A) and NRTI (K65R, Q151M

and M184V) mutations (http://hivdb.stanford.edu/) (Bacheler et al., 2000). The assays can therefore be used to screen HIV-1 patient samples for major reverse transcriptase related drug resistance mutations. If major mutations are detected then samples would be subjected to population sequencing to identify secondary mutations.

HRMA assays are cost effective, require less technical expertise than other population sequencing and a single specialized melting machine. Therefore, the assays can be implemented to genotype specific major HIV-1 reverse transcriptase drug resistance mutations in resource limited settings. In this way, the sequencing burden can be decreased by > 60%-90%, as only samples generating no result require sequencing.

The detection of major drug resistance mutations is integral to the treatment success of patients receiving ARV drug therapy. Due to the expansion of ARVs drug resistance is an increasing problem in resource limited areas. As a result of increased resistance, transmission of drug resistant viruses may increase which will compromise the treatment of drug naïve patients (WHO/UNAIDS, 2008). Consequently drug resistance testing for surveillance of the prevalence of resistance and transmitted resistance is essential (Bennett et al., 2008). Additionally, resistance testing is helpful for the formulation of appropriate drug regimens in cases of treatment failure (Torre and Tambini, 2002). Due to the cost, expertise and equipment requirements, population sequencing for resistance testing has not been widely implemented in resource limited areas. The advantages HRMA has over population sequencing may allow for, after further development, rapid and cost effective resistance testing for surveillance and clinical purposes.

Appendix A: Primer Sequences

The primers for the nested RT-PCR, cDNA synthesis and Sanger population sequencing (Table A1) were manufactured by the University of Cape Town. The primers for site-directed mutagenesis (Table A2) were manufactured by Invitrogen (USA).

Table A1. Primer sequences for cDNA synthesis, nested RT-PCR and population sequencing.

Name	Sequence (5'-3')	Tm (°C)	Product Length
IN3	TCTCAGCCATCTAAAAATAGTACTTTCCTGATTCC	71	n/a
pFor-out	AAAATGATAGGAGGAATTGG	52	1129bp
pRev-out	CATGGAGTATATTATGACCCAT	56	
pFor-in	CACCTGTCAACATAATTGG	53	986bp
pRev-in	GCAGAGAACAGGGAAATT	51	
LC-outFor	TTCAGGGAACTCAATAAAAG	52	n/a
M8	CTGTATATCATTGACAGTCCAG	58	n/a

n/a = Not applicable, as the primers were used for cDNA synthesis or population sequencing.

Table A2. Primer sequences for site-directed mutagenesis.

Name	Sequence (5'-3')	Modification	G+C (%)	T_m (°C)
M41La	GCATTAACAGCAATTTGTGAAGAATTGGAAAAGGAAGG	ATG→TTG	36	57
M41La-as	CCTTCCTTTTCCAATTCTTCACAAATTGCTGTTAATGC		36	57
M41Lb	GCATTAACAGCAATTTGTGAAGAACTGGAAAAGGAAGG	ATG→CTG	39	58
M41Lb-as	CCTTCCTTTTCCAGTTCTTCACAAATTGCTGTTAATCG		39	58
D67Na	CCAGTATTTGCCATAAAAAAGAAGAACAGTACCAAGTGGAG	GAC→AAC	39	59
D67Na-as	CTCCACTTGGTACTGTTCTTCTTTTTTATGGCAAATACTGG		39	59
D67Nb	CCAGTATTTGCCATAAAAAAGAAGAATAGTACCAAGTGGAG	GAC→AAT	36	58
D67Nb-as	CTCCACTTGGTACTATTCTTCTTTTTTATGGCAAATACTGG		36	58
K70Ra	GAAGGACAGTACCAGGTGGAGAAAATTAGTAGATTTCAGGG	AAG→AGG	43	61
K70Ra-as	CCCTGAAATCTACTAATTTTCTCCACCTGGTACTGTCCTTC		43	61
Q151Ma	CAATATAATGTGCTTCCAATGGGATGGAAAGGATCACC	CAG→ATG	42	59
Q151Ma-as	GGTGATCCTTTCCATCCCATTGGAAGCAGATTATATTG		42	59
G190a	GGATGACTTGTATGTAGCATCTGATTTAGAAATAAAGCAACATAGAGC	GGA→GCA	35	60
G190a-as	GCTCTATGTTGCTTTATTTCTAAATCAGATGCTACATACAAGTCATCC		35	60
T215a	CTATTAAAGTGGGGATTTTTCACACCAGACAAGAAACATCAG	ACC→TTC	38	59
T215a-as	CTGATGTTTCTTGTCTGGTGTGAAAAATCCCCACTTTAATAG		38	59
T215b	CTATTAAAGTGGGGATTTTTTACACCAGACAAGAAACATCAG	ACC→TTT	35	58
T215b-as	CTGATGTTTCTTGTCTGGTGTAAAAAATCCCCACTTTAATAG		35	58
T215c	CTATTAAAGTGGGGATTTTACACACCAGACAAGAAACATCAG	ACC→ACT	38	59
T215c-as	CTGATGTTTCTTGTCTGGTGTGTAGTAAAATCCCCACTTTAATAG		38	59
T215d	CTATTAAAGTGGGGATTTTACACACCAGACAAGAAACATCAG	ACC→TAC	38	59
T215d-as	CTGATGTTTCTTGTCTGGTGTGTAAAATCCCCACTTTAATAG		38	59
P225Ha	GAAACATCAGAAAGAACACCCATTTCTTTGGATGGGG	CCC→CAC	43	59
P225Ha-as	CCCCATCCAAAGAAATGGGTGTTCTTTCTGATGTTTC		43	59

Appendix B: Vector Map

The following diagram depicts the vector map of the pCR 2.1-TOPO vector (Invitrogen, USA).

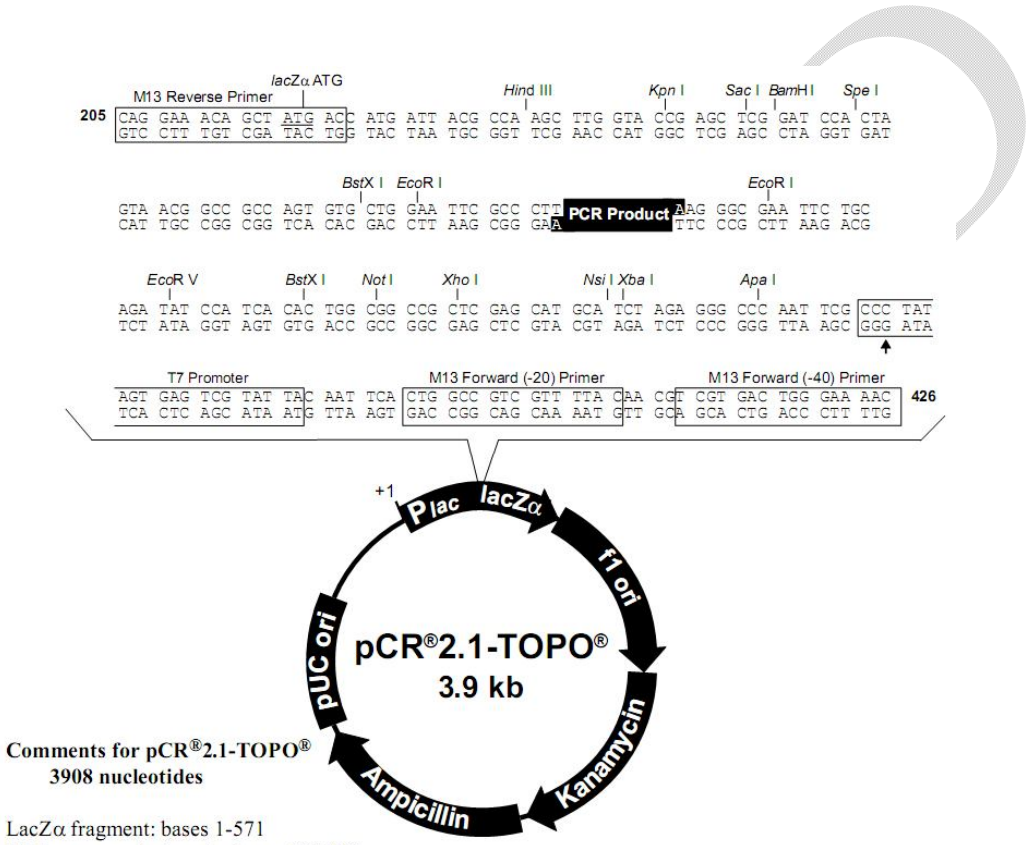

Comments for pCR®2.1-TOPO®
3908 nucleotides

LacZα fragment: bases 1-571
M13 reverse priming site: bases 205-221
Multiple cloning site: bases 234-357
T7 promoter/priming site: bases 364-383
M13 Forward (-20) priming site: bases 391-406
M13 Forward (-40) priming site: bases 411-426
f1 origin: bases 548-962
Kanamycin resistance ORF: bases 1296-2090
Ampicillin resistance ORF: bases 2108-2968
pUC origin: bases 3113-3786

Figure B1. Diagram of pCR 2.1 TOPO vector.

Appendix C: Media and Reagents

Bacterial Culture Reagents

- **Ampicillin (100 mg/mL)**

Mixed 1 g of ampicillin with 10 mL of dH_2O, stored at -20 °C, used within 6 months.

- **Lysogeny broth (LB)**

LB Ultra pure (USB, USA): 10 g/L casein peptone, 5 g/L Yeast extract and 5 g/L NaCl. Added 25 g of LB to 1 L of dH_2O. Mixed thoroughly and autoclaved for 20 minutes at 121 °C. Cooled and added 100 mg of ampicillin.

- **LB agar**

LB agar (Lennox L agar, Invitrogen, USA): 10g/L select peptone 140, 5 g/L select yeast extract, 5 g/L NaCl and 12 g/L select agar. Added 32 g of LB agar to 1 L of dH_2O. Mixed and autoclaved for 20 minutes at 121 °C. Cooled and added 100 mg of ampicillin. After mixing aliquoted 25 mL into agar plates.

- **X-Galactosidase (40 mg/mL)**

Added 0.4 g of X-Gal to 10 mL of dimethylformamide. Protected from light and stored at -20 °C.

Agarose Gel Electrophoresis Solutions

- **TAE Buffer (1x)**

50 x TAE (per 1 x solution): 40 mM Tris, 20 mM acetic acid and 1 mM EDTA. Added 20 mL of 50 x TAE to 1800 mL of dH_2O.

- **Agarose Gels**

For 1% agarose gel, added 0.5 g of agarose (Bioline, London, UK) to 50 mL of 1 x TAE buffer. Mixed and then boiled in a microwave. Cooled to ~ 60 °C and added 5 µL of 10 mg/mL ethidium bromide (Biorad, California, USA). Mixed and poured into agarose gel mould with well comb in place, allowed to set for 20 minutes. For 2% agarose gel, followed same method, but added 1 g of agarose to 50 mL of 1 x TAE buffer.

- **Tracking Dye**

Added 0.025% bromophenol blue to 30% glycerol in TE.

DNA Buffer

- **Tris-HCl (pH 8)**

Added 12.11 g of Tris to 90 mL of dH_2O. Adjusted to pH 8 with HCl, made up to 100 mL with dH_2O.

Appendix D: HRMA Results

The following Tables contain the Sanger population sequencing results and HRMA predictions for the K103N (D2), Y181C (D3), M184V (D4), Q151M (D5), G190A (D6), K65R (D7) and V106M (D8) HIV-1 RT mutation codons. Samples with discordant HRMA results are in red and samples with no result (NR) are in blue. A guide to the nomenclature used in the following Tables is in Table D1.

Table D1. DNA bases and incompletely specified bases.

A	Adenine
C	Cytosine
T	Thymine
G	Guanine
R	G or A
Y	T or C
M	A or C
S	G or C
W	A or T
H	A or C or T

Table D2. Population sequences and HRMA predictions for the 103 assay.

Patient sample	103 Sequence	103 HRM	Altered primer	Ambiguous probe
Sample 1a	AAA	AAA		
Sample 1b	AAM	AAM		
Sample 2a	AAA	AAA		
Sample 2b	AAM	AAM		
Sample 3a	AAA	AAA		
Sample 3b	AAA	AAA		
Sample 4a	AAA	AAR		
Sample 4b	AAM	AAM		
Sample 5a	AAA	NR	AAA	AAA
Sample 5b	AAA	NR	AAA	AAM
Sample 6a	AAA	AAA		
Sample 6b	AAC	AAC		
Sample 7a	AAA	AAA		
Sample 7b	AAM	AAM		
Sample 8a	AAA	AAA		
Sample 8b	AAA	NR	NR	AAA
Sample 9a	AAA	AAA		
Sample 9b	AAA	AAA		
Sample 10a	AAA	AAA		
Sample 10b	AAM	NR	NR	AAT
Sample 11a	AAA	AAA		
Sample 11b	AAW	NR	NR	AAA
Sample 12a	AAA	AAA		
Sample 12b	AAM	NR	AAA	NR
Sample 13a	AAA	AAA		
Sample 13b	AAM	AAM		
Sample 14	AAA	AAA		
Sample 15	AAA	AAA		
Sample 16	AAA	AAA		
Sample 17	AAA	AAA		
Sample 18	AAA	AAA		
Sample 19	AAM	AAM		
Sample 20	AGA	AAA		
Sample 21	AAA	AAA		
Sample 22	AAC	NR	AAC	NR
Sample 23	AAA	AAA		
Sample 24	AAC	AAC		
Sample 25	AAA	AAA		
Sample 26	AAA	AAA		
Sample 27	AAA	AAA		
Sample 28	AAA	NR	AAA	AAA
Sample 29	AAC	AAC		
Sample 30	AAT	AAY		
Sample 31	AAA	AAA		
Sample 32	AGA	NR	NR	AAA
Sample 33	AGA	NR	NR	NR
Sample 34	AAC	AAC		
Sample 35	AAA	AAA		
Sample 36	AAC	AAC		
Sample 37	AAA	AAA		
Sample 38	AAC	AAY		
Sample 39	AAG	AAR		
Sample 40	AAC	NR	AAC	NR
Sample 41	AAC	AAC		
Sample 42	AAA	AAA		
Sample 43	AAC	AAC		
Sample 44	AAT	AAT		
Sample 45	AAA	AAA		
Sample 46	AAA	NR	NR	AAC
Sample 47	AAG	AAG		
Sample 48	AAC	AAC		
Sample 49	AAR	AAR		
Sample 50	AAA	NR	AAA	NR
Sample 51	AAA	AAA		
Sample 52	AAC	AAC		
Sample 53	AAA	AAA		
Sample 54	AGT	AAG		
Sample 55	AAA	AAA		
Sample 56	AAC	AAC		
Sample 57	AAC	AAC		
Sample 58	AAA	AAA		
Sample 59	AAA	AAA		
Sample 60	AAM	NR	AAC	NR
Sample 61	AAA	AAA		
Sample 62	AAC	AAC		
Sample 63	AAT	AAT		
Sample 64	AAA	AAA		
Sample 65	AAA	AAA		
Sample 66	AAA	AAA		
Sample 67	AGA	NR	AAA	NR
Sample 68	AAA	NR	AAA	AAA
Sample 69	AAA	AAA		
Sample 70	AAA	AAA		
Sample 71	AGC	NR	NR	NR
Sample 72	AAC	AAC		
Sample 73	AAT	AAY		
Sample 74	AAG	AAG		
Sample 75	AAA	AAA		
Sample 76	AAT	AAT		
Sample 77	AAA	NR	NR	NR
Sample 78	AAC	AAC		
Sample 79	AAA	NR	AAA	NR
Sample 80	AAA	AAA		
Sample 81	AAA	AAA		
Sample 82	AAA	AAA		
Sample 83	AAA	AAA		
Sample 84	AAC	AAC		
Sample 85	AAA	AAA		
Sample 86	AAG	AAG		
Sample 87	AAC	AAC		
Sample 88	AAA	AAA		
Sample 89	AAG	AAG		
Sample 90	AAA	AAA		
Sample 91	AAG	AAG		
Sample 92	AAC	AAC		
Sample 93	AAA	AAA		
Sample 94	AAC	NR	AAC	AAC
Sample 95	AAA	AAA		
Sample 96	AAA	AAA		
Sample 97	AAA	NR	NR	NR
Sample 98	AAA	AAA		
Sample 99	AAA	AAA		
Sample 100	AAA	AAA		
Sample 101	AAA	AAA		
Sample 102	AAC	AAC		
Sample 103	AAC	AAC		

The AAC, AAT, AGA, AGT or AGC genotypes at codon 103 result in drug resistance.

Table D3. Population sequences and HRMA predictions for the 181 assay.

Patient sample	181 Sequence	181 HRM	Deletion probe	Universal probe
Sample 1a	TAT	TAT		
Sample 1b	TRT	TRT		
Sample 2a	TAT	TAT		
Sample 2b	TAT	TAT		
Sample 3a	TAT	TAT		
Sample 3b	TRT	TRT		
Sample 4a	TAT	TAT		
Sample 4b	TAT	TAT		
Sample 5a	TAT	TAT		
Sample 5b	TAT	TAT		
Sample 6a	TAT	TAT		
Sample 6b	TAT	TRT		
Sample 7a	TAT	TAT		
Sample 7b	TAT	TAT		
Sample 8a	TAT	TAT		
Sample 8b	TAT	TAT		
Sample 9a	TAT	TAT		
Sample 9b	TAT	TAT		
Sample 10a	TAT	TAT		
Sample 10b	TRT	TRT		
Sample 11a	TAT	NR	TAT	TAT
Sample 11b	TAT	NR	TAT	TAT
Sample 12a	TAT	TAT		
Sample 12b	TAT	TAT		
Sample 13a	TAT	TAT		
Sample 13b	TAT	TAT		
Sample 14	TAT	TAT		
Sample 15	TAT	NR	TAT	NR
Sample 16	TAT	TAT		
Sample 17	TAT	TAT		
Sample 18	TAT	TAT		
Sample 19	TRT	TRT		
Sample 20	TAT	TAT		
Sample 21	TAT	TAT		
Sample 22	TAT	TAT		
Sample 23	TAT	TAT		
Sample 24	TAT	TAT		
Sample 25	TAT	TAT		
Sample 26	TAT	NR	NR	NR
Sample 27	TAY	TAT		
Sample 28	TAT	TAT		
Sample 29	TAT	TAT		
Sample 30	TAT	TAT		
Sample 31	TAT	TAT		
Sample 32	TAT	TAT		
Sample 33	TAT	TAT		
Sample 34	TAT	NR	TAT	NR
Sample 35	TAT	TAT		
Sample 36	TAT	TAT		
Sample 37	TAT	TAT		
Sample 38	TAT	TAT		
Sample 39	TAT	TAT		
Sample 40	TAT	TAT		
Sample 41	TAT	TAT		
Sample 42	TAT	TAT		
Sample 43	TAT	TAT		
Sample 44	TAT	TAT		
Sample 45	TAT	TAT		
Sample 46	TAT	TAT		
Sample 47	TAT	TAT		
Sample 48	TAT	TAT		
Sample 49	TAT	NR	TAT	NR
Sample 50	TAT	TAT		
Sample 51	TAT	TAT		
Sample 52	TAT	TAT		
Sample 53	TAT	TAT		
Sample 54	TAT	TAT		
Sample 55	TAT	NR	TAT	TAT
Sample 56	TAT	TAT		
Sample 57	TAT	TAT		
Sample 58	TAT	NR	TAT	NR
Sample 59	TAT	TAT		
Sample 60	TAT	TAT		
Sample 61	TAT	TAT		
Sample 62	TAT	NR	NR	NR
Sample 63	TAT	TAT		
Sample 64	TAT	TAT		
Sample 65	TAT	TAT		
Sample 66	TAT	TAT		
Sample 67	TAT	TAT		
Sample 68	TAT	TAT		
Sample 69	TAT	TRT		
Sample 70	TAT	TAT		
Sample 71	TAT	TAT		
Sample 72	TAT	TAT		
Sample 73	TAT	TRT		
Sample 74	TAT	TAT		
Sample 75	TAT	TAT		
Sample 76	TAT	TAT		
Sample 77	TAC	NR	NR	NR
Sample 78	TAT	TAT		
Sample 79	TAT	TAT		
Sample 80	TAT	TAT		
Sample 81	TAT	TAT		
Sample 82	TAT	TAT		
Sample 83	TAT	TAT		
Sample 84	TAT	TAT		
Sample 85	TRT	TRT		
Sample 86	TGT	TRT		
Sample 87	TAT	TAT		
Sample 88	TAT	TAT		
Sample 89	TAT	TAT		
Sample 90	TAC	NR	NR	NR
Sample 91	TAT	TAT		
Sample 92	TAT	TAT		
Sample 93	TRT	TRT		
Sample 94	TAT	TAT		
Sample 95	TAT	TAT		
Sample 96	TAT	TAT		
Sample 97	TAT	TAT		
Sample 98	TAT	TAT		
Sample 99	TAT	TAT		
Sample 100	TAT	TAT		
Sample 101	TAT	TAT		
Sample 102	TAT	TAT		
Sample 103	TAT	TAT		

The TGT genotype at codon 181 results in drug resistance.

Table D4. Population sequences and HRMA predictions for the 184 assay.

Patient sample	184 Sequence	184 HRM	Altered primer
Sample 1a	ATG	ATG	
Sample 1b	ATG	ATG	
Sample 2a	ATG	ATG	
Sample 2b	ATG	ATG	
Sample 3a	ATG	ATG	
Sample 3b	ATG	ATG	
Sample 4a	ATG	ATG	
Sample 4b	ATG	ATG	
Sample 5a	ATG	ATG	
Sample 5b	ATG	ATG	
Sample 6a	ATG	ATG	
Sample 6b	ATG	ATG	
Sample 7a	ATG	ATG	
Sample 7b	ATG	ATG	
Sample 8a	ATG	NR	n/a
Sample 8b	GGA	NR	n/a
Sample 9a	ATG	ATG	
Sample 9b	ATG	ATG	
Sample 10a	ATG	ATG	
Sample 10b	ATG	RTG	
Sample 11a	ATG	ATG	
Sample 11b	ATG	ATG	
Sample 12a	ATG	ATG	
Sample 12b	ATG	ATG	
Sample 13a	ATG	ATG	
Sample 13b	ATG	ATG	
Sample 14	ATG	ATG	
Sample 15	ATG	NR	NR
Sample 16	ATG	ATG	
Sample 17	ATG	ATG	
Sample 18	ATG	ATG	
Sample 19	ATG	ATG	
Sample 20	ATG	ATG	
Sample 21	GTG	GTG	
Sample 22	GTG	GTG	
Sample 23	GTG	GTG	
Sample 24	GTG	RTG	
Sample 25	RTG	RTG	
Sample 26	GTG	GTG	
Sample 27	ATG	ATG	
Sample 28	GTR	GTG	
Sample 29	GTG	GTG	
Sample 30	GTG	GTG	
Sample 31	ATG	ATG	
Sample 32	ATG	NR	NR
Sample 33	GTG	GTG	
Sample 34	ATG	NR	ATG
Sample 35	RTR	ATG	
Sample 36	GTG	GTG	
Sample 37	ATG	ATG	
Sample 38	ATG	ATG	
Sample 39	ATG	ATG	
Sample 40	GTG	GTG	
Sample 41	GTG	GTG	
Sample 42	ATG	ATG	
Sample 43	ATG	ATG	
Sample 44	GTG	GTG	
Sample 45	ATG	NR	NR
Sample 46	RTG	RTG	
Sample 47	GTG	GTG	
Sample 48	GTG	GTG	
Sample 49	GTG	NR	GTG
Sample 50	ATG	ATG	
Sample 51	RTG	RTG	
Sample 52	GTA	NR	NR
Sample 53	GTG	RTG	
Sample 54	GTG	GTG	
Sample 55	ATG	RTG	
Sample 56	ATG	ATG	
Sample 57	GTG	GTG	
Sample 58	ATG	NR	ATG
Sample 59	ATG	ATG	
Sample 60	ATG	ATG	
Sample 61	GTG	GTG	
Sample 62	GTG	NR	GTG
Sample 63	ATG	NR	ATG
Sample 64	ATG	NR	NR
Sample 65	GTR	GTG	
Sample 66	ATG	NR	NR
Sample 67	ATG	ATG	
Sample 68	ATG	ATG	
Sample 69	GTR	GTG	
Sample 70	GTG	GTG	
Sample 71	GTA	NR	NR
Sample 72	GTG	GTG	
Sample 73	ATG	ATG	
Sample 74	ATG	ATG	
Sample 75	GTG	GTG	
Sample 76	ATG	ATG	
Sample 77	ATG	ATG	
Sample 78	GTG	GTG	
Sample 79	GTG	RTG	
Sample 80	GTG	RTG	
Sample 81	ATG	ATG	
Sample 82	ATG	ATG	
Sample 83	ATG	ATG	
Sample 84	ATG	NR	ATG
Sample 85	ATG	NR	n/a
Sample 86	GTG	RTG	
Sample 87	GTG	GTG	
Sample 88	GTG	GTG	
Sample 89	ATG	NR	ATG
Sample 90	GTG	GTG	
Sample 91	GTG	NR	GTG
Sample 92	ATG	RTG	
Sample 93	GTG	GTG	
Sample 94	GTG	RTG	
Sample 95	ATG	ATG	
Sample 96	ATG	ATG	
Sample 97	ATG	ATG	
Sample 98	ATG	ATG	
Sample 99	ATG	NR	ATG
Sample 100	ATG	NR	ATG
Sample 101	ATG	ATG	
Sample 102	GTG	RTG	
Sample 103	ATG	ATG	

n/a = no amplification. The GTG or GTA genotypes at codon 184 result in drug resistance.

Table D5. Population sequences and HRMA predictions for the 151 assay.

Patient sample	151 Sequence	151 HRM MM	151 HRM	Altered primer
Sample 1a	CAG	CAG	CAR	
Sample 1b	CAG	CAG	CAR	
Sample 2a	CAG	CAG	CAR	
Sample 2b	CAG	CAG	CAR	
Sample 3a	CAG	CAG	CAR	
Sample 3b	CAG	CAG	CAG	
Sample 4a	CAG	CAG	CAR	
Sample 4b	CAG	CAG	CAR	
Sample 5a	CAG	CAG	CAR	
Sample 5b	CAG	CAG	CAR	
Sample 6a	CAG	CAG	CAR	
Sample 6b	CAG	CAG	CAR	
Sample 7a	CAA	NR	NR	n/a
Sample 7b	CAA	NR	NR	n/a
Sample 8a	CAA	CAA	CAA	
Sample 8b	CAA	CAA	CAA	
Sample 9a	CAG	CAG	CAR	
Sample 9b	CAG	CAG	CAR	
Sample 10a	CAA	CAA	NR	
Sample 10b	CAA	CAG	CAG	n/a
Sample 11a	CAG	CAG	CAR	
Sample 11b	CAG	CAG	CAR	
Sample 12a	CAG	CAG	CAR	
Sample 12b	CAG	CAG	CAR	
Sample 13a	CAA	NR	NR	NR
Sample 13b	CAA	NR	NR	NR
Sample 14	CAG	CAA	NR	n/a
Sample 15	CAG	CAG	CAG	
Sample 16	CAG	CAG	CAR	
Sample 17	CAG	CAG	CAR	
Sample 18	CAG	NR	NR	NR
Sample 19	CAG	CAG	CAG	
Sample 20	CAG	NR	NR	NR
Sample 21	CAG	NR	NR	NR
Sample 22	CAG	CAG	CAR	
Sample 23	CAG	CAG	CAG	
Sample 24	CAG	CAG	CAR	
Sample 25	CAG	CAG	CAR	
Sample 26	CAG	CAG	CAR	
Sample 27	CAG	CAG	CAR	
Sample 28	CAG	CAG	CAR	
Sample 29	CAA	NR	CAA	CAA
Sample 30	CAA	CAA	CAA	
Sample 31	CAG	CAG	CAR	
Sample 32	CAA	CAA	CAA	
Sample 33	CAG	CAG	CAR	
Sample 34	CAG	NR	NR	CAG
Sample 35	CAG	CAG	CAR	
Sample 36	CAG	CAG	CAG	
Sample 37	CAG	CAG	CAR	
Sample 38	CAG	NR	NR	NR
Sample 39	CAG	CAG	CAR	
Sample 40	CAG	NR	NR	CAG
Sample 41	CAA	CAA	NR	
Sample 42	CAG	NR	NR	CAG
Sample 43	CAA	NR	NR	NR
Sample 44	CAA	NR	NR	NR
Sample 45	CAG	NR	NR	CAG
Sample 46	CAG	CAG	CAG	
Sample 47	CAG	CAG	CAR	
Sample 48	CAA	NR	NR	CAA
Sample 49	CAG	CAG	CAG	
Sample 50	CAG	CAG	CAR	
Sample 51	CAG	CAG	CAG	
Sample 52	CAA	NR	NR	NR
Sample 53	CAG	CAG	CAR	
Sample 54	CAG	CAG	CAG	
Sample 55	CAG	CAG	CAR	
Sample 56	CAG	NR	NR	NR
Sample 57	CAG	NR	NR	CAG
Sample 58	CAG	NR	NR	CAG
Sample 59	CAG	NR	NR	CAG
Sample 60	CAG	CAG	CAG	
Sample 61	CAG	CAG	CAR	
Sample 62	CAG	CAG	CAR	
Sample 63	CAA	NR	CAA	CAA
Sample 64	CAG	NR	NR	CAG
Sample 65	CAG	NR	NR	CAG
Sample 66	CAG	CAG	CAG	
Sample 67	CAG	CAA	NR	
Sample 68	CAG	CAG	CAR	
Sample 69	CAG	CAG	CAG	
Sample 70	CAG	CAA	CAG	
Sample 71	CAG	CAG	CAG	
Sample 72	CAA	CAA	CAA	
Sample 73	CAA	CAA	CAA	
Sample 74	CAG	NR	NR	CAG
Sample 75	CAG	NR	NR	CAG
Sample 76	CAG	NR	NR	CAG
Sample 77	CAA	CAA	CAA	
Sample 78	CAG	CAG	CAR	
Sample 79	CAG	CAG	CAR	
Sample 80	CAG	CAG	CAR	
Sample 81	CAG	CAG	CAG	
Sample 82	ATG	ATG	ATG	
Sample 83	CAG	CAG	CAR	
Sample 84	ATG	ATG	ATG	
Sample 85	ATG	ATG	ATG	
Sample 86	CAG	CAG	CAR	
Sample 87	CAG	CAG	CAG	
Sample 88	CAA	CAA	CAA	
Sample 89	CAG	CAG	CAR	
Sample 90	CAG	NR	NR	NR
Sample 91	CAG	CAG	CAR	
Sample 92	CAG	CAG	CAR	
Sample 93	CAG	CAG	CAR	
Sample 94	CAG	CAG	CAR	
Sample 95	CAG	NR	NR	CAG
Sample 96	CAG	CAG	CAR	
Sample 97	MTG	ATG	ATG	
Sample 98	CAG	CAG	CAR	
Sample 99	CAG	NR	NR	CAG
Sample 100	ATG	ATG	ATG	
Sample 101	CAG	CAG	CAR	
Sample 102	CAG	CAG	CAG	
Sample 103	CAG	NR	NR	CAG

n/a = no amplification. The ATG genotype at codon 151 results in drug resistance.

Table D6. Population sequences and HRMA predictions for the 190 assay.

Patient sample	190 Sequence	190 HRM
Sample 1a	GGA	GGA
Sample 1b	GGA	GGA
Sample 2a	GGA	GGA
Sample 2b	GGA	GGA
Sample 3a	GGA	GGA
Sample 3b	GGA	NR
Sample 4a	GGA	GGA
Sample 4b	GSA	NR
Sample 5a	GGA	NR
Sample 5b	GGA	NR
Sample 6a	GGA	GGA
Sample 6b	GGA	NR
Sample 7a	GGA	GGA
Sample 7b	GGA	GGA
Sample 8a	GGA	GGA
Sample 8b	ACA	GGA
Sample 9a	GGA	GGA
Sample 9b	GGA	NR
Sample 10a	GGA	NR
Sample 10b	GGA	GGA
Sample 11a	GGA	GGA
Sample 11b	GGA	NR
Sample 12a	GGA	GGA
Sample 12b	GSA	GGA
Sample 13a	GGA	GGA
Sample 13b	GGA	GGA
Sample 14	GGA	GGA
Sample 15	GGA	GGA
Sample 16	GGA	GGA
Sample 17	GGA	GGA
Sample 18	GGA	GGA
Sample 19	GGA	NR
Sample 20	GGR	NR
Sample 21	GGA	NR
Sample 22	GGA	GGA
Sample 23	GGA	GGA
Sample 24	GGA	GGA
Sample 25	GGA	NR
Sample 26	GGA	GGA
Sample 27	GGR	GGA
Sample 28	GGA	NR
Sample 29	GGA	GGA
Sample 30	GGA	GGA
Sample 31	GGA	GGA
Sample 32	GGA	NR
Sample 33	GCA	GCA
Sample 34	GGA	GGA
Sample 35	GSA	NR
Sample 36	GGC	NR
Sample 37	GSA	NR
Sample 38	GGA	GGA
Sample 39	GGA	GGA
Sample 40	GGA	GGA
Sample 41	GGA	GGA
Sample 42	GGA	GGA
Sample 43	GGA	GGA
Sample 44	GGA	NR
Sample 45	GGA	GGA
Sample 46	GGA	GGA
Sample 47	GGA	NR
Sample 48	GGA	GGA
Sample 49	GGA	NR
Sample 50	GGA	NR
Sample 51	GGA	GGA
Sample 52	GGA	GGA
Sample 53	GGA	NR
Sample 54	GCA	GCA
Sample 55	GGA	GGA
Sample 56	GGA	GGA
Sample 57	GGA	GGA
Sample 58	GGA	GGA
Sample 59	GGC	NR
Sample 60	GGA	GGA
Sample 61	GGA	NR
Sample 62	GGA	NR
Sample 63	GGA	GGA
Sample 64	GGA	GGA
Sample 65	GGA	NR
Sample 66	GGA	GGA
Sample 67	GGA	GGA
Sample 68	GCA	GCA
Sample 69	GGR	NR
Sample 70	GGA	GGA
Sample 71	GGA	NR
Sample 72	GGA	GGA
Sample 73	GCA	NR
Sample 74	GGA	GGA
Sample 75	GCA	NR
Sample 76	GCA	GCA
Sample 77	GGA	GGA
Sample 78	GGA	NR
Sample 79	GCA	GCA
Sample 80	GGA	GGA
Sample 81	GGA	NR
Sample 82	GGA	GGA
Sample 83	GGA	GGA
Sample 84	GGA	NR
Sample 85	AGC	NR
Sample 86	GGA	NR
Sample 87	GGA	NR
Sample 88	GGA	GGA
Sample 89	GGA	GGA
Sample 90	GGA	GGA
Sample 91	GGA	GGA
Sample 92	GGA	NR
Sample 93	GSA	NR
Sample 94	GGA	GGA
Sample 95	GGA	NR
Sample 96	GGA	GGA
Sample 97	GGA	GGA
Sample 98	GGA	GGA
Sample 99	GGA	GGA
Sample 100	GGA	GGA
Sample 101	GSA	NR
Sample 102	GGA	NR
Sample 103	GGA	GGA

The GCA, ACA or AGC genotypes at codon 190 result in drug resistance.

Table D7. Selected population sequences and HRMA predictions for the 65 assay.

Patient sample	65 sequence	65 HRM
Sample 83	ARG	AGG
Sample 84	ARG	AGG
Sample 97	ARG	AGG

The AGG genotype at codon 65 results in drug resistance.

Table D8. Selected population sequences and HRMA predictions for the 106 assay.

Patient sample	106 sequence	106 HRM
Sample 2b	RTG	ATG
Sample 5b	RTG	NR
Sample 12b	RTG	NR
Sample 21	ATG	ATG
Sample 23	ATG	ATG
Sample 28	ATG	ATG
Sample 32	ATG	ATG
Sample 33	ATG	ATG
Sample 35	ATG	ATG
Sample 40	ATG	ATG
Sample 51	ATG	ATG
Sample 53	ATG	ATG
Sample 62	ATG	ATG
Sample 67	ATG	ATG
Sample 68	ATG	ATG

The ATG genotype at codon 106 results in drug resistance.

Appendix E: Ethics Clearance

UNIVERSITY OF THE WITWATERSRAND, JOHANNESBURG

Division of the Deputy Registrar (Research)

HUMAN RESEARCH ETHICS COMMITTEE (MEDICAL)
R14/49 David Sacks

CLEARANCE CERTIFICATE	**M090360**
PROJECT	Surveillance of HIV Drug Resistance in South Africa (as part of M020725 Prof L Morris)
INVESTIGATORS	David Sacks.
DEPARTMENT	Pathology Department
DATE CONSIDERED	09.03.09
DECISION OF THE COMMITTEE*	Approved unconditionally

Unless otherwise specified this ethical clearance is valid for 5 years and may be renewed upon application.

DATE **CHAIRPERSON** .....
(Professor P E Cleaton Jones)

*Guidelines for written 'informed consent' attached where applicable

cc: Supervisor : Dr G Hunt

DECLARATION OF INVESTIGATOR(S)

To be completed in duplicate and **ONE COPY** returned to the Secretary at Room 10004, 10th Floor, Senate House, University.
I/We fully understand the conditions under which I am/we are authorized to carry out the abovementioned research and I/we guarantee to ensure compliance with these conditions. Should any departure to be contemplated from the research procedure as approved I/we undertake to resubmit the protocol to the Committee. **I agree to a completion of a yearly progress report.**

PLEASE QUOTE THE PROTOCOL NUMBER IN ALL ENQUIRIES...

.....

References

Ahmadian, A., Ehn, M. and Hober, S., 2006. Pyrosequencing: History, Biochemistry and Future. Clinica Chimica Acta 363, 83–94.

Alcorn, T.M. and Faruki, H., 2000. HIV Resistance Testing: Methods, Utility, and Limitations. Molecular Diagnosis 5, 159-168.

Allan, J.S., Coligan, J.E., Barin, F., McLane, M.F., Sodroski, J.G., Rosen, C.A., Haseltine, W.A., Lee, T.H. and Essex, M., 1985. Major Glycoprotein Antigens that Induce Antibodies in AIDS Patients are Encoded by HTLV-III. Science 228, 1091-1094.

Bacheler, L.T., Anton, E.D., Kudish, P., Baker, D., Bunville, J., Krakowski, K., Bolling, L., Aujay, M., Wang, X.V., Ellis, D., Becker, M.F., Lasut, A.L., George, H.J., Spalding, D.R., Hollis, G. and Abremski, K., 2000. Human Immunodeficiency Virus Type 1 Mutations Selected in Patients Failing Efavirenz Combination Therapy. Antimicrobial Agents and Chemotherapy 44, 2475-2484.

Baldanti, F., Paolucci, S., Dossena, L. and Gerna, G., 2004. Assays for Determination of HIV Resistance to Antiviral Drugs. Current Drug Metabolism 5, 317-319.

Barré-Sinoussi, F., Chermann, J., Rey, F., Nugeyre, M., Chamaret, S., Gruest, J., Dauguet, C., Axler-Blin, C., Vézinet-Brun, F., Rouzioux, C., Rozenbaum, W. and Montagnier, L., 1983. Isolation of a T-lymphotropic Retrovirus From a Patient at Risk for Acquired Immune Deficiency Syndrome (AIDS). Science 220, 868-71.

Baxter, J.D., Mayers, D.L., Wentworth, D.N., Neaton, J.D., Hoover, M.L., Winters, M.A., Mannheimer, S.B., Thompson, M.A., Abrams, D.I., Brizz, B.J., Ioannidis, J.P. and Merigan, T.C., 2000. A Randomized Study Of Antiretroviral Management Based On Plasma Genotypic Antiretroviral Resistance Testing In Patients Failing Therapy. CPCRA

046 Study Team For The Terry Beirn Community Programs For Clinical Research On AIDS. AIDS 14, F83-93.

Bennett, D.E., Bertagnolio, S., Sutherland, D. and Gilks, C.F., 2008. The World Health Organization's Global Strategy for Prevention and Assessment of HIV Drug Resistance. Antiviral Therapy 13 Suppl 2, 1-13.

Bieniasz, P.D., 2009. The Cell Biology of HIV-1 Virion Genesis. Cell Host and Microbe 5, 550-558.

Birnboim, H.C. and Doly, J., 1979. A Rapid Alkaline Extraction Procedure For Screening Recombinant Plasmid DNA. Nucleic Acids Research 7, 1513-1523.

Boyer, P.L., Gao, H.-Q. and Hughes, S.H., 1998. Mutation at Position 190 of Human Immunodeficiency Virus Type 1 Reverse Transcriptase Interacts with Mutations at Positions 74 and 75 Via the Template Primer. Antimicrobial Agents and Chemotherapy 42, 447–452.

Boyer, P.L., Sarafianos, S.G., Arnold, E. and Hughes, S.H., 2001. Selective Excision of AZTMP by Drug-Resistant Human Immunodeficiency Virus Reverse Transcriptase. Journal of Virology 75, 4832–4842.

Brenner, B., Turner, D., Oliveira, M., Moisi, D., Detorio, M., Carobene, M., Marlink, R.G., Schapiro, J., Rogerd, M. and Wainberg, M.A., 2003. A V106M Mutation in HIV-1 Clade C Viruses Exposed to Efavirenz Confers Cross-Resistance to Non-Nucleoside Reverse Transcriptase Inhibitors. AIDS 17, F1–F5.

Burke, D.S., 1997. Recombination in HIV: an Important Viral Evolutionary Strategy. Emerging Infectious Diseases 3, 253-259.

Bushmana, F.D., Hoffmanna, C., Ronena, K., Malani, N., Minkaha, N., Rosea, H.M., Tebas, P. and Wang, G.P., 2008. Massively Parallel Pyrosequencing in HIV Research. AIDS 22, 1411–1415.

Centers for Disease Control and Prevention, 2005. Antiretroviral Postexposure Prophylaxis After Sexual, Injection-Drug Use, or Other Nonoccupational Exposure to HIV in the United States: Recommendations from the U.S. Department of Health and Human Services. Morbidity and Mortality Weekly Report 54, 1-19.

Chan, D.C., Fass, D., Berger, J.M. and Kim, P.S., 1997. Core Structure of gp41 from the HIV Envelope Glycoprotein. Cell 89, 263–273.

Chen, Z., Telfer, P., Gettie, A., Reed, P., Zhang, L., Ho, D.D. and Marx, P.A., 1996. Genetic Characterization of New West African Simian Immunodeficiency Virus SIVsm: Geographic Clustering of Household-Derived SIV Strains with Human Immunodeficiency Virus Type 2 Subtypes and Genetically Diverse Viruses from a Single Feral Sooty Mangabey Troop. Journal of Virology 70, 3617–3627.

Cheng, J.-C., Huang, C.-L., Lin, C.-C., Chen, C.-C., Chang, Y.-C., Chang, S.-S. and Tseng, C.-P., 2006. Rapid Detection and Identification of Clinically Important Bacteria by High-Resolution Melting Analysis after Broad-Range Ribosomal RNA Real-Time PCR. Clinical Chemistry 52, 1997–2004.

Cheung, P.K., Wynhoven, B. and Harrigan, P.R., 2004. 2004: Which HIV-1 Drug Resistance Mutations are Common in Clinical Practice? AIDS Reviews 6, 107-116.

Chou, L.-S., Meadows, C., Wittwer, C.T. and Lyon, E., 2005. Unlabeled Oligonucleotide Probes Modified with Locked Nucleic Acids for Improved Mismatch Discrimination in Genotyping by Melting Analysis. Biotechniques 39, 644-647.

Cilliers, T., Willey, S., MSullivan, W., Patience, T., Pugach, P., Coetzer, M., Papathanasopoulos, M., PMoore, J., Trkola, A., Clapham, P. and Morris, L., 2005. Use of Alternate Coreceptors on Primary Cells by Two HIV-1 Isolates. Virology 339, 136-144.

Clavel, F. and Hance, A.J., 2004. HIV Drug Resistance. New England Journal of Medicine 350, 1023-1035.

Connick, E., Lederman, M.M., Kotzin, B., Spritzler, J., Kuritzkes, D.R., St Clair, M., Sevin, A.D., Fox, L., Chiozzi, M.H., Leonard, J.M., Rousseau, F., D'Arc Roe, J., Martinez, A., Kessler, H. and Landay, A., 2000. Immune Reconstitution In The First Year Of Potent Antiretroviral Therapy And Its Relationship To Virologic Response. The Journal of Infectious Diseases 181, 358-363.

Dames, S., Pattison, D.C., Bromley, L.K., Wittwer, C.T. and Voelkerding, K.V., 2007. Unlabeled Probes for the Detection and Typing of Herpes Simplex Virus. Clinical Chemistry 53, 1847–1854.

De Clercq, E., 1998. The Role of Non-Nucleoside Reverse Transcriptase Inhibitors (NNRTIs) in the Therapy of HIV-1 Infection. Antiviral Research 38, 153–179.

De Clercq, E., 2001. New Developments in Anti-HIV Chemotherapy. Current Medicinal Chemistry 8, 1543-1572.

De Clercq, E., 2004. Non-Nucleoside Reverse Transcriptase Inhibitors (NNRTIs): Past, Present, and Future. Chemistry and Biodiversity 1, 44-64.

Delaugerre, C., Mouroux, M., Yvon-Groussin, A., Simon, A., Angleraud, F., Huraux, J.-M., Agut, H., Katlama, C. and Calvez, V., 2001. Prevalence and Conditions of Selection of E44D/A and V118I Human Immunodeficiency Virus Type 1 Reverse Transcriptase Mutations in Clinical Practice. Antimicrobial Agents and Chemotherapy 45, 946–948.

Durant, J., Clevenbergh, P., Halfon, P., Delgiudice, P., Porsin, S., Simonet, P., Montagne, N., Boucher, C.A., Schapiro, J.M. and Dellamonica, P., 1999. Drug-Resistance Genotyping In HIV-1 Therapy: The VIRADAPT Randomised Controlled Trial. Lancet 353, 2195-2199.

El-Khatib, Z., Ekström, A.M., Ledwaba, J., Mohapi, L., Laher, F., Karstaedt, A., Charalambous, S., Petzold, M., Katzenstein, D. and Morris, L., 2009. Risk Factors for Viremia and Drug Resistance Among HIV-1 Patients on Antiretroviral Treatment – A Cross-Sectional Study in Soweto, South Africa. AIDS 24, DOI:10.1097/QAD.0b013e32833a097b.

Erali, M., Voelkerding, K.V. and Wittwer, C.T., 2008. High Resolution Melting Applications for Clinical Laboratory Medicine. Experimental and Molecular Pathology 85, 50-58.

Erice, A., Mayers, D.L., Strike, D.G., Sannerud, K.J., McCutchan, F.E., Henry, K. and Balfour, H.H., 1993. Primary Infection with Zidovudine-Resistant Human Immunodeficiency Virus Type 1. New England Journal of Medicine 328, 1123-1124.

Eshleman, S.H., Hackett Jr, J., Swanson, P., Cunningham, S.P., Drews, B., Brennan, C., Devare, S.G., Zekeng, L., Kaptué, L. and Marlowe, N., 2004. Performance of the Celera Diagnostics ViroSeq HIV-1 Genotyping System for Sequence-Based Analysis of Diverse Human Immunodeficiency Virus Type 1 Strains. Journal of Clinical Microbiology 42, 2711-2717.

Gallo, R.C., Salahuddin, S.Z., Popovic, M., Shearer, G.M., Kaplan, M., Haynes, B.F., Palker, T.J., Redfield, R., Oleske, J. and Safai, B., 1984. Frequent Detection and Isolation of Cytopathic Retroviruses (HTLV-III) From Patients with AIDS and at Risk for AIDS. Science 224, 500-3.

Gao, F., Bailes, E., Robertson, D.L., Chen, Y., Rodenburg, C.M., Michael, S.F., Cummins, L.B., Arthur, L., Peeters, M., Shaw, G.M., Sharp, P.M. and Hahn, B.H., 1999. Origin of HIV-1 in the Chimpanzee *Pan Troglodytes Troglodytes*. Nature 397, 436-441.

Garcia-Lerma, J.G., 2005. Diversity of Thymidine Analogue Resistance Genotypes Among Newly Diagnosed HIV-1-Infected Persons. Journal of Antimicrobial Chemotherapy 56, 265–269.

Gardner, E.M., Burman, W.J., Steiner, J.F., Anderson, P.L. and Bangsberg, D.R., 2009. Antiretroviral Medication Adherence And The development Of Class-Specific Antiretroviral Resistance. AIDS 23, 1035-1046.

Geijtenbeek, T.B. and van Kooyk, Y., 2003. DC-SIGN: a novel HIV receptor on DCs that mediates HIV-1 transmission. Current Topics in Microbiology and Immunology 276, 31-54.

Gelderblom, H.R., Hausmann, E.H.S., Özel, M., Pauli, G. and Koch, M.A., 1987. Fine Structure of Human Immunodeficiency Virus (HIV) and Immunolocalization of Structural Proteins. Virology 156, 171-176.

Gentile, M., Adrian, T., Scheidler, A., Ewald, M., Dianzania, F., Pauli, G. and Gelderblom, H.R., 1994. Determination of the Size of HIV Using Adenovirus Type 2 as an Internal Length Marker. Journal of Virological Methods 48, 43-52.

Giglio, S., Monis, P.T. and Saint, C.P., 2005. *Legionella* Confirmation Using Real-Time PCR and SYTO9 is an Alternative to Current Methodology. Applied and Environmental Microbiology 71, 8944–8948.

Goedert, J.J., Biggar, R.J., Melbye, M., Mann, D.L., Wilson, S., Gail, M.H., Grossman, R.J., DiGioia, R.A., Sanchez, W.C. and Weiss, S.H., 1987. Effect of T4 Count and Cofactors

on the Incidence of AIDS in homosexual men infected with human immunodeficiency virus. Journal Of the American Medical Association 257, 331-334.

Goldschmidt, V. and Marquet, R., 2004. Primer Unblocking by HIV-1 Reverse Transcriptase and Resistance to Nucleoside RT Inhibitors (NRTIs). The International Journal of Biochemistry and Cell Biology 36, 1687–1705.

Gonzales, M.J., Wu, T.D., Taylor, J., Belitskaya, I., Kantor, R., Israelski, D., Chou, S., Zolop, A.R., Fessel, W.J. and Shafer, R.W., 2003. Extended Spectrum of HIV-1 Reverse Transcriptase Mutations in Patients Receiving Multiple Nucleoside Analog Inhibitors. AIDS 17, 791–799.

Grant, R.M., Kuritzkes, D.R., Johnson, V.A., Mellors, J.W., Sullivan, J.L., Swanstrom, R., D'Aquila, R.T., Gorder, M.V., Holodniy, M., Lloyd Jr, R.M., Reid, C., Morgan, G.F. and Winslow, D.L., 2003. Accuracy of the TRUGENE *HIV-1* Genotyping Kit. Journal of Clinical Microbiology 41, 1586–1593.

Greenberg, M.L. and Cammack, N., 2004. Resistance to Enfuvirtide, the First HIV Fusion Inhibitor. Journal of Antimicrobial Chemotherapy 54, 333–340.

Grievink, H. and Stowell, K.M., 2008. Identifcation of Ryanodine Receptor 1 Single-Nucleotide Polymorphisms by High-Resolution Melting Using the LightCycler 480 System. Analytical Biochemistry 374, 396-404.

Gundry, C.N., Vandersteen, J.G., Reed, G.H., Pryor, R.J., Chen, J. and Wittwer, C.T., 2003. Amplicon Melting Analysis with Labeled Primers: A Closed-Tube Method for Differentiating Homozygotes and Heterozygotes. Clinical Chemistry 49, 396–406.

Hanna, G.J. and D'Aquila, R.T., 2001. Clinical Use of Genotypic and Phenotypic Drug Resistance Testing to Monitor Antiretroviral Chemotherapy. Clinical Infectious Diseases 32, 774–782.

Harrigan, P.R., Mo, T., Wynhoven, B., Hirsch, J., Brumme, Z., McKenna, P., Pattery, T., Vingerhoets, J. and Bacheler, L.T., 2005. Rare Mutations at Codon 103 of HIV-1 Reverse Transcriptase can Confer Resistance to Non-Nucleoside Reverse Transcriptase Inhibitors. AIDS 19, 549-554.

Hemelaar, J., Gouws, E., Ghys, P.D. and Osmanov, S., 2006. Global and Regional Distribution of HIV-1 Genetic Subtypes and Recombinants in 2004. AIDS 20, W13–W23.

Herrmann, M.G., Durtschi, J.D., Bromley, L.K., Wittwer, C.T. and Voelkerding, K.V., 2006a. Amplicon DNA Melting Analysis for Mutation Scanning and Genotyping: Cross-Platform Comparison of Instruments and Dyes. Clinical Chemistry 52, 494–503.

Herrmann, M.G., Durtschi, J.D., Voelkerding, K.V. and Wittwer, C.T., 2006b. Instrument Comparison for DNA Genotyping by Amplicon Melting. Journal of the Association for Laboratory Automation 11, 273–277.

Hewson, K., Noormohammadi, A.H., Devlin, J.M., Mardani, K. and Ignjatovic, J., 2009. Rapid Detection and Non-Subjective Characterisation of Infectious Bronchitis Virus Isolates Using High-Resolution Melt Curve Analysis and a Mathematical Model. Archives of Virology 154, 649–660.

Hill, C.E., Duncan, A., Wirth, D. and Nolte, F.S., 2006. Detection and Identification of Cytochrome P-450 2C9 Alleles *1, *2, and *3 by High-Resolution Melting Curve Analysis of PCR Amplicons. American Journal of Clinical Pathology 125, 584-591.

Holland, P.M., Abramson, R.D., Watson, R. and Gelfand, D.H., 1991. Detection of Specific Polymerase Chain Reaction Product by Utilizing the 5'----3' Exonuclease Activity of Thermus Aquaticus DNA Polymerase. Proceedings of the National Academy of Sciences USA 88, 7276–7280.

Huang, H., Chopra, R., Verdine, G.L. and Harrison, S.C., 2008. Structure of a Covalently Trapped Catalytic Complex of HIV-1 Reverse Transcriptase: Implications for Drug Resistance Science 282, 1669-1675.

Iversen, A.K., Shafer, R.W., Wehrly, K., Winters, M.A., Mullins, J.I., Chesebro, B. and Merigan, T.C., 1996. Multidrug-Resistant Human Immunodeficiency Virus Type 1 Strains Resulting from Combination Antiretroviral Therapy. American Society for Microbiology 7, 1086–1090.

Jeffery, N., Gasser, R.B., Steer, P.A. and Noormohammadi, A.H., 2007. Classification of *Mycoplasma Synoviae* Strains Using Single-Strand Conformation Polymorphism and High-Resolution Melting-Curve Analysis of the *vlhA* Gene Single-Copy Region. Microbiology 153, 2679–2688.

Johnson, V.A., Brun-Vézinet, F., Clotet, B., Günthard, H.F., Kuritzkes, D.R., Pillay, D., Schapiro, J.M. and Richman, D.D., 2009. Update of the Drug Resistance Mutations in HIV-1: December 2009. Topics In HIV Medicine 17, 138-145.

Joint United Nations Programme on HIV/AIDS. 2008. 2008 Report on the global AIDS epidemic, Vol. 2009, Geneva, Switzerland.

Kaur, H., Arora, A., Wengel, J. and Maiti, S., 2006. Thermodynamic, Counterion, and Hydration Effects for the Incorporation of Locked Nucleic Acid Nucleotides into DNA Duplexes. Biochemistry 45, 7347-7355.

Keele, B.F., Heuverswyn, F.V., Li, Y., Bailes, E., Takehisa, J., Santiago, M.L., Bibollet-Ruche, F., Chen, Y., Wain, L.V., Liegeois, F., Loul, S., Ngole, E.M., Bienvenue, Y., Delaporte, E., Brookfield, J.F.Y., Sharp, P.M., Shaw, G.M., Peeters, M. and Hahn, B.H., 2006. Chimpanzee Reservoirs of Pandemic and Nonpandemic HIV-1. Science 313, 523-526.

Kibbe, W.A., 2007. OligoCalc: an Online Oligonucleotide Properties Calculator. Nucleic Acids Research 35, W43-W46.

Klein, K.C., Reed, J.C. and Lingappa, J.R., 2007. Intracellular Destinies: Degradation, Targeting, Assembly, and Endocytosis of HIV Gag. AIDS Reviews 9, 150-161.

Knipe, D.M., Howley, P.M., Griffin, D.E., Lamb, R.A., Martin, M.A., Roizman, B. and Straus, S.E., 2007. Field's Virology, Vol. II. Lippincott Williams and Wilkins, Philadelphia

Kosalaraksa, P., Kavlick, M.F., Maroun, V., Le, R. and Mitsuya, H., 1999. Comparative Fitness of Multi-Dideoxynucleoside-Resistant Human Immunodeficiency Virus Type 1 (HIV-1) in an In Vitro Competitive HIV-1 Replication Assay. Journal of Virology 73, 5356–5363.

Koshkin, A.A., Singh, S.K., Nielsen, P., Rajwanshi, V.K., Kumar, R., Meldgaard, M., Olsen, C.E. and Wengel, J., 1998. LNA (Locked Nucleic Acids): Synthesis of the Adenine, Cytosine, Guanine, 5-Methylcytosine, Thymine and Uracil Bicyclonucleoside Monomers, Oligomerisation, and Unprecedented Nucleic Acid Recognition. Tetrahedron 54, 3607-3630.

Kozal, M.J., Shafer, R.W., Winters, M.A., Katzenstein, D.A. and Merigan, T.C., 1993. A Mutation in Human Immunodeficiency Virus Reverse Transcriptase and Decline in CD4 Lymphocyte Numbers in Long-Term Zidovudine Recipients. The Journal of Infectious Diseases 167, 526-532.

Krenková, P., Norambuena, P., Stambergová, A. and Macek, M., Jr, 2009. Evaluation of High-Resolution Melting (HRM) for Mutation Scanning of Selected Exons of the CFTR Gene. Folia Biologica 55, 238-242.

Krypuy, M., Newnham, G.M., Thomas, D.M., Conron, M. and Dobrovic, A., 2006. High Resolution Melting Analysis for the Rapid and Sensitive Detection of Mutations in Clinical Samples: KRAS Codon 12 and 13 Mutations in Non-Small Cell Lung Cancer. BMC Cancer 6, doi:10.1186/1471-2407-6-295.

Kubista, M., Andrade, J.M., Bengtsson, M., Forootan, A., Jonak, J., Lind, K., Sindelka, R., Sjoback, R., Sjogreen, B., Strombom, L., Stahlberg, A. and Zoric, N., 2006. The Real-Time Polymerase Chain Reaction. Molecular Aspects of Medicine 27, 95–125.

Kuiken, C., Leitner, T., Brian Foley, Hahn, B., Marx, P., Francince, McCutchan, Wolinsky, S. and Korber, B., 2009. HIV Sequence Compendium 2009. Los Alamos National Laboratory, Theoretical Biology and Biophysics, Los Alamos, New Mexico. LA-UR 09-03280.

Kwong, P.D., Wyatt, R., Robinson, J., Sweet, R.W., Sodroski, J. and Hendrickson, W.A., 1998. Structure of an HIV gp120 Envelope Glycoprotein in Complex with the CD4 Receptor and a Neutralizing Human Antibody. Nature 393, 648-659.

Lalezari, J.P., Henry, K., O'Hearn, M., Montaner, J.S.G., Piliero, P.J., Trottier, B., Walmsley, S., Cohen, C., Kuritzkes, D.R., J J. Eron Jr, Chung, J., DeMasi, R., Donatacci, L., Drobnes, C., Delehanty, J., Salgo, M. and TORO 1 Study Group, 2009. Enfuvirtide, an HIV-1 Fusion Inhibitor, for Drug-Resistant HIV Infection in North and South America. The New England Journal of Medicine 348, 2175-2185.

Landegren, U., Nilsson, M. and Kwok, P.-Y., 1998. Polymorphism Analysis Reading Bits of Genetic Information: Methods for Single-Nucleotide. Genome Research 8, 769-776.

Larder, B.A., Darby, G. and Richman, D.D., 1989. HIV with Reduced Sensitivity to Zidovudine (AZT) Isolated During Prolonged Therapy. Science 243, 1731-1734.

Larder, B.A., Kellam, P. and Kemp, S.D., 1991. Zidovudine Resistance Predicted by Direct Detection of Mutations in DNA from HIV-Infected Lymphocytes. AIDS 5, 137-144.

Latinovic, O., Kuruppu, J., Davis, C., Le, N. and Heredia, A., 2009. Pharmacotherapy of HIV-1 Infection: Focus on CCR5 Antagonist Maraviroc. Clinical Medicine Insights: Therapeutics 1, 1497–1510.

Lay, M.J. and Wittwer, C.T., 1997. Real-time Fluorescence Genotyping of Factor V Leiden During Rapid-Cycle PCR. Clinical Chemistry 43, 2262–2267.

Lehmann-Che, J. and Saïb, A., 2004. Early Stages of HIV Replication: How to Hijack Cellular Functions for a Successful Infection. AIDS Reviews 6, 199-207.

Liew, M., Pryor, R., Palais, R., Meadows, C., Erali, M., Lyon, E. and Wittwer, C.T., 2004. Genotyping of Single-Nucleotide Polymorphisms by High-Resolution Melting of Small Amplicons. Clinical Chemistry 50, 1156–1164.

Lin, J.-H., Tseng, C.-P., Chen, Y.-J., Lin, C.-Y., Chang, S.-S., Wu, H.-S. and Cheng, J.-C., 2008. Rapid Differentiation of Influenza A Virus Subtypes and Genetic Screening for Virus Variants by High-Resolution Melting Analysis. Journal of Clinical Microbiology 46, 1090–1097.

Lipsky, R.H., Mazzanti, C.M., Rudolph, J.G., Xu, K., Vyas, G., Bozak, D., Radel, M.Q. and Goldman, D., 2001. DNA Melting Analysis for Detection of Single Nucleotide Polymorphisms. Clinical Chemistry 47, 635–644.

Loakes, D., 2001. The Application of Universal DNA Base Analogues. Nucleic Acids Research 29, 2437-2447.

Loakes, D. and Brown, D.M., 1994. 5-Nitroindole as an Universal Base Analogue. Nucleic Acids Research 22, 4039-4043.

Loemba, H., Brenner, B., Parniak, M.A., Ma'ayan, S., Spira, B., Moisi, D., Oliveira, M., Detorio, M. and Wainberg, M.A., 2002. Genetic Divergence of Human Immunodeficiency Virus Type 1 Ethiopian Clade C Reverse Transcriptase (RT) and Rapid Development of Resistance Against Nonnucleoside Inhibitors of RT. Antimicrobial Agents and Chemotherapy 46, 2087-2094.

Lori, F. and Lisziewicz, J., 1999. Mechanisms of Human Immunodeficiency Virus Type 1 Inhibition by Hydroxyurea. Journal of Biological Regulators & Homeostatic Agents 13, 176-180.

Loubser, S., Balfeb, P., Shermanc, G., Hammer, S., Kuhnd, L. and Morris, L., 2006. Decay of K103N Mutants in Cellular DNA and Plasma RNA After Single-Dose Nevirapine to Reduce Mother-to-Child HIV Transmission. AIDS 20, 995–1002.

Luber, A.D., 2005. Genetic Barriers to Resistance and Impact on Clinical Response. Medscape General Medicine 7, 69.

Marconi, V.C., Sunpath, H., Lu, Z., Gordon, M., Koranteng-Apeagyei, K., Hampton, J., Carpenter, S., Giddy, J., Ross, D., Holst, H., Losina, E., Walker, B.D. and Kuritzkes, D.R., 2008. Prevalence of HIV-1 Drug Resistance after Failure of a First Highly Active Antiretroviral Therapy Regimen in KwaZulu Natal, South Africa. Clinical Infectious Diseases 46, 1589–1597.

Margraf, R.L., Mao, R., Highsmith, W.E., Holtegaard, L.M. and Wittwer, C.T., 2007. *RET* Proto-Oncogene Genotyping Using Unlabeled Probes, the Masking Technique, and Amplicon High-Resolution Melting Analysis. Journal of Molecular Diagnostics 9, 184-196.

Margraf, R.L., Mao, R. and Wittwer, C.T., 2006. Masking Selected Sequence Variation by Incorporating Mismatches Into Melting Analysis Probes. Human Mutation 27, 269-278.

Martinez-Picado, J. and Martinez, M.A., 2008. HIV-1 Reverse Transcriptase Inhibitor Resistance Mutations and Fitness: A View From the Clinic and *ex vivo*. Virus Research 134, 104–123.

Martins, S., Ramos, M.J. and Fernandes, P.A., 2008. The Current Status of the NNRTI Family of Antiretrovirals Used in the HAART Regime Against HIV Infection. Current Medicinal Chemistry 15, 1083-1095.

Martinson, N.A., Morris, L., Gray, G., Moodley, D., Pillay, V., Cohen, S., Dhlamini, P., Puren, A., Bhayroo, S., Steyn, J. and McIntyre, J.A., 2007. Selection and Persistence of Viral Resistance in HIV-Infected Children After Exposure to Single-Dose Nevirapine. Journal of Acquired Immune Deficiency Syndromes 44, 148–153.

Martinson, N.A., Morris, L., Johnson, J., Gray, G.E., Pillay, V., Ledwaba, J., Dhlamini, P., Cohen, S., Puren, A., Steyn, J., Heneine, W. and McIntyre, J.A., 2009. Women Exposed to Single-Dose Nevirapine in Successive Pregnancies: Effectiveness and Nonnucleoside Reverse Transcriptase Inhibitor Resistance. AIDS 23, 809-816.

Mellors, J.W., Bazmi, H.Z., Schinazi, R.F., Roy, B.M., Hsiou, Y., Arnold, E., Weir, J. and Mayers, D.L., 1995a. Novel Mutations in Reverse Transcriptase of Human

Immunodeficiency Virus Type 1 Reduce Susceptibility to Foscarnet in Laboratory and Clinical Isolates. Antimicrobial Agents and Chemotherapy 39, 1087–1092.

Mellors, J.W., Kingsley, L.A., Rinaldo, C.R., Jr, Todd, J.A., Hoo, B.S., Kokka, R.P. and Gupta, P., 1995b. Quantitation of HIV-1 RNA in Plasma Predicts Outcome After Seroconversion. Annals of Internal Medicine 122, 573-9.

Menendez-Arias, L., 2008. Mechanisms of Resistance to Nucleoside Analogue Inhibitors of HIV-1 Reverse Transcriptase. Virus Research 134, 124–146.

Millward, H., Samowitz, W., Wittwer, C.T. and Bernard, P.S., 2002. Homogeneous Amplification and Mutation Scanning of the p53 Gene Using Fluorescent Melting Curves. Clinical Chemistry 48, 1321–1328.

Mohey, R., Jørgensen, L.B., Møller, B.K., Black, F.T., Kjems, J. and Obel, N., 2005. Detection and Quantification of Proviral HIV-1 184M/V in Circulating CD4+ T Cells of Patients on HAART With a Viremia Less Than 1000 Copies/ml. Journal of Clinical Virology 34, 257–267.

Montgomery, J., Wittwer, C.T., Palais, R. and Zhou, L., 2007a. Simultaneous mutation scanning and genotyping by high-resolution DNA melting analysis. Nature Protocols 2, 59-66.

Montgomery, J., Wittwer, C.T., Palais, R. and Zhou, L., 2007b. Simultaneous Mutation Scanning and Genotyping by High-Resolution DNA Melting Analysis. Nature Protocols 2, 59-66.

Montgomery, J.L., Sanford, L.N. and Wittwer, C.T., 2010. High-Resolution DNA Melting Analysis in Clinical Research and Diagnostics. Expert Review of Molecular Diagnostics 10, 219-240.

Muller, B., Tessmer, U., Schubert, U. and Krausslich, H.G., 2000. Human Immunodeficiency Virus Type 1 Vpr Protein is Incorporated into the Virion in Significantly Smaller

Amounts than Gag and is Phosphorylated in Infected Cells. Journal of Virology 74, 9727-9731.

Musey, L., Hughes, J., Schacker, T., Shea, T., Corey, L. and McElrath, M.J., 1997. Cytotoxic-T-Cell Responses, Viral Load, And Disease Progression In Early Human Immunodeficiency Virus Type 1 Infection. New England Journal of Medicine 337, 1267-1274.

Naiser, T., Ehler, O., Kayser, J., Mai, T., Michel, W. and Ott, A., 2008. Impact of Point-Mutations on the Hybridization Affinity of Surface-Bound DNA/DNA and RNA/DNA Oligonucleotide-Duplexes: Comparison of Single Base Mismatches and Base Bulges. BMC Biotechnology 8, doi:10.1186/1472-6750-8-48.

Nakagawa, N., Higashi, N. and Nakagawa, T., 2009. Cocirculation of Antigenic Variants and the Vaccine-Type Virus during the 2004–2005 Influenza B Virus Epidemics in Japan. Journal of Clinical Microbiology 47, 352–357.

National Department of Health South Africa 2010. 2010. Clinical Guidelines for the Management of HIV & Aids in Adults and Adolescents. In: National Department of Health (Ed), pp. 1-42.

National Department of Health South Africa, 2004. National Antiretroviral Treatment Guidelines. Jacana, Johannesburg, South Africa.

Ndung'u, T., Renjifo, B. and Essex, M., 2001. Construction and Analysis of an Infectious Human Immunodeficiency Virus Type 1 Subtype C Molecular Clone. Journal of Virology 75, 4964–4972.

Nermut, M.V., Grief, C., Hashmi, S. and Hockley, D.J., 1993. Further Evidence of Icosahedral Symmetry in Human and Simian Immunodeficiency Virus. AIDS Research and Human Retroviruses 9, 929-938.

Nguyen-Dumont, T., Calvez-Kelm, F.L., Forey, N., McKay-Chopin, S., Garritano, S., Gioia-Patricola, L., Silva, D.D., Weigel, R., Breast Cancer Family Registries (BCFR), Kathleen Cuningham Foundation Consortium for research into Familial Breast cancer (kConFab), Sangrajrang, S., Lesueur, F. and Tavtigian, S.V., 2009. Description and Validation of High-Throughput Simultaneous Genotyping and Mutation Scanning by High-Resolution Melting Curve Analysis. Human Mutation 30, 884-890.

Nienke van der Stoep, van Paridon, C.D.M., Janssens, T., Krenkova, P., Stambergova, A., Macek, M., Matthijs, G. and Bakker, E., 2009. Diagnostic Guidelines for High-Resolution Melting Curve (HRM) Analysis: An Interlaboratory Validation of BRCA1 Mutation Scanning Using the 96-Well LightScanner^{TM}. Human Mutation 30, 899-909.

Norambuena, P.A., Copeland, J.A., Křenková, P., Štambergová, A. and Macek, M.J., 2009. Diagnostic method validation: High resolution melting (HRM) of small amplicons genotyping for the most common variants in the MTHFR gene. Clinical Biochemistry.

Odell, I.D., Cloud, J.L., Seipp, M. and Wittwer, C.T., 2005. Rapid Species Identification Within the *Mycobacterium chelonae–abscessus* Group by High-Resolution Melting Analysis of hsp65 PCR Products. American Journal of Clinical Pathology 123, 96-101.

Ohtaka, H. and Freire, E., 2005. Adaptive Inhibitors of the HIV-1 Protease. Progress in Biophysics and Molecular Biology 88, 193–208.

Oliveira, T., Engelbrecht, S., Rensburg, E.J., Gordon, M., Bishop, K., Megede, J., Barnett, S.W. and Cassol, S., 2003. Variability at Human Immunodeficiency Virus Type 1 Subtype C

Protease Cleavage Sites: an Indication of Viral Fitness? Journal of Virology 77, 9422–9430.

Orrell, C., Walensky, R.P., Losina, E., Pitt, J., Freedberg, K.A. and Wood, R., 2009. HIV Type-1 Clade C Resistance Genotypes in Treatment-Naive Patients and After First Virological Failure in a Large Community Antiretroviral Therapy Programme. Antiviral Therapy 14, 523-531.

Osmond, D.H., 1989. Incubation Period of AIDS in San Francisco. Nature 338, 251-253.

Palmer, S., Alaeus, A., Albert, J. and Cox, S., 1998. Drug Susceptibility of Subtypes A,B,C,D, and E Human Immunodeficiency Virus Type 1 Primary Isolates. AIDS Research and Human Retroviruses 14, 157-162.

Palmer, S., Boltz, V., Maldarelli, F., Kearney, M., Halvas, E.K., Rock, D., Falloon, J., Davey, R., Dewar, R.L., Metcalf, J.A., Mellors, J.W. and Coffin, J.M., 2006. Selection and Persistence of Non-Nucleoside Reverse Transcriptase Inhibitor-Resistant HIV-1 in Patients Starting and Stopping Non-Nucleoside Therapy. AIDS 20, 701-710.

Paredes, R., Marconi, V.C., Campbell, T.B. and Kuritzkes, D.R., 2007. Systematic Evaluation of Allele-Specific Real-Time PCR for the Detection of Minor HIV-1 Variants With Pol and Env Resistance Mutations. Journal of Virological Methods 146, 136–146.

Parkin, N.T., Gupta, S., Chappey, C. and Petropoulos, C.J., 2006. The K101P and K103R/V179D Mutations in Human Immunodeficiency Virus Type 1 Reverse Transcriptase Confer Resistance to Nonnucleoside Reverse Transcriptase Inhibitors. Antimicrobial Agents and Chemotherapy 50, 351–354.

Perelson, A.S., Neumann, A.U., Markowitz, M., Leonard, J.M. and Ho, D.D., 1996. HIV-1 Dynamics *in vivo*: Virion Clearance Rate, Infected Cell Life-Span, and Viral Generation Time. Science 271, 1582-6.

Pettersson, E., Lundeberg, J. and Ahmadian, A., 2009. Generations of Sequencing Technologies. Genomics 93, 105–111.

Phillips, A.N., Lee, C.A., Elford, J., Janossy, G., Timms, A., Bofill, M. and Kernoff, P.B., 1991. Serial CD4 Lymphocyte Counts and Development of AIDS. Lancet 337, 389-392.

Piatak Jr, M., Saag, M.S., Yang, L.C., Clark, S.J., Kappes, J.C., Luk, K.C., Hahn, B.H., Shaw, G.M. and Lifson, J.D., 1993. High Levels of HIV-1 in Plasma During all Stages of Infection Determined by Competitive PCR. Science 19, 1749-5174.

Pillay, V., Pillay, C., Kantor, R., Venter, F., Leon Levin and Morris, L., 2008. HIV Type 1 Subtype C Drug Resistance Among Pediatric and Adult South African Patients Failing Antiretroviral Therapy. AIDS Research and Human Retroviruses 24, 1449-1454.

Plantier, J.-C., Leoz, M., Dickerson, J.E., Oliveira, F.D., Cordonnier, F., Lemee, V., Damond, F., Robertson, D.L. and Simon, F., 2009. A New Human Immunodeficiency Virus Derived from Gorillas. Nature Medicine 15, 871-872.

Poláková, K.M., Lopotová, T., Klamová, H. and Moravcová, J., 2008. High-Resolution Melt Curve Analysis: Initial Screening for Mutations in BCR-ABL Kinase Domain. Leukemia Research 32, 1236-1243.

Pollard, V.W. and Malim, M.H., 1998. The HIV-1 Rev Protein. Annual Review of Microbiology 52, 491–532.

Poulson, M.D. and Wittwer, C.T., 2007. Closed-Tube Genotyping of Apolipoprotein E by Isolated-Probe PCR With Multiple Unlabeled Probes and High-Resolution DNA Melting Analysis. BioTechniques 43, 87-91.

Preston, B.D., Poiesz, B.J. and Loeb, L.A., 1988. Fidelity of HIV-1 Reverse Transcriptase. Science 242, 1168-1171.

Price, E.P., Smith, H., Huygens, F. and Giffard, P.M., 2007. High-Resolution DNA Melt Curve Analysis of the Clustered, Regularly Interspaced Short-Palindromic-Repeat Locus of *Campylobacter jejuni*. Applied and Environmental Microbiology 73, 3431–3436.

Reed, G.H. and Wittwer, C.T., 2004. Sensitivity and Specificity of Single-Nucleotide Polymorphism Scanning by High-Resolution Melting Analysis. Clinical Chemistry 50, 1748–1754.

Reed, R., Holmes, D., Weyers, J. and Jones, A., 2003. Practical Skills in Biomolecular Sciences. Ashford Colour Press Ltd, Gosport.

Reja, V., Kwok, A., Stone, G., Yang, L., Missel, A., Menzel, C. and Bassam, B., 2010. ScreenClust: Advanced Statistical Software for Supervised and Unsupervised High Resolution Melting (HRM) Analysis. Methods In Press: doi:10.1016/j.ymeth.2010.02.006.

Ren, J. and Stammers, D.K., 2008. Structural Basis For Drug Resistance Mechanisms For Non-Nucleoside Inhibitors of HIV Reverse Transcriptase. Virus Research 134, 157–170.

Rhee, S.-Y., Liu, T., Ravela, J., Gonzales, M.J. and Shafer, R.W., 2004. Distribution of Human Immunodeficiency Virus Type 1 Protease and Reverse Transcriptase Mutation Patterns in 4,183 Persons Undergoing Genotypic Resistance Testing. Antimicrobial Agents and Chemotherapy 48, 3122–3126.

Ririe, K.M., Rasmussen, R.P. and Wittwer, C.T., 1997. Product Differentiation by Analysis of DNA Melting Curves during the Polymerase Chain Reaction. Analytical Biochemistry 245, 154–160.

Roberts, J.D., Bebenek, K. and Kunkel, T.A., 1988. The Accuracy of Reverse Transcriptase from HIV-1. Science 242, 1171-1173.

Rouleau, E., Lefol, C., Bourdon, V., Coulet, F., Noguchi, T., Soubrier, F., Bieche, I., Olschwang, S., Sobol, H. and Lidereau, R., 2009. Quantitative PCR High-Resolution Melting (qPCR-HRM) Curve Analysis, a New Approach to Simultaneously Screen Point Mutations and Large Rearrangements: Application to MLH1 Germline Mutations in Lynch Syndrome. Human Mutation 30, 867–875.

Sabol, I., Cretnik, M., Hadzisejdic, I., Si-Mohamed, A., Matovina, M., Grahovac, B., Levanat, S. and Grce, M., 2009. A New Approach for the Evaluation of the Human Papillomavirus Type 16 Variability With High Resolution Melting Analysis. Journal of Virological Methods 162, 142-147.

Saracino, A., Monno, L., Scudeller, L., Cibelli, D.C., Tartaglia, A., Punzi, G., Torti, C., Caputo, S.L., Mazzotta, F., Scotto, G., Carosi, G. and Angarano, G., 2006. Impact of Unreported HIV-1 Reverse Transcriptase Mutations on Phenotypic Resistance to Nucleoside and Non-Nucleoside Inhibitors. Journal of Medical Virology 78, 9–17.

Sarafianos, S.G., Marchand, B., Das, K., Himmel, D.M., Parniak, M.A., Hughes, S.H. and Arnold, E., 2009. Structure and Function of HIV-1 Reverse Transcriptase: Molecular Mechanisms of Polymerization and Inhibition. Journal of Molecular Biology 385, 693–713.

Shafer, R.W., 2002. Genotypic Testing for Human Immunodeficiency Virus Type 1 Drug Resistance. Clinical Microbiology Reviews 15, 247–277.

Shafer, R.W. and Schapiro, J.M., 2008. HIV-1 Drug Resistance Mutations: an Updated Framework for the Second Decade of HAART. AIDS Reviews 10, 67-84.

Shisana, O., Rehle, T., Simbayi, L.C., Zuma, K., Jooste, S., Pillay-van-Wyk, V., Mbelle, N., Zyl, J.V., Parker, W., Zungu, N.P., Pezi, S. and SABSSM III Implementation Team, 2009. South African National HIV Prevalence, Incidence, Behaviour and Communication Survey 2008: A Turning Tide Among Teenagers? HSRC Press, Cape Town.

Sichtig, N., Sierra, S., Kaiser, R., Daumer, M., Reuter, S., Schulter, E., Altmann, A., Fatkenheuer, G., Dittmer, U., Pfister, H. and Esser, S., 2009. Evolution of Raltegravir Resistance During Therapy. Journal of Antimicrobial Chemotherapy 64, 25–32.

Simeonov, A. and Nikiforov, T.T., 2002. Single Nucleotide Polymorphism Genotyping Using Short, Fluorescently Labeled Locked Nucleic Acid (LNA) Probes and Fluorescence Polarization Detection. Nucleic Acids Research 30, e91.

Simi, L., Pratesi, N., Vignoli, M., Sestini, R., Cianchi, F., Valanzano, R., Nobili, S., Mini, E., Pazzagli, M. and Orlando, C., 2008. High-Resolution Melting Analysis for Rapid Detection of KRAS, BRAF, and PIK3CA Gene Mutations in Colorectal Cancer. American Journal of Clinical Pathology 130, 247-253.

Simon, V., Ho, D.D. and Karim, Q.A., 2006. HIV/AIDS Epidemiology, Pathogenesis, Prevention, and Treatment. Lancet 368, 489–504.

Steer, P.A., Kirkpatrick, N.C., O'Rourke, D. and Noormohammadi, A.H., 2009. Classification of Fowl Adenovirus Serotypes by Use of High-Resolution Melting-Curve Analysis of the Hexon Gene Region. Journal of Clinical Microbiology 47, 311–321.

Stuyver, L., Wyseur, A., Rombout, A., Louwagie, J., Scarcez, T., Verhofstede, C., Rimland, D., Schinazi, R.F. and Rossau, R., 1997. Line Probe Assay (LiPa) for Rapid Detection of Drug-Selected Mutations in the Human Immunodeficiency Virus Type 1 Reverse Transcriptase Gene. . Antimicrobial Agents and Chemotherapy 41, 284–291.

Svicher, V., Sing, T., Santoro, M.M., Forbici, F., Rodrıguez-Barrios, F., Bertoli, A., Beerenwinkel, N., Bellocchi, M.C., Gago, F., Monforte, A.d.A., Antinori, A., Lengauer, T., Ceccherini-Silberstein, F. and Perno, C.F., 2006. Involvement of Novel Human Immunodeficiency Virus Type 1 Reverse Transcriptase Mutations in the Regulation of Resistance to Nucleoside Inhibitors. Journal of Virology 80, 7186–7198.

Tajiri-Utagawa, E., Hara, M., Takahashi, K., Watanabe, M. and Wakita, T., 2009. Development of a Rapid High-Throughput Method for High-Resolution Melting Analysis for Routine Detection and Genotyping of Noroviruses. Journal of Clinical Microbiology 47, 435–440.

Tochikura, T.S., Nakashima, H. and Yamamoto, N., 1989. Antiviral Agents with Activity Against Human Retroviruses. Journal of Acquired Immune Deficiency Syndromes 2, 441-447.

Toi, C.S. and Dwyer, D.E., 2008. Differentiation Between Vaccine and Wild-Type Varicella-Zoster Virus Genotypes by High-Resolution Melt Analysis of Single Nucleotide Polymorphisms. Journal of Clinical Virology 43, 18-24.

Toni, T.A., Asahchop, E.L., Moisi, D., Ntemgwa, M., Oliveira, M., Masquelier, B., Brenner, B.G. and Wainberg, M.A., 2009. Detection of Human Immunodeficiency Virus (HIV) Type 1 M184V and K103N Minority Variants in Patients With Primary HIV Infection. Antimicrobial Agents and Chemotherapy 53, 1670-1672.

Torre, D. and Tambini, R., 2002. Antiretroviral Drug Resistance Testing in Patients with HIV-1 Infection: A Meta-Analysis Study. HIV Clinical Trials 3, 1-8.

Tozzi, V., 2010. Pharmacogenetics of Antiretrovirals. Antiviral Research 85, 190-200.

Tural, C., Ruiz, L., Holtzer, C., Schapiro, J., Viciana, P., González, J., Domingo, P., Boucher, C., Rey-Joly, C., Clotet, B. and Havana Study Group, 2002. Clinical Utility Of HIV-1 Genotyping And Expert Advice: The Havana Trial. AIDS 16, 209-218.

Ugozzoli, L.A., Latorra, D., Pucket, R., Arar, K. and Hambya, K., 2004. Real-time Genotyping with Oligonucleotide Probes Containing Locked Nucleic Acids. Analytical Biochemistry 324, 143–152.

Vahey, M., Nau, M.E., Barrick, S., Cooley, J.D., Sawyer, R., Sleeker, A.A., Vickerman, P., Bloor, S., Larder, B., Michael, N.L. and Wegner, S.A., 1999. Performance of the Affymetrix GeneChip HIV PRT 440 Platform for Antiretroviral Drug Resistance Genotyping of Human Immunodeficiency Virus Type 1 Clades and Viral Isolates with Length Polymorphisms. Journal of Clinical Microbiology 37, 2533-2537.

van der Stoep, N., van Paridon, C.D.M., Janssens, T., Krenkova, P., Stambergova, A., Macek, M., Matthijs, G. and Bakker, E., 2009. Diagnostic Guidelines for High-Resolution Melting Curve (HRM) Analysis: An Interlaboratory Validation of BRCA1 Mutation Scanning Using the 96-Well LightScanner^{TM}. Human Mutation 30, 899-909.

Van Harmelen, J.H., Van Der Ryst, E., Loubser, A.S., York, D., Madurai, S., Lyons, S., Wood, R. and Williamson, C., 1999. A Predominantly HIV Type 1 Subtype C-Restricted Epidemic in South African Urban Populations. AIDS Research and Human Retroviruses 15, 395-398.

Vandersteen, J.G., Bayrak-Toydemir, P., Palais, R.A. and Wittwer, C.T., 2007. Identifying Common Genetic Variants by High-Resolution Melting. Clinical Chemistry 53, 1191-1198.

Vaughn, C.P. and Elenitoba-Johnson, K.S.J., 2004. High-Resolution Melting Analysis for Detection of Internal Tandem Duplications. Journal of Molecular Diagnostics 6, 211-216.

Veronese, F.D., DeVico, A.L., Copeland, T.D., Oroszlan, S., Gallo, R.C. and Sarngadharan, M.G., 1985. Characterization of gp41 as the Transmembrane Protein Coded by the HTLV-III/LAV Envelope Gene. Science 229, 1402-1405.

Vossen, R.H.A.M., Aten, E., Roos, A. and den Dunnen, J.T., 2009a. High-Resolution Melting Analysis (HRMA)—More Than Just Sequence Variant Screening. Human Mutation 30, 860-866.

Vossen, R.H.A.M., Aten, E., Roos, A. and den Dunnen, J.T., 2009b. High-Resolution Melting Analysis (HRMA) - More Than Just Sequence Variant Screening. Human Mutation 30, 860-866.

Wallis, C., Sanne, I., Venter, F., Mellors, J. and Stevens, W., 2009. Varied Patterns of HIV-1 Drug Resistance on Failing First-Line Antiretroviral Therapy in South Africa. Journal of Acquired Immune Deficiency Syndromes.

Wallis, C.L., Mahomed, I., Morris, L., Chidarikire, T., Stevens, G., Rekhviashvili, N. and Stevens, W., 2005. Evaluation of an Oligonucleotide Ligation Assay for Detection of Mutations in HIV-1 Subtype C Individuals Who Have High Level Resistance to Nucleoside Reverse Transcriptase Inhibitors and Non-Nucleoside Reverse Transcriptase Inhibitors. Journal of Virological Methods 125, 99-109.

Watkins Jr, N.E. and SantaLucia Jr, J., 2005. Nearest-Neighbor Thermodynamics of Deoxyinosine Pairs in DNA Duplexes. Nucleic Acids Research 33, 6258–6267.

Weller, I.V.D. and Williams, I.G., 2001. ABC of AIDS Antiretroviral Drugs. British Medical Journal 322, 1410-1412.

WHO/UNAIDS. 2008. Towards Universal Access - Scaling Up Priority HIV/AIDS Interventions in the Health Sector. Progress Report 2008, WHO Press, Geneva, Switzerland.

Wilk, T., Gross, I., Gowen, B.E., Rutten, T., Haas, F., Welker, R., Krausslich, H.G., Boulanger, P. and Fuller, S.D., 2001. Organization of Immature Human Immunodeficiency Virus Type 1. Journal of Virology 75, 759–771.

Willmore-Payne, C., Holden, J.A., Tripp, S. and Layfield, L.J., 2005. Human Malignant Melanoma: Detection of BRAF- and c-Kit-Activating Mutations by High-Resolution Amplicon Melting Analysis. Human Pathology 36, 486-493.

Wilson, J.W., Bean, P., Robins, T., Graziano, F. and Persing, D.H., 2000. Comparative Evaluation of Three Human Immunodeficiency Virus Genotyping Systems: the HIV-GenotypR Method, the HIV PRT GeneChip Assay, and the HIV-1 RT Line Probe Assay. Journal of Clinical Microbiology 38, 3022–3028.

Wittwer, C.T., Mark G. Herrmann, Gundry, C.N. and Elenitoba-Johnson, K.S.J., 2001. Real-Time Multiplex PCR Assays. Methods 25, 430–442.

Wittwer, C.T., Reed, G.H., Gundry, C.N., Vandersteen, J.G. and Pryor, R.J., 2003. High-Resolution Genotyping by Amplicon Melting Analysis Using LCGreen. Clinical Chemistry 49, 853–860.

Witvrouw, M., Pannecouque, C., Laethem, K.V., Desmyter, J., De Clercq, E. and Vandamme, A.-M., 1999. Activity of Non-Nucleoside Reverse Transcriptase Inhibitors Against HIV-2 and SIV. AIDS 13, 1477–1483.

Wojdacz, T.K. and Dobrovic, A., 2007. Methylation-Sensitive High Resolution Melting (MS-HRM): a New Approach for Sensitive and High-Throughput Assessment of Methylation. Nucleic Acids Research 35, e41 doi:10.1093/nar/gkm013.

World Health Organization (WHO). 2007. WHO Case Definitions of HIV For Surveillance and Revised Clinical Staging And Immunological Classification Of HIV-Related Disease in Adults and Children, WHO Press, Geneva, Switzerland.

Wu, J.-H., Hong, P.-Y. and Liu, W.-T., 2009. Quantitative Effects of Position and Type of Single Mismatch on Single Base Primer Extension. Journal of Microbiological Method 77, 267–275.

Wyatt, R. and Sodroski, J., 1998. The HIV-1 Envelope Glycoproteins: Fusogens, Antigens, and Immunogens. Science 280, 1884 - 1888.

Xu, H.-T., Martinez-Cajas, J.L., Ntemgwa, M.L., Coutsinos, D., Frankel, F.A., Brenner, B.G. and Wainberg, M.A., 2009. Effects of the K65R and K65R/M184V Reverse Transcriptase Mutations in Subtype C HIV on Enzyme Function and Drug Resistance. Retrovirology 6, doi:10.1186/1742-4690-6-14.

Zheng, L., Gibbs, M.J. and Rodoni, B.C., 2008. Quantitative PCR Measurements of the Effects of Introducing Inosines into Primers Provides Guidelines for Improved Degenerate Primer Design. Journal of Virological Methods 153, 97–103.

Zheng, Y.H., Lovsin, N. and Peterlin, B.M., 2005. Newly Identified Host Factors Modulate HIV Replication. Immunology Letters 97, 225–234.

Zhou, L., Myers, A.N., Vandersteen, J.G., Wang, L. and Wittwer, C.T., 2004. Closed-Tube Genotyping with Unlabeled Oligonucleotide Probes and a Saturating DNA Dye. Clinical Chemistry 50, 1328–1335.

Zhou, L., Wang, L., Palais, R., Pryor, R. and Wittwer, C.T., 2005. High-Resolution DNA Melting Analysis for Simultaneous Mutation Scanning and Genotyping in Solution. Clinical Chemistry 51, 1770–1777.

Zhuang, J., Jetzt, A.E., Sun, G., Yu, H., Klarmann, G., Ron, Y., Preston, B.D. and Dougherty, J.P., 2002. Human Immunodeficiency Virus Type 1 Recombination: Rate, Fidelity, and Putative Hot Spots. Journal of Virology 76, 11273–11282.